

**GAC-MAC  
WINNIPEG  
2013**



**AT THE  
CENTRE OF  
THE CONTINENT**

**AU  
CENTRE DU  
CONTINENT**



*Pirate Island - Paint Lake by Nancy-lyne Hughes*

**FIELD TRIP GUIDEBOOK**

**Field Trip Guidebook FT-C3 / Open File OF2013-6  
The Volcanological and Structural Evolution of the Paleoproterozoic  
Flin Flon Mining District, Manitoba: The Anatomy of a Giant VMS  
System**

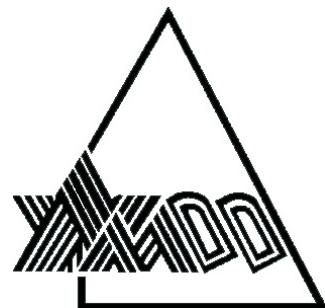
Harold Gibson, Bruno Lafrance, Sally Pehrsson, Michelle DeWolfe,  
Kelly Gilmore, Renée-Luce Simard and Brett Pearson



Held in conjunction with  
**GAC®-MAC • AGC®-AMC**  
Joint Annual Meeting • Congrès annuel conjoint  
May 22–24, 2013



**This field trip was sponsored by the  
Mineral Deposits Division of the  
Geological Association of Canada**



**In-kind support provided by  
HudBay Minerals Inc.**

**HUDBAY**



---

Open File OF2013-6

## Field Trip Guidebook FT-C3

# The Volcanological and Structural Evolution of the Paleoproterozoic Flin Flon Mining District, Manitoba: The Anatomy of a Giant VMS System

by Harold Gibson, Bruno Lafrance, Sally Pehrsson, Michelle DeWolfe, Kelly Gilmore, Renée-Luce Simard and Brett Pearson

Geological Association of Canada–Mineralogical Association of Canada Joint Annual Meeting,  
Winnipeg  
May, 2013

---

Innovation, Energy and Mines

Hon. Dave Chomiak  
Minister

Grant Doak  
Deputy Minister

Mineral Resources Division

John Fox  
Assistant Deputy Minister

Manitoba Geological Survey

C.H. Böhm  
A/Director



©Queen's Printer for Manitoba, 2013

Every possible effort is made to ensure the accuracy of the information contained in this report, but Manitoba Innovation, Energy and Mines does not assume any liability for errors that may occur. Source references are included in the report and users should verify critical information.

Any digital data and software accompanying this publication are supplied on the understanding that they are for the sole use of the licensee, and will not be redistributed in any form, in whole or in part, to third parties. Any references to proprietary software in the documentation and/or any use of proprietary data formats in this release do not constitute endorsement by Manitoba Innovation, Energy and Mines of any manufacturer's product.

When using information from this publication in other publications or presentations, due acknowledgment should be given to the Manitoba Geological Survey. The following reference format is recommended:

Gibson, H., Lafrance, B., Pehrsson, S., DeWolfe, M., Gilmore, K., Simard, R-L. and Pearson, B. 2013: The Volcanological and Structural Evolution of the Paleoproterozoic Flin Flon Mining District, Manitoba: The Anatomy of a Giant VMS System; Geological Association of Canada–Mineralogical Association of Canada Joint Annual Meeting, Field Trip Guidebook FT-C3; Manitoba Innovation, Energy and Mines, Manitoba Geological Survey, Open File OF2013-6, 47 p.

**NTS grid:** 63K

**Keywords:** Manitoba; Flin Flon; Trans-Hudson orogen; Flin Flon Belt; Amisk collage; Paleoproterozoic; VMS deposits; 777 deposit; synvolcanic subsidence structure

**Author addresses:**

Harold Gibson, Bruno Lafrance, Michelle DeWolfe  
Mineral Exploration Research Centre, Laurentian University, Sudbury, ON, P3E 2C6

Sally Pehrsson  
Geological Survey of Canada, 601 Booth Street, Ottawa, ON

Michelle DeWolfe  
Mount Royal University, Calgary, AB

Kelly Gilmore  
Box 95, Flin Flon, MB, R8A 1M6

Brett Pearson  
Hudbay Minerals Inc., P.O. Box 1500, Flin Flon, MB

Renée-Luce Simard  
Northern Shield Resources Inc., Ottawa, ON

**Published by:**

Manitoba Innovation, Energy and Mines  
Manitoba Geological Survey  
360–1395 Ellice Avenue  
Winnipeg, Manitoba  
R3G 3P2 Canada  
Telephone: (800) 223-5215 (General Enquiry)  
(204) 945-4154 (Publication Sales)  
Fax: (204) 945-8427  
E-mail: [minesinfo@gov.mb.ca](mailto:minesinfo@gov.mb.ca)  
Website: [manitoba.ca/minerals](http://manitoba.ca/minerals)

This publication is available to download free of charge at [manitoba.ca/minerals](http://manitoba.ca/minerals)

## SAFETY INFORMATION

### General Information

The Geological Association of Canada (GAC) recognizes that its field trips may involve hazards to the leaders and participants. It is the policy of the GAC to provide for the safety of participants during field trips, and to take every precaution, reasonable in the circumstances, to ensure that field trips are run with due regard for the safety of leaders and participants. Field trip safety is a shared responsibility. The GAC has a responsibility to take all reasonable care to provide for the safety of the participants on its field trips. Participants have a responsibility to give careful attention to safety-related matters and to conduct themselves with due regard to the safety of themselves and others while on the field trips.

Field trip participants should be aware that any geological fieldwork, including field trips, can present significant safety hazards. Foreseeable hazards of a general nature include inclement weather, slips and falls on uneven terrain, falling or rolling rock, insect bites or stings, animal encounters and flying rock from hammering. **The provision and use of appropriate personal protective equipment (e.g., rain gear, sunscreen, insect repellent, safety glasses, work gloves and sturdy boots) is the responsibility of each participant.** Each field trip vehicle will be equipped with a moderate sized first-aid kit, and the lead vehicle will carry a larger, more comprehensive kit of the type used by the Manitoba Geological Survey for remote field parties.

Participants should be prepared for the possibility of inclement weather. In Manitoba, the weather in May is highly unpredictable. The average daily temperature in Winnipeg is 12°C, with record extremes of 37°C and -11°C. North-central Manitoba (Thompson) has an average daily temperature of 7°C, with record extremes of 33°C and -18°C (*Source*: Environment Canada). Consequently, participants should be prepared for a wide range of temperature and weather conditions, and should plan to dress in layers. A full rain suit and warm sweater are essential. Gloves and a warm hat could prove invaluable if it is cold and wet, and a sunhat and sunscreen might be just as essential in the heat and sun.

Above all, field trip participants are responsible for acting in a manner that is safe for themselves and their co-participants. This responsibility includes using personal protective equipment (PPE) when necessary or when recommended by the field trip leader, or upon personal identification of a hazard requiring PPE use. It also includes informing the field trip leaders of any matters of which they have knowledge that may affect their health and safety or that of co-participants. Field Trip participants should pay close attention to instructions from the trip leaders and GAC representatives at all field trip stops. Specific dangers and precautions will be reiterated at individual localities.

### Specific Hazards

Some of the stops on this field trip may require short hikes, in some cases over rough, rocky, uneven or wet terrain. Participants should be in good physical condition and accustomed to exercise. Sturdy footwear that provides ankle support is strongly recommended. Some participants may find a hiking stick a useful aid in walking safely. Steep outcrop surfaces require special care, especially after rain. Access to bush outcrops may require traverses across muddy or boggy areas; in some cases it may be necessary to cross small streams or ditches. Field trip leaders are responsible for identifying such stops and making participants aware well in advance if waterproof footwear is required. Field trip leaders will also ensure that participants do not go into areas for which their footwear is inadequate for safety. In all cases, field trip participants must stay with the group.

Other field trip stops are located adjacent to roads, some of which may be prone to fast-moving traffic. At these stops, participants should pay careful attention to oncoming traffic, which may be distracted by the field trip group. Participants should exit vehicles on the shoulder-side of the road, stay off roads when examining or photographing outcrops, and exercise extreme caution in crossing roads.

Road cuts or rock quarries also present specific hazards, and participants **MUST** behave appropriately for the safety of all. Participants must be aware of the danger from falling debris and should stay well back from overhanging cliffs or steep faces. Participants must stay clear of abrupt drop-offs at all times, stay with the field trip group, and follow instructions from leaders.

Participants are asked to refrain from hammering rock. It represents a significant hazard to the individual and other participants, and is in most cases unnecessary. Many stops on this field trip include outcrop with unusual features that should be preserved for future visitors. If a genuine reason exists for collecting a sample, please inform the field trip leader, and then make sure it is done safely and with concern for others, ideally after the main group has departed the outcrop.

Subsequent sections of this guidebook contain the stop descriptions and outcrop information for the field trip. In addition to the general precautions and hazards noted above, the introductions for specific localities make note of any specific safety concerns. Field trip participants must read these cautions carefully and take appropriate precautions for their own safety and the safety of others.



## TABLE OF CONTENTS

	<b>Page</b>
Safety information .....	iii
Introduction .....	1
Acknowledgements .....	1
Field trip program .....	1
Regional Geology and Background .....	1
Trans-Hudson orogen .....	1
The Flin Flon – Glennie Complex .....	3
Amisk collage .....	4
History of Exploration .....	4
Geology, Structure and VMS deposits of the Flin Flon District .....	6
Terminology .....	7
Flin Flon formation .....	8
Club member .....	8
Blue Lagoon member .....	8
Millrock member .....	8
Mill Rock Hill Station .....	9
South Main Section .....	10
Smelter Section .....	11
Callinan Section .....	11
Millrock member west of the Flin Flon Lake Fault .....	12
Reconstruction .....	12
Hidden formation .....	12
1920 unit .....	12
Reservoir member .....	14
Stockwell member .....	14
Carlisle Lake member .....	14
Louis formation .....	14
Tower member .....	14
Icehouse member .....	15
Undivided Louis formation rocks .....	15
Structure and Metamorphism .....	15
3D Architecture of the Flin Flon District .....	15
Stop Descriptions .....	17
Stop 1: Meridian-West Arm shear zone and the Missi unconformity .....	17
Stop 1.1 Meridian – West Arm Shear Zone .....	17
Co-ordinates .....	17
Overview .....	17
Stop description .....	17
Stop 1.2: Missi unconformity .....	18
Co-ordinates .....	18
Overview .....	18
Stop description .....	19
Stop 2. Millrock Hill Section .....	20
Stops 2.1 to 2.3 .....	20
Stratigraphy .....	20
Co-ordinates .....	20

Stop Descriptions .....	20
Stops 2.4 to 2.7.....	22
Co-ordinates.....	22
Structure.....	22
Stop 3. South Main Section .....	23
Co-ordinates.....	23
Stop Descriptions.....	23
Stop 4. Smelter Section.....	25
Stops 4.1 to 4.8: Blue Lagoon member.....	25
Co-ordinates.....	25
Stop Descriptions.....	25
Stop 5. Lower Callinan Section .....	27
Stops 5.1 to 5.2.....	27
Co-ordinates.....	27
Stop Descriptions.....	27
Stops 5.3 to 5.5.....	28
Co-ordinates.....	28
Stop Descriptions.....	28
Stop 6. Beaver Road Anticline.....	28
Stops 6.1 to 6.10.....	28
Co-ordinates.....	28
Stop Descriptions.....	29
Stop 7. Upper Callinan section .....	31
Stop 7.1: Columnar jointed vent facies of the 1920 unit cryptoflow .....	31
Co-ordinates.....	31
Stop Descriptions.....	31
Stop 7.2: Facies transitions within the 1920 unit: Field evidence for emplacement as a cryptoflow .....	32
Co-ordinates.....	32
Stop Description.....	32
Stop 7.3: Sheared rhyolitic tuff breccia of the Millrock member along the Upper Railway fault.....	33
Co-ordinates.....	33
Stop Description.....	33
Stop 7.4: Sheared 1840 Ma Phantom Lake dikes and 1872 Ma gabbroic dikes along the Upper Railway fault .....	34
Co-ordinates.....	34
Stop Description.....	34
Stop 7.5: Missi wedge.....	35
Co-ordinates.....	35
Stop Description.....	35
Stop 8: 777 Underground Tour .....	37
Mine Geology .....	37
The Massive Sulphide.....	38
Underground tour.....	39
Stop 9 – Hanging wall to the Schist Lake and Mandy ore bodies .....	39
Stop 9.1: Lava tubes and megabreccias within the Hidden formation: Evidence for vent proximity .....	39
Co-ordinates.....	39
Stop Description.....	40
Stop 9.2: Spatter rampart and synvolcanic dikes within the Hidden formation: Evidence for vent proximity .....	41

Co-ordinates.....	41
Stop Description.....	41
Stop 10. Cliff Lake Pluton .....	41
Stop 10.1: Contact between the Cliff Lake Pluton and the Hooke Lake Block.....	41
Co-ordinates.....	41
Stop Description.....	41
Stop 10.2: Contact between the Cliff Lake Pluton and the Hooke Lake Block.....	42
Co-ordinates.....	42
Stop Description.....	42
Stop 11. Icehouse member, Louis Formation, near Louis Lake .....	42
Stop 11.1: Massive and pillows lava flows of the Icehouse member .....	42
Co-ordinates.....	42
Stop Description.....	42
Stop 11.2: Pillow lavas, pillow breccia and overlying volcanoclastic rocks of the Icehouse member.....	42
Co-ordinates.....	42
Stop Description.....	42
References.....	42

## TABLES

Table 1: Major mines of the Flin Flon-Glennie complex.....	3
Table 2: Ore Reserves at the 777 Mine as of January 1, 2012 (Hudbayminerals.com).....	37

## FIGURES

Figure 1: Simplified map of the Trans-Hudson Orogen.....	2
Figure 2: Map of the Flin Flon Belt.....	2
Figure 3: Temporal evolution of the Flin Flon district.....	4
Figure 4: Geology and structure of the Flin Flon District showing stop locations.....	5
Figure 5: Schematic stratigraphic sections of the Flin Flon area.....	6
Figure 6: Generalized lithofacies through the Flin Flon, Hidden and Louis formations.....	7
Figure 7: Stratigraphic sections through the Flin Flon Formation.....	9
Figure 8: Possible reconstruction of the sequence of volcanic events that produced the facies architecture of the Millrock member at Millrock Hill.....	10
Figure 9: Facies architecture and volcanic environment post formation of the Flin Flon, Callinan and 777 VMS deposits.....	11
Figure 10: Sequence of interpreted volcanic, subsidence and VMS ore-forming events.....	13
Figure 11: 3D block diagram of the Flin Flon mine camp.....	16
Figure 12: Geological map of the Meridian Creek-Hutton Bay (Meridian Lake) area.....	18
Figure 13: Structure of “Missi outlier”.....	19
Figure 14: Idealized stratigraphic section through the Millrock member at Millrock Hill.....	21
Figure 15: Idealized stratigraphic section through the Millrock member at South Main.....	24
Figure 16: Idealized stratigraphic section through the Millrock member, Smelter section.....	25
Figure 17: Simplified geology and structure within the Blue Lagoon member.....	29
Figure 18: Details of synvolcanic graben showing Stop locations.....	30
Figure 19: Pre-diking and pre-folding reconstruction of the area in Figures 17 and 18.....	30
Figure 20: Geology and Structure of the Hidden formation within the Hidden lake Syncline.....	32
Figure 21: Geology of the 1920 unit at Stop 7.2.....	33

Figure 22: Details of the geology and structure of the Railway thrust faults at Stop 7.3. .... 34

Figure 23: Geology and structure of the Upper Railway thrust fault at Stop 7.4. .... 35

Figure 24: Geology and structure of the “Missi Wedge” ..... 36

Figure 25: Generalized 3D Geology of the 1262 m level of the 777 Deposit. .... 38

Figure 26: Geological map of the 1082 m level. .... 38

Figure 27: Geological map of the 1080 m level. .... 39

Figure 28: Geology and structure of the Hidden formation..... 40

Figure 29: Geology at the location of Stop 10..... 41

Figure 30: Geology and structure of the Louis formation (Ice House member at Louis Lake). .... 43

## Introduction

The Paleoproterozoic Flin Flon greenstone belt is a world-class Volcanic-hosted Massive Sulphide (VMS) district, host to 27 present and past-producing mines and hosting over 400 million tonnes sulphide in its VMS deposits alone. The smelter at Flin Flon, and production from the 777, Trout Lake and Chisel North mines, sustains the communities of Creighton, Saskatchewan and Flin Flon, Manitoba and a host of other smaller regional communities. Over the past decades the Manitoba and Saskatchewan geological surveys, Natural Resources Canada (Targeted Geoscience Initiative-1 and -3 programs), Natural Sciences and Engineering Research Council (NSERC) and Hudbay Minerals Inc. ('Hudbay'), have supported a variety of projects aimed at understanding the volcanological and structural setting of Cu-Zn deposits in this uniquely well exposed area.

This field trip is an outgrowth of these collective efforts and presents a significant new interpretation of the volcanic and structural control of the deposits that will be useful to researchers and explorationists in VMS terranes of any era. *This guidebook is a modified version of GAC-MAC 2011 Field Trip Guidebook 3B, from which the stop descriptions are taken (Gibson et al., 2011).*

The principal objectives of the field trip are to:

- Place the Flin Flon District in the context of the tectonic and magmatic evolution of the Flin Flon Belt and Trans Hudson Orogen
- Introduce the stratigraphy, lithofacies and structural elements of the Flin Flon District
- Illustrate the role of volcanism and subsidence in the formation and location of VMS deposits by reconstructing the volcanic and structural architecture and history of the district. In particular to demonstrate evidence for a large, syn-volcanic subsidence structure, referred to as the Flin Flon cauldron, that hosts the VMS deposits, and to demonstrate how subsequent deformation events have modified this primary volcanic feature and its contained ore deposits.

## Acknowledgments

Field trip leaders gratefully acknowledge permission of Hudbay to conduct the tour on company property and for their logistical and organizational support. Harold Gibson would like to acknowledge funding from TGI-1, an NSERC-Hudbay-Laurentian University CRD grant, TGI-3, NSERC Discovery Grants, and the Manitoba and Saskatchewan geological surveys that funded and provided logistical support for 10 years of research at Flin Flon, and supported 6 M.Sc. (Christine Devine, Dianne Mitchinson, Nicole Tardif, Kim Bailey, Eilidh Cole and David Lewis), 1 Ph.D. (Michelle DeWolfe) and 12 undergraduate students. We gratefully acknowledge the contributions of the TGI-3 Flin Flon team, in particular Ernst Schetselaar, Don White, Maggie Currie and Doreen Ames. David Price is thanked for discussions and field tours.

## Field trip program

Participants will assemble in the Victoria Inn, Flin Flon on the evening of May 25 for an orientation session. The field trip

will focus on the Flin Flon Mine District. On Day 1 an evening talk will cover the district geology and exploration history of the Flin Flon belt and on Day 3 an evening talk will present the new 2D and 3D architecture of the Flin Flon district. The last day of the field trip (Day 3) will include an underground tour at the 777 VMS deposit.

Parts of the field trip surface tour take place on the Hudbay Plant property. This area is restricted to the public and entrance to the property requires the permission of Hudbay, an appropriate safety/orientation course provided by Hudbay, registration at the Main Gate House, and a daily Travel Pass obtained from the Gate House. Field trip participants will take the orientation on the evening of Saturday May 25. Participants going underground at 777 mine require an additional safety briefing and fit testing for a respirator. They *must* be clean shaven to pass the respirator fit test. No one will be allowed underground unless they are clean shaven for a respirator. Where access to outcrops is on town roads or near private homes we ask that you respect private property.

**A note on safety hazards:** Outcrops and logs may be slippery, especially if wet and lichen-covered. Outcrops are commonly steep and care is advised. Participants are asked to remain alert while on company property and obey all directives. A working railway is part of the property and vehicle activity is high.

## Regional Geology and Background

### *Trans-Hudson orogen*

The Flin Flon VMS district is situated within the southwestern Trans-Hudson Orogen (Figures 1 and 2; THO), the largest Paleoproterozoic orogenic belt of Laurentia (Hoffman, 1988). THO is the site of closure of the Manikewan Ocean (Stauffer et al., 1975) and one of a series of orogenic belts that formed during the interval 2.0–1.78 Ga during amalgamation of the supercontinent *Nuna*.

The Flin Flon belt is situated in the orogen internides of Saskatchewan and Manitoba, which are also referred to as the "Reindeer zone" by Lewry and Collerson (1990). This region preserves accreted oceanic crust and subjacent microcontinent fragments (Sask craton and East Kiseynew domain) caught during convergence of the larger Hearne and Superior cratons. Due to space limitations this guidebook cannot give a complete overview. The interested reader is referred to Corrigan et al. (2007) and references therein for a more complete overview. Additional material can be found in the numerous reports published by the Saskatchewan and Manitoba Geological Surveys.

The southwestern Trans-Hudson Orogen is a tectonic collage consisting of at least five main entities: 1) the reactivated Archean Hearne and Superior Craton margins and associated Paleoproterozoic cover sequences (Cree Lake zone and Superior boundary zone); 2) the Flin Flon – Glennie Complex (Ashton et al., 2005), an intra-oceanic assemblage composed of ca. 1.91–1.88 Ga primitive to evolved island arc, ocean floor, ocean plateau and associated sedimentary and plutonic rocks that developed during closure of the Manikewan Ocean (e.g. Stauffer et al., 1975; Syme and Bailes, 1993; Lucas et al., 1996; Ansdell, 2005); 3) the northwestern Reindeer zone, an

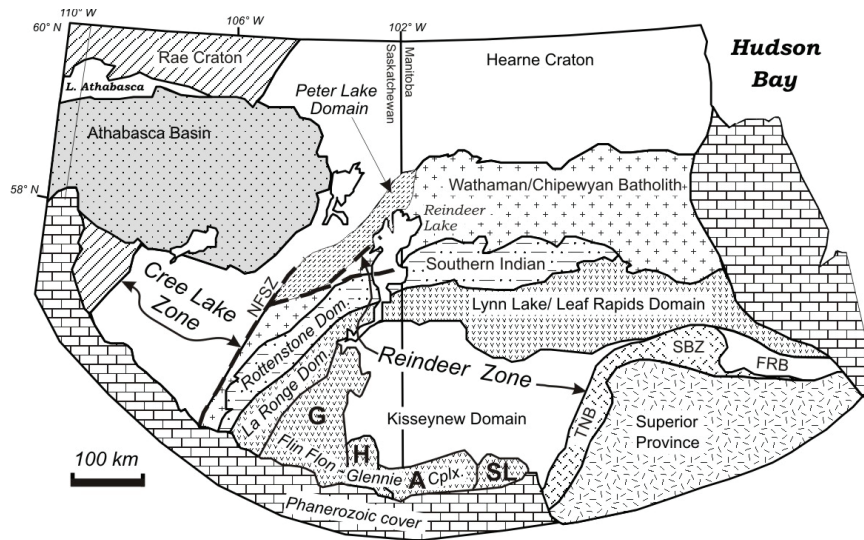


**Figure 1:** Simplified map of the Trans-Hudson Orogen showing main lithotectonic domains of the Reindeer Zone and bounding domains, after Corrigan et al. (2009). Cree Lake zone is the reactivated portion of the Hearne Craton. Abbreviations: A, Amisk Lake block; FRB, Fox River belt; G, Glennie domain; H, Hanson Lake block; NFSZ, Needle Falls shear zone; SBZ, Superior Boundary Zone; SL, Snow Lake belt; TNB, Thompson Nickel Belt.

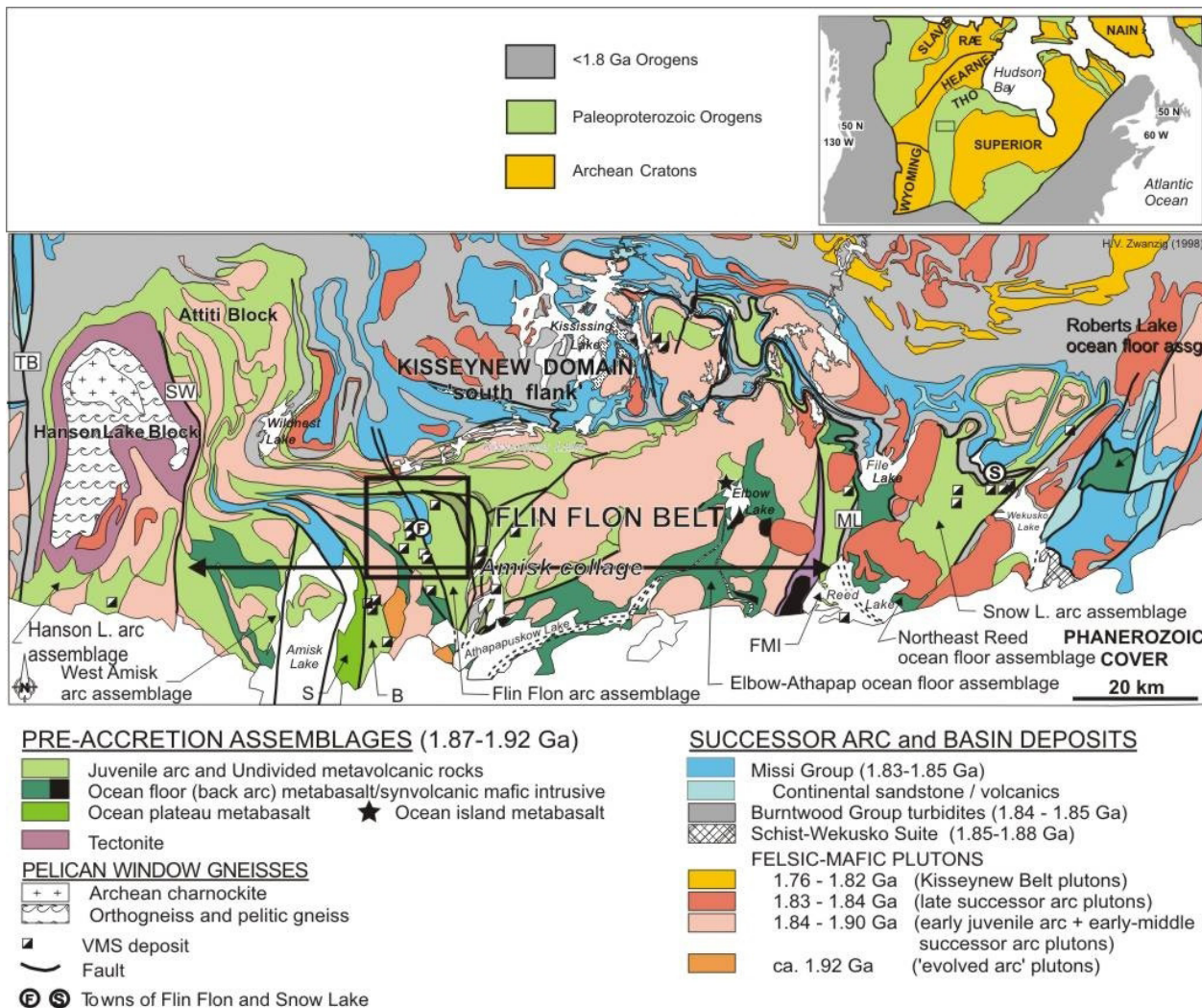


**Figure 2:** Map of the Flin Flon Belt after Galley et al. (2007, and references therein), illustrating tectonostratigraphic assemblages, the location of various accretionary assemblages, and major mineral deposits. Abbreviations: B, Birch Lake assemblage; FMI, Four-mile Island assemblage; ML, Morton Lake fault zone; S, Sandy Bay assemblage; TB, Tabernor fault zone.

accretionary orogen comprising ocean arc, back-arc, ocean crust and associated sediments, and sub-arc plutonic rocks of the 1.92–1.88 Ga La Ronge-Lynn Lake-Partridge Breast belts, pericratonic arcs that amalgamated before accretion to the southeastern Hearne Craton margin (Maxeiner et al., 2005; Corrigan et al. 2007; Kremer and Simard, 2007), 4) the ca. 1.86–1.84 Ga Wathaman-Chipewyan batholith, an Andean-type continental magmatic arc emplaced along the northwestern Reindeer zone; and 5) marginal, successor and molasse basins developed during the interval 1.85–1.84 Ga. (Hoffman, 1988; Lewry and Collerson, 1990; Lewry et al., 1990; Lucas et al., 1996, 1996; Ansdell, 2005). All were penetratively deformed and metamorphosed during the late syn-collisional stage of the Trans-Hudson Orogeny, ca. 1.82–1.80 Ga (Lewry et al., 1990; Ansdell, 2005).

The Trans- Hudson Orogen preserves a relatively complete tectonostratigraphic record from early ca. 2.45–1.95 Ga rift to drift sedimentary assemblages deposited along Archean cratonic margins, to formation and accretion of ca. 2.0–1.88 Ga juvenile crust, to finally 1.88–1.83 Ga post-accretion foredeep and collisional basins and successor arcs (Ansdell, 2005). The resulting wide range of preserved tectonic and magmatic settings are host to a variety of mineral deposit types. A combina-

tion of moderate overthickening, microcontinent accretion and promontory–re-entrant geometry along Superior craton (e.g., Bleeker, 1990) has fostered wide areas of greenschist to lower amphibolite metamorphic conditions and upper to mid-crustal levels favourable to VMS preservation.

### *The Flin Flon – Glennie Complex*

From east to west the Flin Flon – Glennie Complex comprises the Snow Lake arc assemblage, the Amisk collage, Hanson Lake block and the Glennie Domain (Figure 2) all amalgamated at ca. 1.87–1.85 Ga as a result of intraoceanic accretion (Lewry and Collerson, 1990; Lucas et al., 1996). The complex is host to 27 present- and past-producing VMS deposits (Table 1) now preserved in fold-repeated and thrust-stacked tectonostratigraphic assemblages, that structurally overlie the Archean to earliest-Paleoproterozoic Sask Craton (Ashton et al., 2005). The Flin Flon – Glennie complex developed through five main stages (Lucas et al., 1996; Stern et al., 1999), consisting of: 1) 1.91–1.88 Ga formation of juvenile or pericratonic arcs, back-arc basins and ocean plateaus; 2) 1.88–1.87 Ga intra-oceanic accretion; 3) 1.87–1.84 Ga post-accretion development of successor arc intrusions and inter-arc basins; and 4) 1.84–1.83 Ga terminal collision stage, first with the Sask Craton at

**Table 1: Major mines of the Flin Flon-Glennie complex.\*production plus remaining resource, historical estimates not NI 43-101 compliant.**

Mine	Tonnes	Au g/t	Ag g/t	Cu %	Zn %	Discovered	Method
Mandy	125,000	3.02	60.15	8.22	11.38	1915	Prospecting
Flin Flon	62,485,362	2.72	41.28	2.21	4.11	1915	Prospecting
Sherridon	7,739,471	0.63	18.96	2.37	2.28	1922	Prospecting
Dickstone	1,077,462	1.56	9.49	3.91	2.15	1935	Prospecting
Cuprus	462,094	1.3	28.8	3.25	6.4	1941	Prospecting
Birch Lake	272,898	0.1	4.11	6.21	0	1950	Prospecting
Schist Lake	1,846,656	1.3	37.03	4.3	7.27	1947	Geological
Don Jon	79,329	0.96	15.09	3.09	0.01	1950	Geophysics
North Star	241,691	0.34	0.57	6.11	0	1950	Geophysics
Flexar	305,937	1.3	6.51	3.76	0.5	1952	Geophysics
Coronation	1,281,719	2.06	5.14	4.25	0.24	1953	Geophysics
Osborne	2,807,471	0.27	4.11	3.14	1.5	1953	Prospecting
Chisel	7,153,532	1.76	44.76	0.54	10.6	1956	Geophysics
Stall	6,381,129	1.41	12.34	4.41	0.5	1956	Geophysics
Ghost & Lost	581,438	1.2	39.09	1.34	8.6	1956	Geophysics
Anderson	2,510,000	0.62	7.54	3.4	0.1	1963	Geophysics
White Lake	849,784	0.72	27.1	1.98	4.64	1963	Geophysics
Centennial	2,366,000	1.51	26.4	1.56	2.2	1969	Geophysics
Rod	735,219	1.71	16.11	6.63	2.9	1970	Geological
Westarm	1,394,149	1.56	17.49	3.21	1.48	1973	Geophysics
Spruce Point	1,865,095	1.68	19.54	2.06	2.4	1973	Geophysics
Trout Lake	21,612,296	1.56	16.02	1.74	4.97	1976	Geophysics
Hanson Lake	147,332	1.09	137.14	0.51	9.99	1984	Geophysics
Callinan	7,773,725	2.06	24.63	1.36	4	1984	Geological
Chisel North	2,606,212	0.58	21.43	0.21	9.49	1985	Geological
777	21,903,539	2.12	26.94	2.59	4.39	1993	Geological
Konuto	1,645,691	1.99	8.91	4.2	1.63	1994	Geophysics

ca. 1.84–1.83 Ga and later, at 1.83–1.80 Ga, with the Superior Craton (Bleeker, 1990; Ashton et al., 2005). Only those parts of the complex visited on this trip will be discussed here.

### Amisk collage

The Amisk collage is subdivided into a number of distinct juvenile arc and ocean floor, island or plateau assemblages (Figure 2), all separated by faults and shear zones. From west to east these comprise the West Amisk arc assemblage, Sandy Bay ocean-plateau assemblage, Birch nascent arc assemblage, Mystic evolved arc assemblage, Flin Flon arc assemblage, Elbow-Athapapuskow ocean floor assemblage, and Fourmile Island arc assemblage. Within the Flin Flon arc assemblage, distinct juvenile arc, arc-rift and mature-arc sequences host 16 VMS deposits mined to date, including the past-producing Flin Flon, Callinan and Trout Lake mines and the present producing 777 mine (Galley et al., 2007). In general, there is an evolution from primitive arc tholeiites to evolved calc-alkaline arc rocks (Stern et al., 1995a) between 1.91 and 1.88 Ga and < 10 Ma between VMS formation and accretion (Figure 3). Although the arcs are broadly juvenile, Nd isotopic and zircon inheritance data suggest variable input from Archean crust, either via sediment recycling off-board of a cratonic margin or direct formation on rifted microcontinental fragments (Stern et al., 1995b; Pehrsson et al., 2009). Archean crust is preserved as thrust-imbricated slices interleaved with juvenile arc and back-arc, ocean floor crust (Lucas et al., 1996; Syme et al., 1999).

Following the early stage of intraoceanic accretion (ca. 1.88–1.87 Ga) continental and pericratonic successor arcs and their related basins formed on the accreted collage (Whalen et al., 1999). The Missi group, a ca. 1.85 Ga alluvial-fluvial molasse sequence of sandstone and conglomerate was deposited on uplifted and eroded rocks of the Amisk collage, contemporaneously with development of major northwest-vergent THO fold-thrust belts. Various mafic through felsic intrusive

rocks of two distinct suites of successor arc magmatism intrude the imbricated volcano-sedimentary stack (Stern et al., 1995a).

### History of Exploration

Prospecting in the Flin Flon belt coincided with the beginning of the 20<sup>th</sup> century, likely following on the work of J.B. Tyrrell of the Geological Survey of Canada in the 1890's and E.L Bruce also of the GSC from 1914 to 1918. Exploration quickly gained momentum with the construction of the rail line to Churchill that shortened the length of travel time to get into the belt (Coombe Consultants 1984). The earliest prospecting appears to have been in 1896 by a Mr. Loucks who made an expedition to Reed Lake where he staked a claim (R.C. Wallace). Prospectors travelled along the major river systems from Prince Albert and subsequently from The Pas mainly looking for gold and, in 1913, gold was discovered on the shore of Beaver Lake (now Amisk Lake) by the prospecting party of Thomas Creighton, Jack Mosher and Leon Dion (Coombe Consultants 1984). Gold showings and generally small deposits occur throughout the belt and there were several gold mines in production in the Wekusko Lake area prior to 1920 (Wallace, 1984) and later in the Amisk, Elbow, Douglas and Tartan Lake areas. The belt is also host to the New Britannia mine, which had total production of over 1.6 million ounces of gold from two periods of production (1949–1958 and 1995–2005).

The Flin Flon Belt is now of course best known for its base metal production from volcanogenic massive sulphide deposits. The first base metal mines in the belt were discovered in 1915 by the same Creighton-Mosher-Dion prospecting team who were shown what became the Flin Flon Mine by local trapper David Collins. In 1917 the Mandy Mine (Figure 4), also discovered in 1915 by another party, became the first producing base metal mine in Manitoba. Ore was transported by barge and wagons to the rail head at The Pas and then to Trail B.C. for processing. Although the world-class Flin Flon Mine was discovered in 1915 it was not put into production until 1930

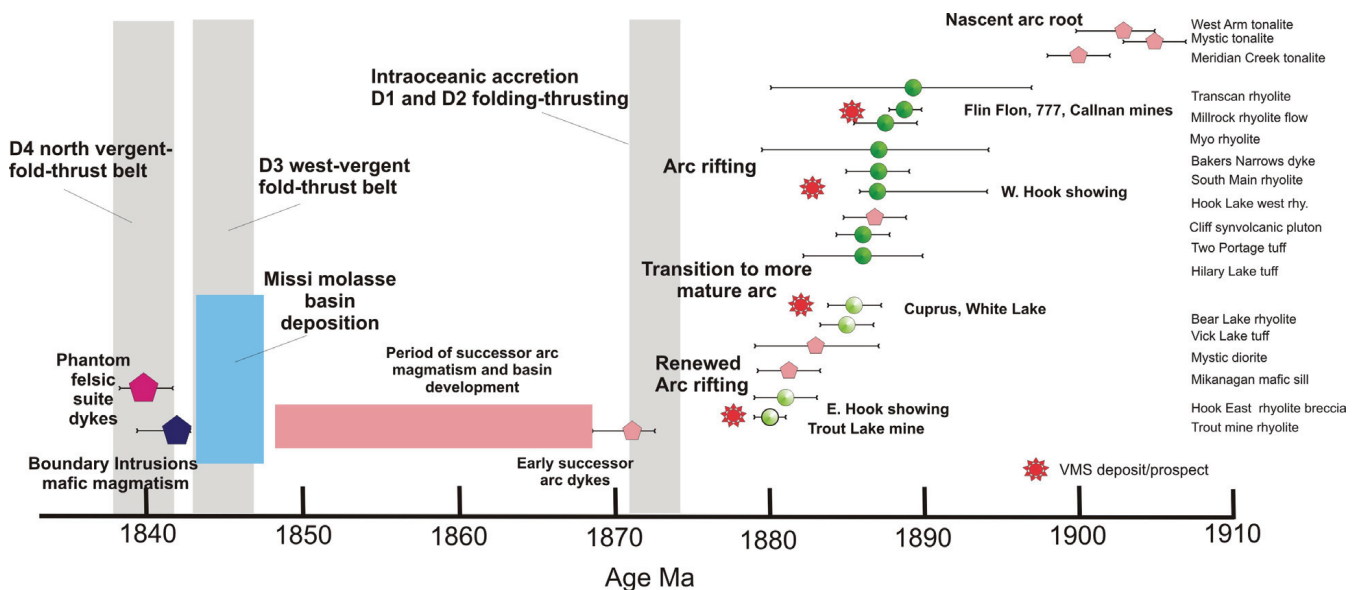


**Figure 3:** Temporal evolution of the Flin Flon district. U-Pb ages from Lafrance et al. (submitted), Rayner (2010) and Stern et al. (1995a, b), and references therein. Note VMS-forming events associated with successive phases of arc-rifting over a 10 Ma time period, and the short time frame between VMS formation and D1 accretion (ca. 8 Ma).

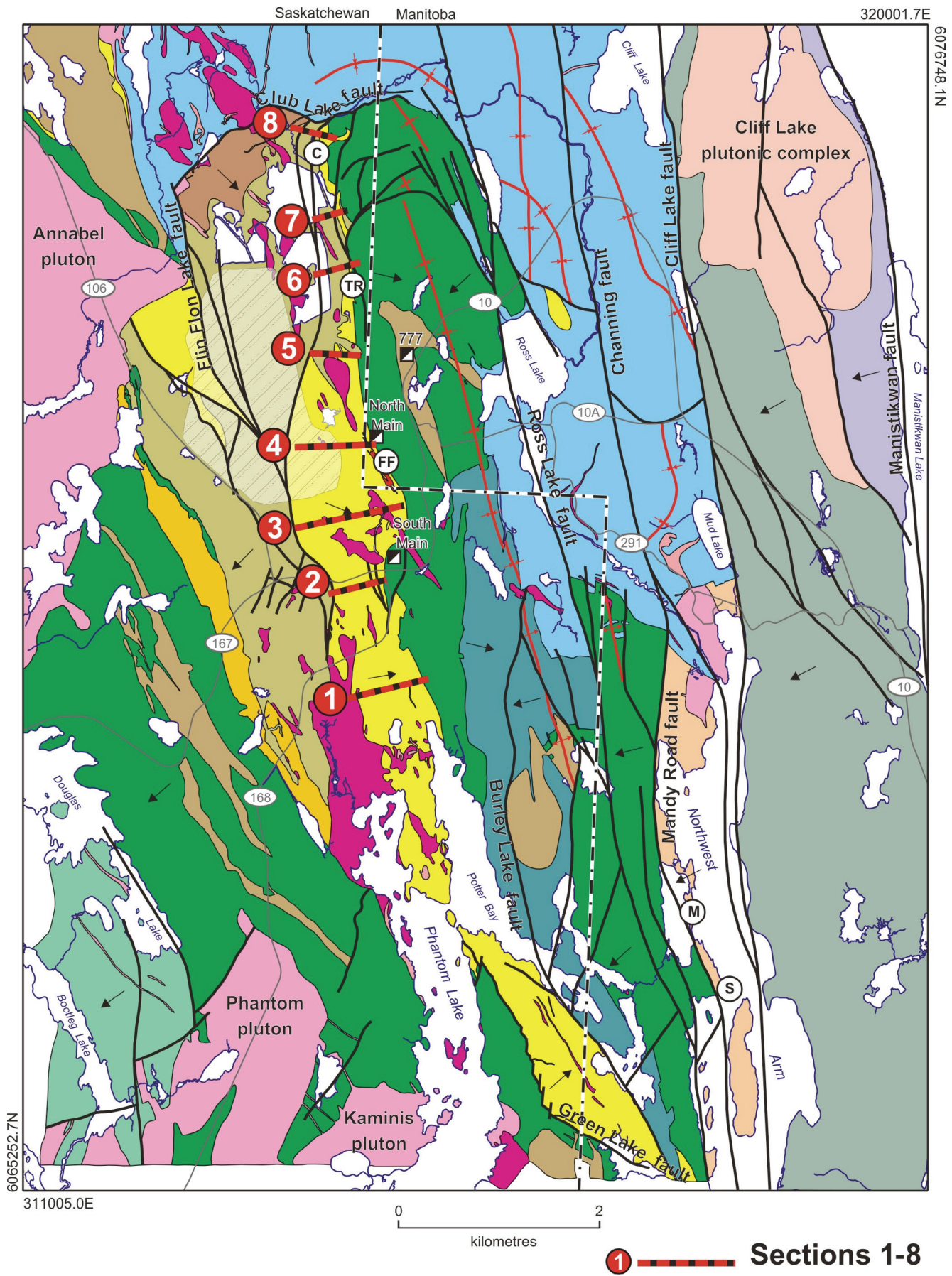
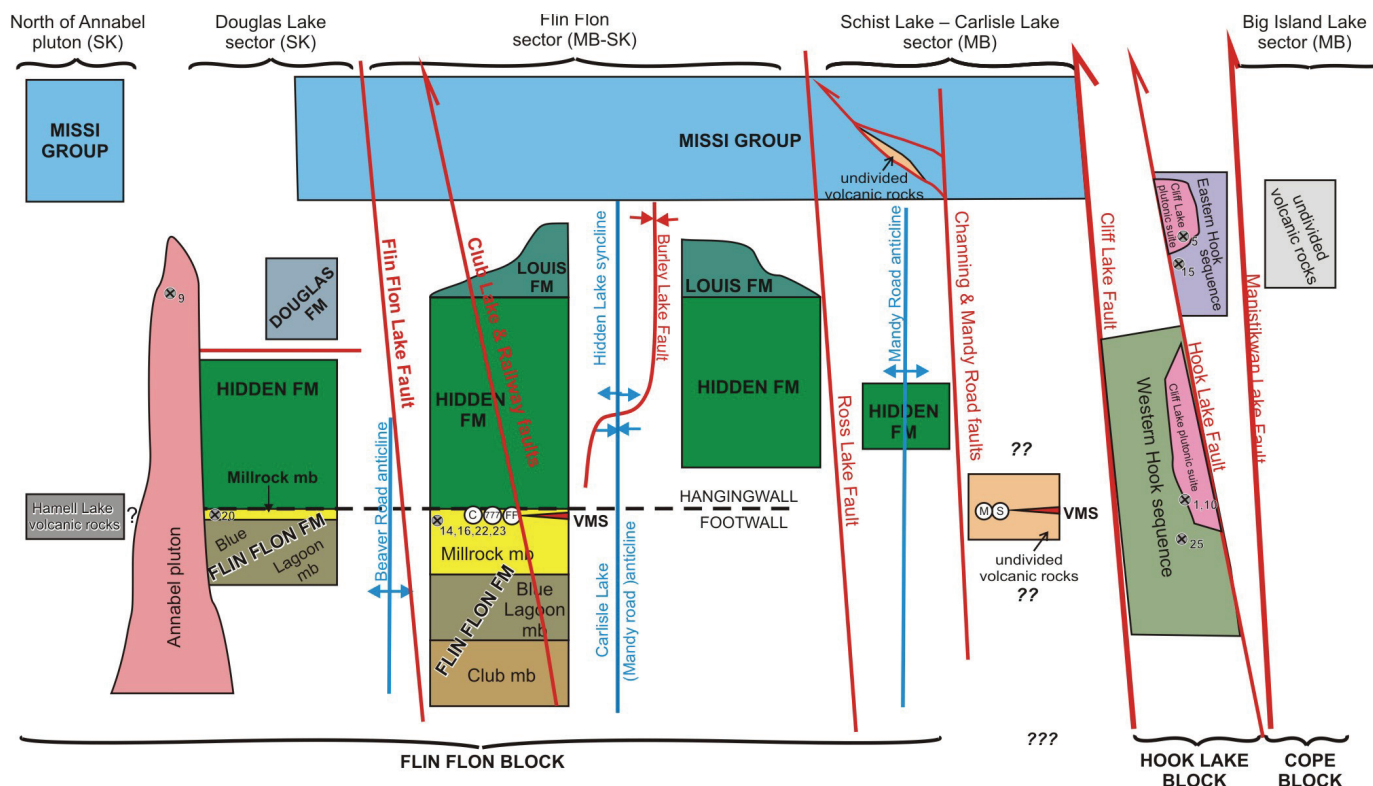


Figure 4: Geology and structure of the Flin Flon District showing the location of stops and transects. Legend as in Figure 5 with Boundary Intrusions (1842 Ma; Figure 3) in bright red (modified after Simard et al., 2010).



**Figure 5:** Schematic stratigraphic sections of the Flin Flon area (after Simard et al., 2010). For simplicity only pre-Missi folds are shown. Red lines represent faults, blue lines folds and arrows represent facing directions on either side of a given structure. Circles denote VMS deposits: C, Callinan; FF, Flin Flon; M, Mandy; S, Schist Lake (MB, Manitoba; SK, Saskatchewan).

after metallurgical problems related to the fine grained nature of the ore were solved by using flotation methods. With total production exceeding 62 million tonnes at a grade of 2.64% copper, 4.13% zinc, 2.64 grams/tonne gold and 41.49 grams/tonne silver the deposit is by far the largest in the belt.

To date there have been approximately 28 producing VMS deposits in the belt of which two, 777 and Chisel North, are currently being mined by Hudbay (Figure 2). Prospectors found 7 of the deposits prior to 1953 and the advent of electromagnetic geophysical technology. Since 1950, geophysical methods have been the dominant exploration method and sixteen mines, including Trout Lake, were found by drill testing geophysical targets.

In more recent times, the discovery of deposits, including 777 and Chisel North, are attributed to drill testing geological or structural targets in the vicinity of known mines. Although the Flin Flon mine is the largest deposit in the belt, there has been a trend to finding deposits larger than the average of 5.8 million tonnes (MT) with the Trout Lake (21.6 MT), Callinan (7.8 MT), 777 (21.9 MT) and most recently the Lalor deposit which now stands at >30 million tonnes and is in a development stage. There has also been a trend to finding the deposits at deeper depths as demonstrated by 777 and Lalor which lie at depths of 500 to 1500 meters. Much of the exploration activity has also shifted to the south, exploring under the Paleozoic cover of flat lying carbonate rocks (Figure 2). Nickel and PGE occurrences are also common throughout the belt and one nickel mine, Namew Lake, operated from 1988 to 1993, producing 2.3 million tonnes at a grade of 0.63% copper and 1.79% nickel from

a deposit under the Paleozoic cover. Exceptionally high PGE concentrations occur at the McBratney Lake occurrence where a drill hole intersected 7.3 meters that assayed 15.4 g/t Pd, 3.2 g/t Pt, 1.6% Cu, 1.2% Ni and 21.5 g/t Au. Lithium-bearing pegmatites are known and actively explored east of Wekusko Lake.

### Geology, Structure and VMS deposits of the Flin Flon District

The Flin Flon District is divisible into a >1.88 Ga juvenile, oceanic arc assemblage comprising basalt, basaltic andesite, rhyolite and synvolcanic intrusions (formerly Amisk Group; Syme and Bailes, 1993), and a <1.88 Ga assemblage consisting of calc-alkaline “early successor arc” plutons (pre-Missi intrusive rocks), fluvial sedimentary rocks of the Missi Group, and “late successor arc” intrusions such as the Boundary intrusions (Bailes and Syme, 1989; Stauffer, 1990; Stern et al., 1999). A major outcome of research conducted under TGI-1, an NSERC-Hudbay-Laurentian University CRD (supported by the Manitoba and Saskatchewan Geological Surveys) and TGI-3 was the development of an informal stratigraphy for strata of the Flin Flon District. This informal stratigraphy has, for the first time, allowed stratigraphic correlation within the district, and this has resulted in a new geological map for the Flin Flon District (Figure 4; Simard et al., 2010), which provided the basis for the new volcanic and structural reconstructions presented herein (Gibson et al., 2009a, 2011). Strata within the Flin Flon block were subdivided into four informal and conformable formations which, from oldest to youngest, include the Flin Flon, Hidden, Louis and Douglas formations as illustrated in Figure 5

(Devine et al., 2002, 2003; Gibson et al., 2003a, b; 2005; 2009a, b; MacLachlan and Devine, 2007; DeWolfe, 2008; DeWolfe et al. 2009a, b; Simard et al., 2010). However, as the structural architecture of the Flin Flon District and the geometry of mapped formations have been shaped by multiple generations of folding, thrusting and strike-slip faulting it is prudent to recognize that within the Flin Flon Block, major north-north-west striking early thrust faults and late strike-slip faults have dissected the block into structural panels as illustrated in Figure 5 (Simard et al., 2010). Lithofacies within each formation can differ somewhat between panels and the correlation of units between panels cannot always be done with certainty. Thus, the description of each formation and lithofacies that follows is generalized, but details regarding lithofacies are provided, and uncertainties in stratigraphic correlation discussed, within the Stop descriptions. An idealized stratigraphic column for the Flin Flon, Hidden and Louis formations, and their members, is illustrated in Figure 6.

### Terminology

The terminology for clastic volcanic rocks is controversial, so it is important to define the terms that are being used in order to avoid confusion. Herein, the term volcaniclastic is used to describe a clastic rock composed entirely or dominantly of volcanic material and may include primary autoclastic (including hyaloclastite), pyroclastic and peperite deposits, and their redeposited, syneruptive equivalents (White and Houghton, 2006). As many primary and resedimented volcaniclastic lithofacies are difficult to distinguish, these lithofacies are classified using the same non-genetic granulometric nomenclature as proposed by Fisher (1966), Fisher and Schmincke (1984), Gibson et al. (1999) and White and Houghton (2006), which is based on the size and percentage of clasts (material >2 mm in size) relative to matrix (material <2 mm) into tuff, lapilli tuff, lapillistone and tuff breccia.

The term “*peperite*” is used with a genetic meaning according to the definition of White et al. (2000): “*peperite* (n): a genetic term applied to a rock formed essentially in situ by disintegration of magma intruding and mingling with unconsolidated or poorly consolidated, typically wet sediment”.

The term “*cryptoflow*” is used to describe high level intrusive sills that possess many of the features typical of flows, including aspect ratio, but were emplaced into unconsolidated volcaniclastic deposits just below the seafloor (Gibson et al., 2003a; DeWolfe et al., 2009a). It includes both massive and pillowed lithofacies that are characterized by peperite along the upper (and lower) contacts. The term megabreccia is used to describe coarse, block-rich, mafic volcaniclastic lithofacies in which the predominant clasts are angular to subangular blocks of massive and pillowed basalt, with lesser amoeboid-shaped and scoriaceous lapilli in a matrix comprising fine, cusped, shard-like lapilli and tuff. The coarse block of massive and pillowed basalt attain sizes of up to 50 m and can be difficult to distinguish from coherent flows. Megabreccia occupies and defines fault bounded basins, and was transported primarily as high concentration mass flows (debris flows) that were triggered by the collapse of fault scarps during or immediately following subsidence (Gibson et al., 2009a, b).

The term “*included tuff*” is used to describe inclusions of tuff within massive coherent flows or between pillows, but not within individual pillows (DeWolfe et al., 2009a). In pillowed flows, if the bedding within the tuff inclusions is well-developed and parallel to the flow contacts then the tuff is interpreted to have settled out of the water column as a suspension deposit during and after emplacement of the pillowed flow (DeWolfe et al., 2009a). If the bedding within the tuff inclusions is irregular, contorted, or absent the included tuff is interpreted to have been squeezed or injected between pillows as the flow moved over or was emplaced within unconsolidated volcaniclastic deposits (DeWolfe et al., 2009a). In the latter case the pillows may be brecciated, in situ brecciated, or veined by tuff and/or have margins composed of peperite.

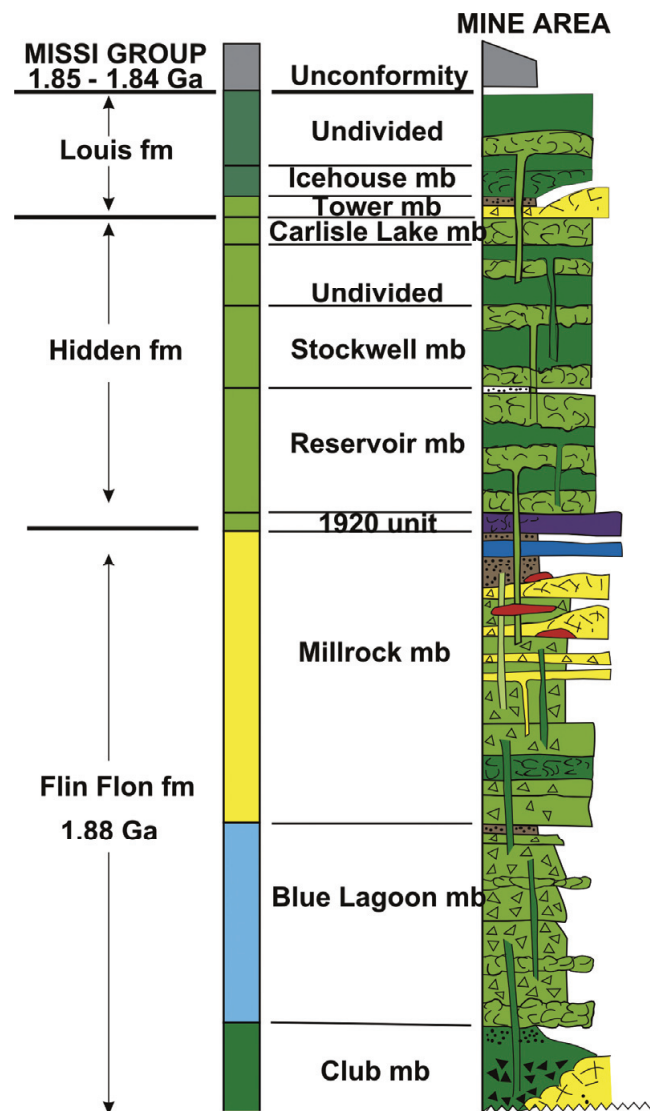


**Figure 6:** Idealized stratigraphic column showing generalized lithofacies through the Flin Flon, Hidden and Louis formations east of the Flin Flon Lake Fault and on the west limb of the Hidden Lake Syncline (after Gibson et al., 2007, 2009a). Lithofacies colour: yellow, rhyolitic lithofacies (triangles denote breccia); lighter and darker green, massive flow/sill/dike (uniform) and pillowed lithofacies (pillow masses); lighter green with triangles, volcaniclastic lithofacies, primarily megabreccia; brown, bedded tuff lithofacies; red, massive sulphide.

The term *sedimentary* is used to describe epiclastic terrigenous and chemical sedimentary rocks; the former refers to rocks composed of material derived through chemical or mechanical weathering. Epiclastic sedimentary lithofacies are classified according to the percentages of gravel, sand, silt, and clay-sized particles, as defined by Wentworth (1922). The term “*epidote-quartz alteration*” refers to round or amoeboid patches consisting of a granular mosaic of epidote and quartz with minor actinolite in mafic volcanic rocks. Epidote-quartz alteration is attributed to relatively high-temperature (>300°C, <400°C) evolved seawater-rock interaction within semi-conformable hydrothermal alteration zones associated with some VMS districts (Galley, 1993; Gibson and Kerr, 1993; Alt, 1995; 1999; Harper, 1999; Banerjee et al., 2000; Banerjee and Gillis, 2001).

The term *cauldron*, as used herein follows the definition proposed by Smith and Bailey (1968) to include “all volcanic subsidence structures regardless of shape, size, depth of erosion, or connection with surface volcanism”. Cauldron is preferred over caldera as the deformation and erosion precludes reconstructing the original geometry and size of the Flin Flon subsidence structure, and the mechanisms proposed for subsidence are not unequivocally understood.

### ***Flin Flon formation***

The Flin Flon formation is exposed on both sides of the Flin Flon Lake Fault (Figure 4, 5) and is subdivided in three mappable members, which from oldest to youngest, include the Club, Blue Lagoon and Millrock members (Figure 6; Devine et al., 2002; Devine, 2003; Gibson et al., 2003a and b; Gibson et al., 2009a).

#### **Club member**

The Club member is only exposed north and west of the tailing ponds where it occurs as a shallowly dipping, south-southeast facing succession ~500 m thick (apparent thickness; Figure 4). The Club member is truncated at its base by the Club Lake Fault to the north and it is conformably overlain by the Blue Lagoon member to the south and east (Figure 4).

The Club member consists of massive, aphyric coherent rhyolite, monolithic rhyolite breccia, and rhyolite-clast-bearing mafic volcanoclastic and bedded tuff lithofacies intercalated with lesser aphyric mafic flows. The coherent rhyolite associated volcanoclastic lithofacies are interpreted as part of rhyolite flow or dome complexes with their in-situ and transported flank breccias (Devine, 2003; Gibson et al., 2005). The associated heterolithic mafic volcanoclastic rocks are interpreted to have been derived from the proximal resedimentation of pre-existing mafic and to a lesser extent felsic volcanoclastic lithofacies and their localized accumulation within basin(s) suggests that strata of the Club member were erupted and deposited during or after subsidence. The fine, well bedded tuff is interpreted to be a product of suspension sedimentation and low-concentration density currents resulting from concomitant mafic pyroclastic eruptions that accompanied effusive mafic and felsic volcanism.

#### **Blue Lagoon member**

The Blue Lagoon member (Figure 4) is characterized by distinctly plagioclase phyric flow lithofacies (15–20 % plagioclase up to 1.2cm) and plagioclase crystal-rich volcanoclastic lithofacies. East of the Flin Flon Lake Fault, the Blue Lagoon member lies conformably on the Club member and is conformably to unconformably overlain by rocks of the Millrock member (Figure 4 and sections 5–8 in Figure 7). The base of the Blue Lagoon member is characterized by the intercalation of plagioclase-phyric pillowed lithofacies with the plagioclase-crystal-rich volcanoclastic lithofacies which suggests the latter, in part, may be transported autoclastic deposits of the former (Devine, 2003). Where the volcanoclastic units contain clasts of aphyric basalt and/or rhyolite the volcanoclastic units are interpreted to be syneruptive, redeposited deposits generated through subsidence and collapse of faults scarp walls (Devine, 2003; Gibson, et al., 2006, 2009a). The upper portion of the Blue Lagoon member is characterized by thick, heterolithic, plagioclase-crystal-rich volcanoclastic and flow lithofacies. The volcanoclastic lithofacies are interpreted as primary pyroclastic deposits, their syneruptive redeposited equivalents and /or subsidence induced megabreccias, deposited by mass flows into rapidly subsiding, fault-controlled basins (Devine, 2003; Gibson et al., 2005, 2006, 2009a, b). The Blue Lagoon member is characterized by abrupt changes in the thickness and limited lateral continuity of units indicate the presence of several distinct synvolcanic fault blocks (Figure 7). The dominance of coarse volcanoclastic versus flow lithofacies within the Blue Lagoon member east of the Flin Flon Lake Fault is interpreted to a product of extensive and long-lived, subsidence-triggered, mass-flow sedimentation (Gibson et al., 2006, 2007, 2009a).

West of the Flin Flon Lake Fault, the Blue Lagoon member is characterized by a localized thick accumulation of coarse plagioclase-crystal-rich heterolithic mafic volcanoclastic, mega-breccia, and tuff lithofacies interbedded with aphyric and plagioclase-phyric mafic flow lithofacies. The volcanoclastic lithofacies occur within synvolcanic ‘sub-basins’ in the dominantly mafic flow lithofacies and collectively define a larger subsidence structure (Gibson et al., 2003, 2006, 2007; MacLachlan and Devine, 2007).

#### **Millrock member**

The Millrock member is host to over 80 million tonnes of massive sulphide ore with average grades of 4.4% Zn, 2.2% Cu, 2.2g/t Au and 32g/t Ag within the Flin Flon, Callinan and 777 VMS deposits (Thomas, 1990). The Millrock member is exposed east and west of the Flin Flon Lake Fault (Figure 4). East of the Flin Flon Lake Fault, the Millrock member is traceable along strike for >5 km where it ranges in apparent thickness from <10m in the north to >500m in the south. Its lithofacies are discontinuous and define syn-volcanic basins that range from tens to several hundreds of metres in width (Gibson et al., 2006, 2009a). Because of this lateral variability in lithofacies thickness and extent, the Millrock member will be described for the four sections examined during the field trip: the Millrock Hill (and south), South Main, Smelter and Callinan sections (sections 2, 3, 5 and 8: Figures 4, 7).

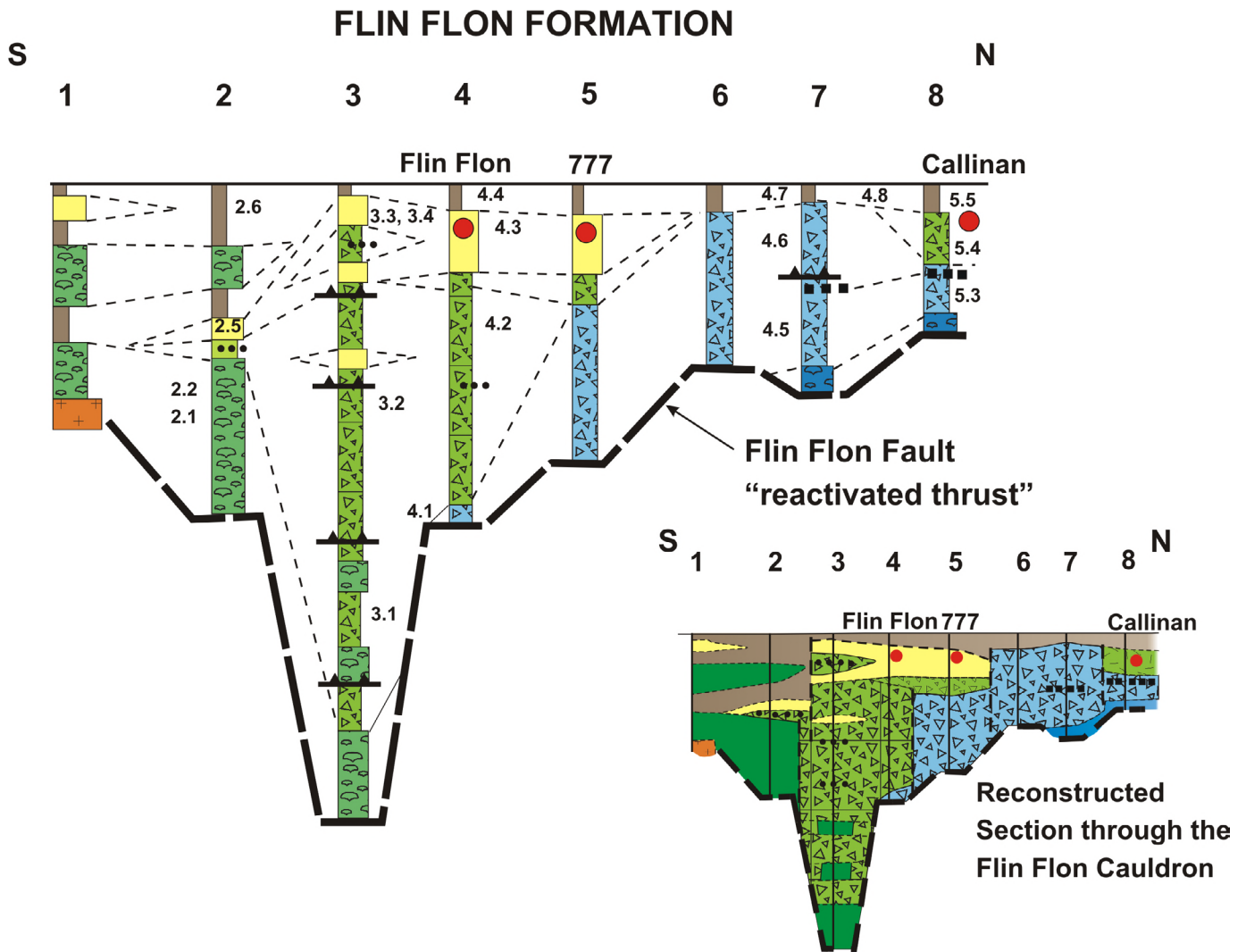


**Figure 7:** Stratigraphic sections through the Flin Flon Formation on the west limb of the Hidden Lake Syncline (excluding the Club member) showing generalized lithofacies, thrust faults and Stop locations. (after Gibson et al., 2009a; see Figure 4 for section locations). Lithofacies: dark blue and light blue with triangles, coherent flow and volcaniclastic (megabreccia) lithofacies of the Blue Lagoon member; dark green and lighter green with triangles, coherent flow/sill and volcaniclastic (megabreccia) lithofacies; yellow, coherent and breccia lithofacies; brown, bedded tuff lithofacies of the Millrock member; red circle, massive sulphide deposit; orange, Boundary intrusion. Sections represent a south to north cross section through the Flin Flon cauldron and illustrate its facies architecture.

### Mill Rock Hill Section

The Millrock member has an apparent maximum thickness of 600 m, dips moderately and faces to the east and consists, from oldest to youngest, of an aphyric to sparsely plagioclase porphyritic basaltic pillowed flow lithofacies (section 2: Figures 4 and 7). Intercalated with the pillowed lithofacies is an amoeboid breccia lithofacies that increases in abundance upwards. The amoeboid breccia facies consists of irregular to bomb-like, fluidal, amygdaloidal (up to 20% quartz amygdules) basaltic fragments with distinctly chilled margins in a finer-grained matrix composed of mm-sized, cusped, chloritized lapilli. The amoeboid clasts are intact and broken, and the breccia is crudely bedded, where beds are defined by an abrupt change in the size and abundance of amoeboid fragments; the beds are discontinuous. The amoeboid breccia lithofacies is conformably overlain and gradational into a basaltic scoria lithofacies that consists of rounded to irregular, fluidal, bomb-like clasts

within a matrix composed of mm-sized, cusped chloritic shards and finer tuff. The principal difference between the amoeboid breccia and basaltic scoria lithofacies is that the former is clast to matrix supported and intercalated with pillowed flow lithofacies, whereas the latter is dominantly matrix supported and the scoria clasts are smaller and many have a more fluidal form. The amoeboid breccia facies is interpreted to be a product of mild fire-fountain eruptions, and essentially represent submarine spatter deposits (Figure 8.1), that along with intercalated pillowed flows constructed small, low relief pillow volcanoes (Gibson et al., 2009a, b). The basalt scoria lithofacies is a product of more vigorous fire-fountain eruptions, which blanketed the pillow volcano with fine tephra and fluidal bombs (Figure 8.1 and 8.2; Gibson et al., 2009a).

The basaltic scoria lithofacies is conformably overlain by coherent, quartz-feldspar phyric rhyolite and heterolithic and monomictic rhyolite breccia lithofacies. The coherent quartz-

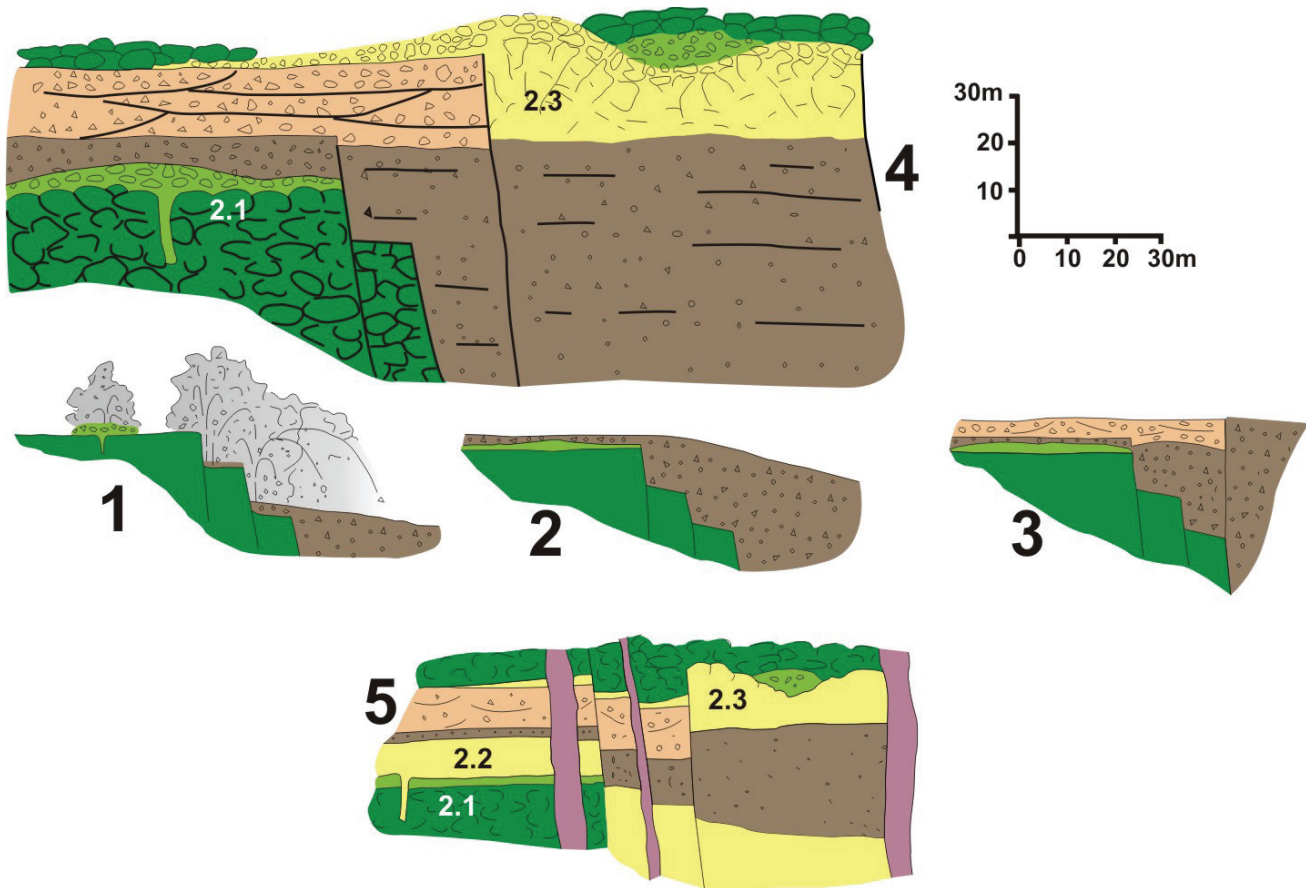


**Figure 8:** Possible reconstruction of the sequence of volcanic events (1 to 5) that produced the facies architecture of the Millrock member at Millrock Hill (after Gibson et al., 2009a). Lithofacies: dark green, pillow and lesser amoeboid breccia lithofacies; light green, amoeboid breccia lithofacies; darker brown, scoria lithofacies; lighter brown, heterolithic rhyolite-basalt lithofacies; yellow, coherent and monolithic rhyolite breccia lithofacies; dark green and light green, pillowed and amoeboid breccia lithofacies above the rhyolite belonging to the Hidden formation.

phyric rhyolite facies grades outwards and upwards into in situ brecciated, then clast rotated breccia and into monomictic, transported rhyolite breccias comprised of angular blocks of rhyolite up to 1 m in size. This transition from coherent rhyolite to rhyolite breccia is interpreted to define a coherent rhyolite dome, its carapace breccia and flank breccias produced by mass wasting (over steepening) of the dome (Figure 8.3 and 8.4; Gibson et al., 2006, 2009a; e.g. McPhie et al., 1993). The coherent and monomictic rhyolite breccia yielded a U-Pb zircon age of  $1888.9 \pm 1.6$  Ma (Rayner, 2010). More sparsely quartz-porphyrific rhyolite sills or cryptodomes occur throughout the Millrock member (Figure 8.5) and along with the coherent rhyolite flow define a rhyolitic vent area that is coincident with the older basaltic vent area that constructed the underlying pillow volcano (Gibson et al., 2009a). This was followed by faulting and emplacement of basalt dikes that are feeders for the overlying Hidden Formation basaltic flows (Figure 8.5).

### South Main Section

At South Main, the Millrock member is a moderately-dipping, east- to northeast-facing succession with a total apparent thickness, including thrust repetitions, of approximately 1000m

(sections 3 and 4 of Figures 4, 7). The base and bulk of the Millrock member consists of a thick megabreccia lithofacies and lesser coarse mafic volcaniclastic lithofacies that are locally intercalated with aphyric to sparsely plagioclase-phyric and lesser plagioclase-phyric (15–20% plagioclase) basaltic flow lithofacies (Gibson et al., 2006). The mafic volcaniclastic lithofacies, mainly tuff breccia and breccia, are characteristically monolithic, and composed of aphyric, scoriaceous, amoeboid-to fluidal-shaped basalt fragments, and more rounded, equant basalt fragments. The megabreccia lithofacies consists mainly of angular to subangular blocks, up to 10's of metres in size, of aphanitic, amygdaloidal, massive and pillowed basalt, with minor amoeboid and scoriaceous clasts in a finer-grained, tuff to lapilli tuff matrix (Gibson et al., 2006, 2009a). Volcaniclastic lithofacies composed entirely, or dominated by fluidal, amoeboid (“spatter”) and scoriaceous clasts have been interpreted as products of fire-fountain and/or strombolian eruptions (Gibson et al., 2006, 2009a). The thick, poorly sorted and crudely bedded megabreccia lithofacies, previously referred to as the Creighton member of the Flin Flon formation (Devine, 2003), is interpreted to represent subsidence-triggered, debris-avalanche deposits derived from the collapse of fault scarp walls composed of pillowed flows, and mafic volcaniclastic deposits

(Gibson et al., 2006, 2009a). Lateral variations in the thickness of megabreccia units are consistent with their emplacement by high-concentration mass flows into localized, fault-controlled depositional basins within a larger subsidence structure (Figure 9) (Devine, 2003; Gibson et al., 2006).

The mega breccia lithofacies fines upward, is intercalated with aphyric pillowed basalt flows, and is conformably overlain by coherent quartz(feldspar)-phyric rhyolite and breccia lithofacies interpreted to represent rhyolite domes and cryptodomes (Bailes et al., 2003). The rhyolite domes, cryptodomes and bedded tuff lithofacies are interpreted to define the Flin Flon mine stratigraphic interval. A coherent, quartz-feldspar phyric rhyolite dome at South Main yielded a U-Pb zircon age of  $1887.1 \pm 2.2$  Ma (sample PQB-1707-08; Rayner, 2010).

### Smelter Section

The Millrock member in the Smelter section consists, from oldest to youngest, of a monolithic basalt breccia lithofacies, a quartz-phyric coherent rhyolite and breccia lithofacies, a heterolithic breccia and tuff lithofacies, and a bedded tuff lithofacies (section 5 in Figures 4, 7). The monolithic basalt breccia facies is framework supported, crudely bedded and is interpreted to be a finer, more distal facies of the megabreccia lithofacies in the South Main section. The coherent rhyolite and breccia lithofacies is interpreted to represent rhyolite domes whereas the heterolithic breccia and tuff lithofacies are interpreted to represent carapace and flank breccias to the rhyolite flows or domes (Devine, 2003; Gibson et al., 2006; Gibson et al., 2009a; e.g. McPhie et al., 1993). The bedded tuff lithofacies is interpreted to represent the same bedded tuff as at South Main and along with the quartz-phyric coherent rhyolite and breccia, are interpreted to define the Flin Flon-777-Callinan stratigraphic interval. However, the massive base of a quartz-phyric rhyolite dome located at the Smelter section and interpreted to repre-

sent the immediate footwall to the Flin Flon VMS deposit was dated at  $1903 \pm 7/-5$  Ma, in marked contrast to the 1888 Ma age obtained from interpreted stratigraphic equivalent rhyolite domes at South Main and at Millrock Hill (sample FF92-1; Stern et al., 1999). More geochronological work is required to clarify this  $\sim 10$  Ma age discrepancy.

Within the Millrock member the coherent and volcanoclastic rhyolite units define localized “felsic volcanic centres”. Massive sulphide lenses at the Flin Flon, 777 and Callinan deposits occur principally at or near the top, but also within, below and lateral to rhyolite flow dome complexes indicating a long-lived hydrothermal event where felsic volcanism was accompanied by ore deposition (Figure 9). The bedded tuff lithofacies occurs above the massive sulphide deposits and defines the top of the Millrock member (Figures 7, 9; Gibson et al., 2007, 2009 a, b).

### Callinan Section

North of the mine site, the Millrock member constitutes a steeply-dipping, northeast-facing succession that is 10–150m thick (apparent thickness). Its uppermost unit, the bedded tuff lithofacies, is the same as that described at the previous sections and in this section its thickness ranges from 5 to 40 m. It is underlain either by Blue Lagoon volcanoclastic lithofacies (sections 6 and 7 of Figures 4 and 7) or by a massive to crudely-bedded, heterolithic mafic breccia lithofacies of the Millrock member that ranges up to 150m in thickness and is restricted to the Callinan section (section 8 of Figures 4 and 7). The base of the heterolithic mafic breccia lithofacies occupies scour channels within the underlying crystal-rich lithofacies of the Blue Lagoon member. The localized lateral extent of the heterolithic mafic breccia lithofacies is consistent with emplacement into a distinct fault-bounded basin (Devine, 2003) and the crude layering has been interpreted to suggest emplacement by mass

## VMS Ore Environment - Flin Flon Cauldron

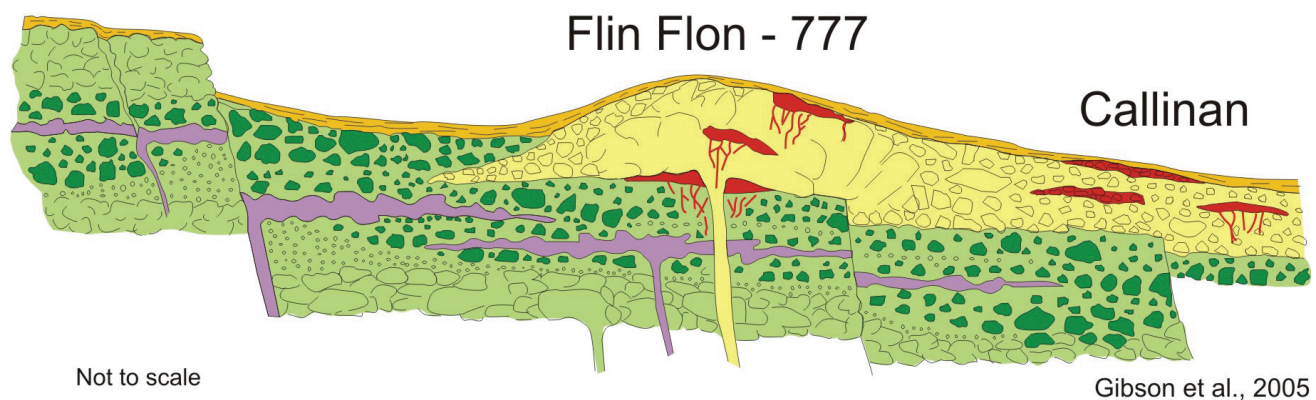


**Figure 9:** Reconstruction showing the facies architecture and volcanic environment post formation of the Flin Flon, Callinan and 777 VMS deposits (pre-hidden formation volcanism, modified after Gibson et al., 2005). Millrock member lithofacies as follows: light green with symbols, pillowed flows; light green with darker green clasts, coarse volcanoclastic and megabreccia lithofacies; lighter green with circles, scoria-rich lithofacies; purple, basalt sills (peperite on margins); yellow, coherent and monomictic rhyolite breccia lithofacies; darker yellow, bedded tuff lithofacies; red, massive sulphide.

flows into a rapidly subsiding structurally controlled basin (Devine, 2003).

The mafic bedded tuff lithofacies is dominantly ash-sized with minor lapilli-sized scoria clasts, plagioclase crystals, and beds containing accretionary lapilli (Gibson et al., 2006). The lateral continuity of bedded tuff lithofacies (along the entire strike length of the Millrock member; Figure 9), dominance of plane-parallel beds, and occurrence of accretionary lapilli support deposition by suspension sedimentation and, to a lesser extent, by low concentration density currents where the eruption column(s) at times broke the water-air interface to form the accretionary lapilli that occur within the water-lain bedded tuffs (e.g., Cas and Wright, 1987; Fisher and Schmincke, 1984; McPhie et al., 1993; Gibson et al., 1999, 2006). Local cross-bedding and scour structures are interpreted to result from bottom current reworking (Gibson et al., 2006). The bedded tuff unit represents a significant hiatus in effusive volcanism that followed emplacement of rhyolite domes and cryptodomes, and formation of the VMS deposits (Figure 9; Devine, 2003; Gibson et al., 2003b, 2009a).

#### ***Millrock member west of the Flin Flon Lake Fault***

West of the Flin Flon Lake Fault (Figure 4), the Millrock member occurs in three thrust panels. The first is located immediately west of the Flin Flon Lake Fault near the Creighton landfill site, where the Millrock member occurs as screens of monolithic and heterolithic mafic breccia, felsic tuff and lapilli tuff, and coherent to brecciated quartz-phyric and quartz-plagioclase-phyric coherent rhyolite within a “fault-bounded” mafic dike and sill complex (Bailey, 2006; MacLachlan, 2006a, b, c; MacLachlan and Devine, 2007; Bailey et al., submitted). A sample of the quartz-phyric lapilli to block breccia lithofacies (that may either represent a cryptodome or a dome) yielded an U-Pb zircon age of  $1889 \pm 9$  Ma (sample PQB07-KM157-01-01; Rayner, 2010). This age is interpreted to represent the maximum age of the breccia and is consistent with the other dated Millrock member rhyolite dome rocks except for the rhyolite dome in the Smelter section.

Stockwell (1960) and Hudbay recognized a monolithic felsic breccia lithofacies, interpreted to be Millrock member, under what is now the southeast corner of the tailings pond. Millrock member also occurs at Hilary Lake, where it consists of a thin-bedded to laminated mafic and felsic tuff lithofacies, a felsic volcanoclastic lithofacies, and remnants of an extrusive coherent rhyolite lithofacies at Myo Lake to the south (Bailey, 2006; MacLachlan and Devine, 2007; Bailey et al., submitted). A sample of the finely bedded felsic tuff lithofacies southeast of Hilary Lake yielded a U-Pb zircon age of  $1886 \pm 4$  Ma (sample PQB07-KM156-01-01; Rayner, 2010). A sample of a quartz-plagioclase phyric, synvolcanic felsic sill collected approximately 2 km southeast, near Myo Lake where it transgresses the southern extension of the felsic tuff lithofacies, yielded an age of  $1888.9 \pm 1.7$  Ma (sample 05MYO-01; Bailey, 2006).

#### ***Reconstruction***

The cross-section through the Millrock member in Figure 7 was constructed using the four sections described above, plus

four other sections as shown in Figure 4 (Gibson et al., 2009a). In order to minimize non-stratigraphic variations in thickness, the reconstruction is restricted to the west limb of the Hidden Lake syncline, and sections were located to minimize structural thickening due to thrust fault duplication (Gibson et al., 2009a). As illustrated in Figure 7, the abrupt lateral change from coherent basaltic flow lithofacies south of Millrock Hill to the thick discontinuous basaltic volcanoclastic and megabreccia lithofacies between Millrock Hill and the Smelter section is interpreted to define one structural margin of a larger subsidence structure or cauldron that hosts the Flin Flon-Callinan-777 VMS deposits (Syme and Bailes, 1993; Gibson et al., 2006, 2007, 2009a; MacLachlan and Devine, 2007). Abrupt lateral changes in thickness in the volcanoclastic and megabreccia lithofacies are interpreted to reflect their deposition within smaller fault bounded basins within the larger cauldron (Devine, 2003; Gibson et al., 2003b; 2009a). The package of coherent mafic flow lithofacies and the overlying intercalated volcanoclastic rocks and mafic flows observed south of Millrock Hill are interpreted to lie outside or inwards, along the structural margin of the cauldron (Gibson et al., 2009a, b). The Flin Flon, Callinan, and 777 deposits formed within this large, subaqueous cauldron, where they are spatially and temporally associated with the construction of rhyolite flow and dome complexes that were emplaced during the waning stage of Flin Flon formation volcanism (Devine, 2003; Gibson et al., 2006, 2009a). Millrock rhyolitic volcanism and VMS ore-formation was followed by a period of explosive basaltic volcanism from vents located primarily at, and south of Millrock Hill (Gibson et al., 2009a). The bedded tuff lithofacies that extends across the cauldron and south of Millrock Hill is a product of these eruptions. A simplified, diagrammatic illustration of the sequence of volcanic, tectonic (subsidence) and VMS ore-forming events is illustrated in Figure 10 (Gibson et al., 2007).

#### ***Hidden formation***

The Hidden formation is composed of mafic flows, sills and volcanoclastic rocks, with subordinate basaltic-andesite flows, rhyolite flows and felsic volcanoclastic rocks (Stockwell, 1960; Bailes and Syme, 1989; DeWolfe and Gibson, 2004, 2005, 2006; DeWolfe, 2008). It is divisible into four mappable units: the 1920 unit and the Reservoir, Stockwell and Carlisle Lake members (DeWolfe et al., 2009a; Figure 6). The base of the Hidden formation is placed at the last occurrence of tuff and/or rhyolite of the underlying Millrock member of the Flin Flon formation, and is marked by: 1) aphyric to sparsely plagioclase porphyritic basalt flows and/or sills of the Reservoir member; or 2) amphibole-porphyroblastic basaltic andesite rocks of the 1920 unit (DeWolfe, 2008, 2009a). Although localized, alteration associated with the Flin Flon-Callinan-777 ore system has been traced into the Hidden formation (Ames et al., 2002, 2003; Tardif, 2003).

#### ***1920 unit***

The 1920 unit occurs on the west limb of the Hidden Lake syncline (Figure 4) where it comprises aphyric Fe-Ti-P basaltic andesite cryptoflows or high-level sills (DeWolfe et al., 2009a, b).

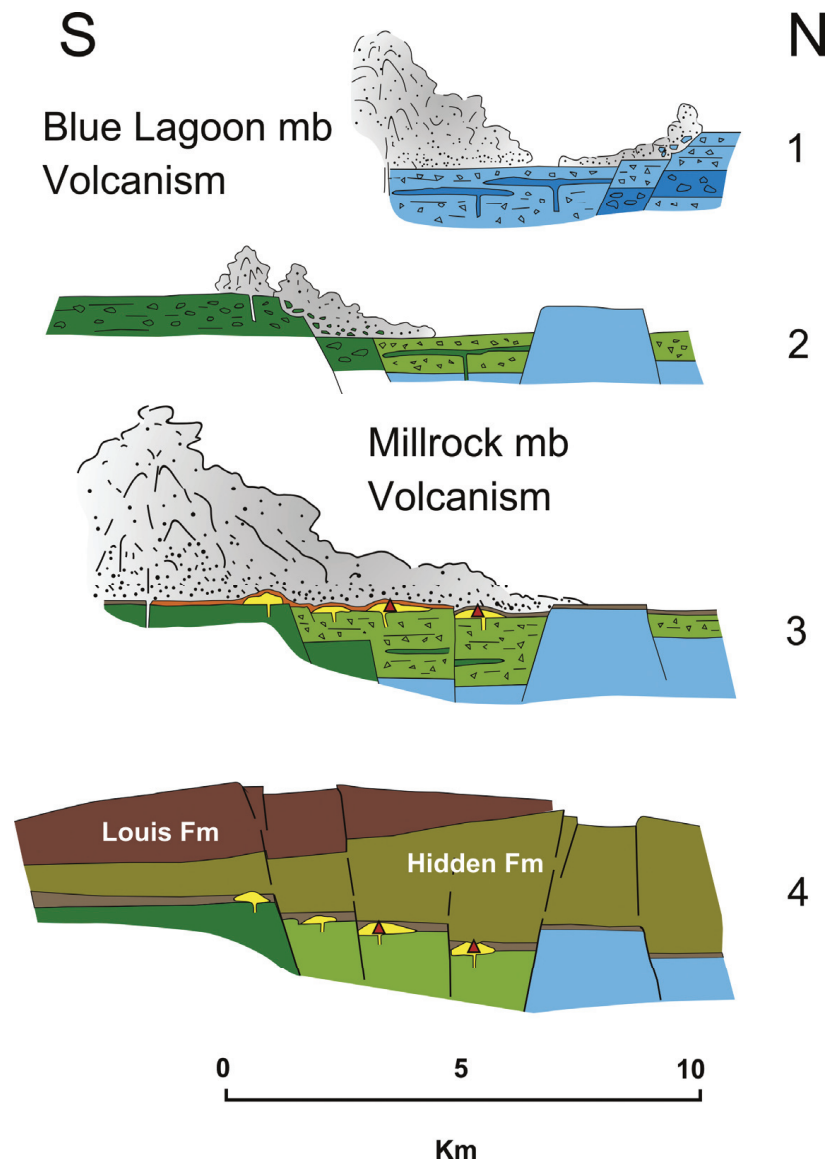


**Figure 10:** Sequence (1 to 4) of interpreted volcanic, subsidence and VMS ore-forming events (modified after Gibson et al., 2009a; legend colour scheme as in Figure 9): **1)** Localized subsidence accompanied Blue Lagoon effusive and pyroclastic eruptions. Piece-meal collapse into nested basins and redeposition of volcaniclastic lithofacies (megabreccias). Subsidence centred in the north. **2)** Initial effusive eruptions of the Millrock member constructed small basaltic lava shield on the “then” south margin of the cauldron. Piece-meal collapse in the north and along south margin triggered collapse of the lava shield to produce thick mega-breccia deposits. Collapse was accompanied by pyroclastic and effusive eruptions, within the Flin Flon cauldron. **3)** Eruption rhyolite localized to nested faults basins within the cauldron led to the construction of rhyolite flow-dome complexes. High-temperature hydrothermal discharge was localized in time and space to rhyolite dome construction to form the Flin Flon, Callinan and 777 deposits. Ore formation was followed by voluminous basaltic pyroclastic eruptions that were centred along the south margin but tephra blanketed the entire cauldron and south margin. **4)** Dominantly effusive eruption of basalt (lesser andesite) constructed the Hidden and Louis formation lava shields that buried the Flin Flon cauldron and VMS deposits (DeWolfe et al., 2009a). Lava shield construction was accompanied by localized and minor subsidence.

North of the Railway fault, the 1920 unit is easily recognisable by its abundant randomly oriented acicular amphibole porphyroblasts (25–50%) and by its light metallic blue colour on fresh surface. It forms a thick massive to pillowed aphyric basaltic-andesite cryptoflow (DeWolfe, 2008) with an approximate strike length of 1.1 km. East of the Flin Flon open-pit and south toward Phantom Beach the unit forms a thin east-facing succession with a total apparent thickness of 50–200m. Here the sills lack the amphibole porphyroblasts so characteristic in

the north; the regional “amphibole-in” metamorphic isograd runs east-west around Hidden Lake, between the two 1920 unit occurrences.

The 1920 unit, although more correctly identified as Fe-Ti basalt or Fe-Ti basaltic-andesite, has been referred to as “icelandite” in the immediate Flin Flon surrounding because of its more andesitic composition relative to surrounding basalt, and its Fe-Ti-enrichment, which resembles true mid-ocean-ridge-derived icelandite as first described by Carmichael (1967)

(DeWolfe et al., 2009b). Fe-Ti basalt or Fe-Ti basaltic-andesite in arc environments have been recognized before where they were interpreted to have been derived through the assimilation of hydrated mafic crust (older lavas) by mafic magma emplaced into shallow-level (<2 km) magma chambers in a rift environment (DeWolfe et al., 2009b; Barrie and Pattison, 1999; Perfit et al., 1999; Embly et al., 1988). Such shallow-level magma chambers are a manifestation of high-temperature rift environments that could have generated and sustained the high-temperature convective hydrothermal systems necessary for the formation of massive sulphide mineralization, like at Flin Flon (DeWolfe et al., 2009b), which make the recognition of “ice-landite-like” unit a potential VMS exploration tool.

### **Reservoir member**

The Reservoir member forms a steeply- to moderately-dipping succession with an apparent thickness of 400-800m which is folded around the Hidden Lake syncline and the Burley Lake fault. It can be traced along strike for >6 km from the Club Lake fault to the north to Phantom Lake in the south. The Reservoir and Stockwell members and the 1920 unit are thrust-repeated by a set of two north-east trending thrust faults, and the Upper and Lower Railway, and Catherine thrusts faults. East of the Flin Flon open-pit, portions of the Reservoir member are repeated along with the top of the Millrock member of the Flin Flon formation by a west-verging north-trending thrust fault. West of the Flin Flon Lake fault, the Reservoir member forms a homoclinal steeply-dipping southwest-facing sequence with an apparent thickness of >1000m.

The Reservoir member comprises aphyric, plagioclase-phyric and pyroxene-plagioclase-phyric basalt flows, with minor of volcanoclastic rocks (DeWolfe et al., 2009a). The flows are mainly massive (>70% in volume) and pillowed (>30% in volume) and contain some large lava tubes. Aphyric massive flows are usually 5–15 m thick and pillowed flows usually 10–50 m thick. The majority of flows is variably peperitic, or contains included tuff. Both massive and pillowed flows commonly show light green quartz-epidote alteration patches, usually elongated and parallel to flow contact in the massive flows, and ovoid to amoeboid in shape in the pillowed flows. Volcanoclastic rocks occur as thin, discontinuous units between flows and pillows, or included in flows (peperitic).

### **Stockwell member**

The Stockwell member occurs north of the Lower Railway fault where it forms a generally south facing moderately-dipping sequence with an apparent thickness up to 300 m that is thrust-repeated with portions of the Reservoir member and 1920 unit (Figure 4). The Stockwell member comprises massive, pillowed and breccia facies of strongly plagioclase (15–50%) and pyroxene (>5%) porphyritic basalt flows and is locally overlain by a mafic volcanoclastic unit (DeWolfe et al., 2009a).

### **Carlisle Lake member**

The Carlisle Lake member occurs between the Burley Lake fault and the Channing-Mandy Road fault (Figure 4). South of Carlisle Lake, the Carlisle Lake member forms a homoclinal

steeply-dipping west-facing sequence with an apparent thickness >800m including potential structural thickening by the Ross Lake fault. North of Carlisle Lake, on the east side of the Ross Lake fault, the Carlisle Lake member rocks are folded/faulted around the Mandy Road anticline and form an east-facing sequence >400m thick truncated to the east by the Channing-Mandy Road fault. The base of the Carlisle Lake member is truncated to the east by the West Mandy Road Fault, but the top is exposed on the peninsula between Burley Lake and Potter Bay of Phantom Lake.

The Carlisle Lake member comprises aphyric to sparsely plagioclase-phyric, plagioclase-phyric basalt flows, mafic volcanoclastic rocks, and minor amount of felsic volcanic rocks and is interpreted to represent a lateral equivalent to the Reservoir member (DeWolfe, 2008; Simard and Creaser, 2007). Where the Reservoir member is interpreted to record the onset of mafic magmatism forming the Hidden shield volcano above the Flin Flon subsidence structure, the Carlisle Lake member most likely occupies a subsidence structure on the side of the main volcanic edifice (DeWolfe, 2008; Simard and Creaser, 2007).

### **Louis formation**

The Louis formation is composed of basalt flows and mafic volcanoclastic rocks, with subordinate amount of rhyolitic flows and felsic volcanoclastic rocks (Figures 4, 7). It represents a second episode of mafic volcanism following that of the Hidden formation (DeWolfe et al., 2009a).

The Louis formation is subdivided in two members, the Tower and Icehouse members, as well as a package of undivided basalt flows (Figure 6; DeWolfe et al., 2009a). The base of the Louis formation is placed at the first occurrence of rhyolite and associated volcanoclastic rocks of the Tower member. Where the Tower member is not present, the base of the Louis formation is defined by the first occurrence of plagioclase-pyroxene porphyritic basalt flows. The top of the Louis formation is not exposed and is represented by the present-day erosion surface.

### **Tower member**

The Tower member occurs at the base of the Louis formation and consists of massive to in situ-brecciated, aphyric or sparsely plagioclase- and quartz-phyric rhyolite overlain by, and locally underlain, by mafic tuff (DeWolfe et al., 2009a). Where the coherent rhyolite portion of the Tower member is not present, the member is defined by a laterally extensive mafic tuff which includes lapilli-tuff beds containing rhyolite fragments derived from the coherent rhyolite portions (DeWolfe et al., 2009a).

The coherent portion of the Tower member rhyolite occurs near the northern extent of Louis and Burley lakes. The rhyolite is interpreted to have been emplaced as a flow or dome with associated autoclastic breccias, and marked the onset of a new magmatic episode in the hangingwall of the Flin Flon-Callinan-Triple 7 VMS deposits (DeWolfe et al., 2009a).

### Icehouse member

The Icehouse member occurs on the east side of the Burley Lake fault where it forms a steeply-dipping, east-facing sequence (25–100 m thick) of strongly plagioclase-pyroxene-phyric basaltic, pillowed to massive flows and mafic volcanoclastic rocks near the base of the Louis formation. From north to south the Icehouse member changes from a thick (~100 m) single facies massive flow to a thin (~25 m) multi-facies flow with a massive bottom and a pillowed top (DeWolfe et al., 2009a). There is a gradational contact along strike where the massive facies grades into pillowed facies over a distance of 1–2 m. Finely laminated epidote-quartz-altered mafic tuff commonly occurs between the pillows. The upper margin of the pillowed facies of the Icehouse member is irregular and broken, with a gradation over a distance of 1 m from intact pillows to pillow breccia to an overlying volcanoclastic facies.

North of Louis Lake, the massive facies is overlain by a plane-bedded mafic tuff or a mafic lapillistone. The mafic tuff is  $\leq 2$  m thick and is strongly silicified. West of Louis Lake, overlying the pillowed facies, is a 20 m thick, normally graded, crudely bedded, heterolithic volcanoclastic unit.

The massive Icehouse member flow is interpreted to have formed from the ponding of lava within an inner fault-bounded graben parallel to the feeding fissure (DeWolfe et al., 2009a). Where it grades laterally and vertically from massive facies into pillowed facies as the flow becomes thinner is likely the result of the flow overriding the wall of an inner graben that ponded the Icehouse member flows to the north (DeWolfe et al., 2009a).

### Undivided Louis formation rocks

The undivided rocks of the Louis formation account for >90% of the formation, and are present on both sides of the Burley Lake fault. They consist of aphyric to sparsely plagioclase-phyric, plagioclase-phyric, and plagioclase-pyroxene-phyric massive and pillowed basalt flows intercalated with subordinate amount of mafic volcanoclastic rocks (DeWolfe, 2008). West of the Burley Lake fault, the undivided Louis formation rocks sit conformably over either mafic volcanoclastic unit of the Icehouse member, mafic tuff of the Tower member, or aphyric flows of the Reservoir member, Hidden formation. On the east side of the Burley Lake fault, they rest directly on aphyric flows of the Carlisle Lake member, Hidden formation. The top of the undivided Louis formation rocks occurs at the present-day erosion surface.

### Structure and Metamorphism

Six ductile deformation events  $D_1$  to  $D_6$  are recorded in rocks of the Flin Flon mining district (Lafrance et al., in press).  $D_1$  and  $D_2$  occurred during intraoceanic accretion of the Flin Flon arc to other volcanic terranes prior to the emplacement of a suite of ca. 1872 Ma gabbroic dikes (Figure 3; Rayner, 2010) and deposition of the Missi Group as a cover sedimentary sequence unconformably on volcanic basement. The basement volcanic rocks were folded and possibly faulted during the development of the  $D_1/F_1$  Burley Lake syncline, and were refolded by the NNW-striking  $D_2/F_2$  Hidden Lake fold system, comprising the prominent Beaver Road anticline, Hidden Lake syncline, and

Mandy Road anticline. The  $F_1$  Burley Lake syncline is a faulted syncline that lacks the weak axial plane cleavage that is associated with the  $F_2$  Hidden Lake fold system.

During  $D_3$ , the development of a fold-thrust system, possibly in response to the final accretion of the Flin Flon terrane to the Glennie terrane, produced west-verging, map-scale folds (Pipeline, Mud Lake and Grant Lake synclines) within stacked, east-dipping, thrust sheets of basement and cover rocks bounded by NNW-striking thrust faults (e.g. 1920 fault). Because  $D_3$  and Missi deposition are both bracketed between ca. 1847 Ma, the age of the youngest Missi detrital zircon, and ca. 1842 Ma, the age of crosscutting Boundary intrusions (Figure 3), uplift and erosion of the basement, and deposition of Missi sediment must have occurred early during  $D_3$  with the Missi basins quickly thereafter deformed during migration of the  $D_3$  orogenic front.

Collision of the amalgamated Flin Flon-Glennie complex with the Sask craton began as the intervening stretch of oceanic crust between the two microcontinents disappeared through subduction beneath the Flin Flon-Glennie complex. This  $D_4$  collisional event produced N-directed thrust faults (Club Lake, Railway, Catherine faults) and east-trending folds (Flin Flon Creek syncline) that truncate the early west-directed fold-thrust system.  $D_4$  was broadly coeval with but outlasted the emplacement of ca. 1840 Ma Phantom Lake dikes. A strong, SE-plunging, stretching lineation formed during thrusting, and the axis of pre-existing regional folds were rotated into near-parallelism with the lineation, deforming the  $F_3$  Pipeline syncline into a km-scale sheath fold.

The first penetrative regional cleavage ( $S_5$ ) formed during  $D_5$ .  $S_5$  is a continuous chloritic foliation that wraps around flattened pillows and volcanic fragments in basement volcanic rocks, is defined by the flattening of pebbles and cobbles in conglomerate, and occurs as a disjunctive to continuous cleavage defined by insoluble opaque material, white mica, and chlorite cleavage planes in sandstone and conglomerate matrix.  $S_5$  strikes NW–NNW (320–350°) and dips moderately to steeply (50–80°) to the NE. It transects the axial plane of regional  $F_3$  and  $F_4$  folds in the Missi cover rocks and is associated with dextral reactivation and shearing of  $D_3$  thrust faults and lithological contacts near the hinge and along the NW-striking limbs of the Hidden Lake syncline. A strong SE-plunging, stretching lineation is associated with  $D_5$  shear zones. It is interpreted as a composite lineation that represents the total finite strain during  $D_4$  and  $D_5$ , that is, it initially formed during  $D_4$  and then was rotated and intensified during  $D_5$ .

The last regional ductile structures in the Flin Flon mining district formed during  $D_6$  during terminal closure of the Manikewan Ocean and collision of the Sask craton and Flin Flon-Glennie complex with the Superior craton at ca. 1.83–1.79 Ga. ESE–WNW compression during  $D_6$  produced a second, regional, NNE-striking cleavage and reactivated E-striking  $D_4$  thrust faults as dextral shear zones and NW-striking lithological contacts,  $D_3$  thrust faults and  $D_5$  dextral shear zones as sinistral shear zones.

### 3D Architecture of the Flin Flon District

A key component of the Flin Flon Targeted Geoscience Initiative-3 project was development of a ‘3D knowledge cube’

of the Flin Flon mine camp. The ‘cube’ is a model built from serial lithostratigraphic and fault surfaces represented in 3D space that also contains the background drill hole and map constraints. The 3D modelling experiment was designed to test new methods of 3D data analysis and integration (Schetselaar et al., 2010), as well as testing existing structural models for extension of the mine horizon at depth.

The 3D geological model (Figure 11) was created from integrated analysis of drill core, mine and surface geological maps and new 2D and 3D seismic data (Schetselaar et al., 2010). Evaluation of the topology of the 3D lithostratigraphic surfaces and numerous shear zones and thrust faults suggest that the Flin Flon mine camp is underlain by an E-dipping stack of thrust imbricates formed by pre- to post-Missi Group  $D_{1-3}$  deformation events. The dominantly east-dipping stack, although still controlling the overall geometry at depth, was subsequently deformed by E-trending  $D_4$  ductile thrust faults that internally imbricated the Missi metasedimentary rocks and overthrust juvenile Flin Flon arc assemblages on top of younger Missi Group rocks with a northerly vergence.

The VMS-hosting Millrock member has been stacked on at least four structural levels due to a combination of the two phases of west-directed thrusting and the latest north-directed thrusting. This has enhanced the VMS potential in the footwall and hangingwall of the orebodies where both thrust systems intersect, by bringing Millrock member prospective units to shallower depths. Drilling in the footwall of 777 mine, underpinned by this new model, lead to the recent discovery of a new Zn-rich ore lens, termed the West zone (Malinowski et al., 2008; Pehrsson et al., 2009). The Millrock member and contained ores have furthermore formed a detachment surface at the broad scale relative to the more competent Hidden and Blue Lagoon mafic volcanic sequences.

Thrusting within the Missi cover has also enhanced exploration potential as it brought discrete thrust slices of Flin Flon arc assemblage rocks up into the basin. These slices host the known Lakeview Cu-Zn showing which outcrops and recently discovered mineralization contained within a wholly blind panel 100’s m below the basin (Pehrsson et al., 2009). Late N-trending brittle-ductile subvertical faulting, in part reactivating

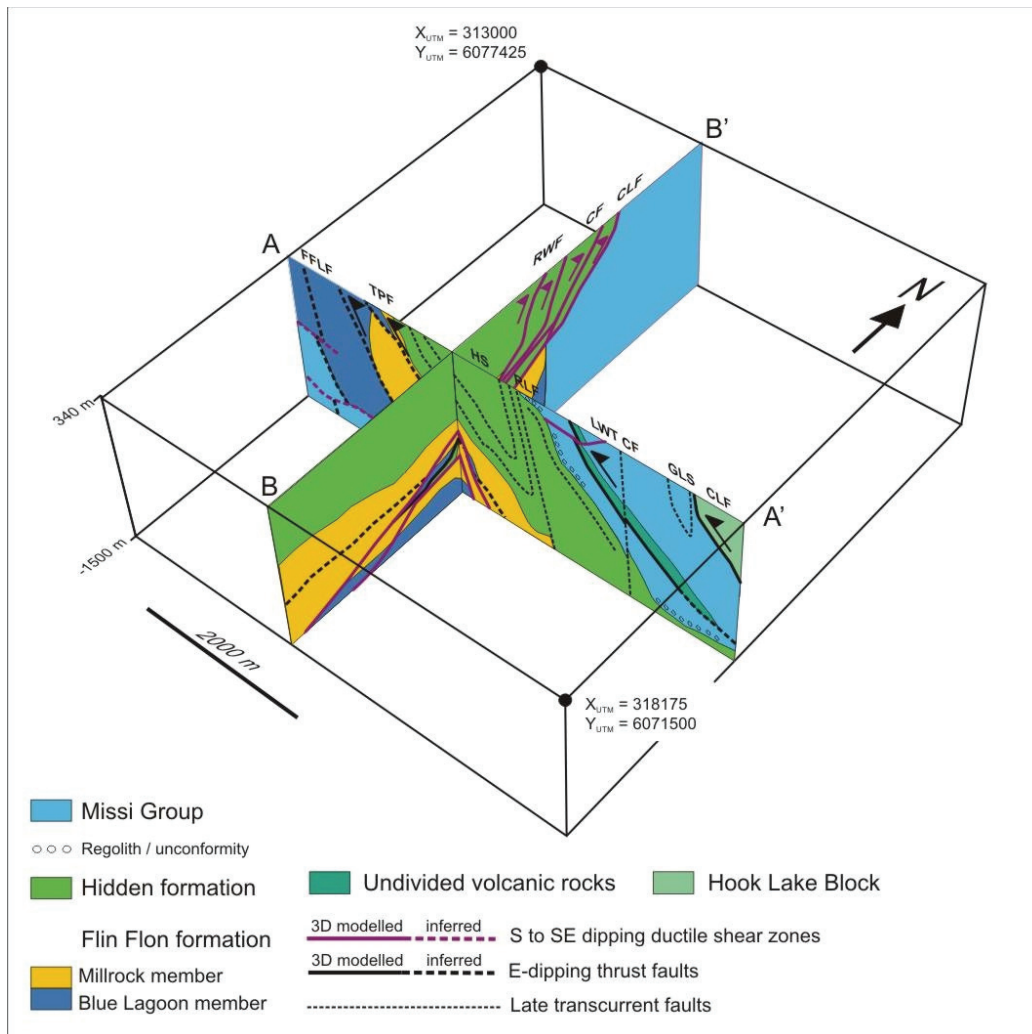


**Figure 11:** 3D block diagram of the Flin Flon mine camp showing modelled and inferred lithostratigraphic units and faults on E–W (A–A’) and N–S (B–B’) sections (after Schetselaar et al., 2010). Abbreviations: CLF, Club Lake fault; CF, Catherine fault; RWF, Railway faults; FFF, Flin Flon Lake fault; TPF, Tailings pond faults; LWT, Lakeview thrust; CF, Channing fault; CLF, Cliff Lake fault; HS, Hidden syncline; GLS, Grant Lake syncline.

older west-vergent thrusts, has further segmented the imbricate stack, complicating the correlation of lithostratigraphic successions across them.

## Stop Descriptions

During Days 1 through 3, variations in the lithofacies and volcanic architecture of the Flin Flon District, as well as a key structural features and their timing, will be demonstrated by examining seven stops through the Flin Flon stratigraphy as illustrated in Figures 4 and 7. However, the first two stops (stop 1) include the Meridian-West Arm shear zone and the Missi unconformity. The next four stops are sections through lithofacies that comprise the Flin Flon formation and, in particular the Millrock member, which demonstrate evidence for synvolcanic subsidence and that exhibit primary volcanic and deformational features. The first Stop is the Millrock Hill section (Stop 2) followed by the South Main (Stop 3), Smelter (Stop 4), Lower Callinan sections (Stop 5), and then across the Flin Flon Lake Fault to the Beaver Road Anticline section (Stop 6). Stop 6 illustrates lithofacies that are indicative of subsidence early in the development of the Flin Flon cauldron, and the role of synvolcanic faults and subsequent deformational events in shaping the Beaver Road Anticline. The Upper Callinan section (Stop 7), provides a section through basaltic and andesitic lithofacies that comprise the Hidden formation, in particular the 1920 unit, along the west limb of the Hidden Lake Syncline. Structural features, such as the Railway thrust faults, which offset the VMS-hosting Millrock member, will be examined at several key localities within Stop 7. Viewed from a larger perspective, Stops 2 through 7 provide a south to north cross-section through the lithofacies and architecture of the structurally modified Flin Flon cauldron, starting with its south structural margin at Millrock Hill and moving northward into the interior of the cauldron where numerous, nested “basins”, which comprise the subsidence structure, contain the Flin Flon, Callinan and 777 VMS deposits (Figures 4, 7, 10).

Stop 8 is an underground tour at the 777 mine and Stop 9, located on the east limb of the Hidden Lake Syncline, will illustrate volcanic- and subsidence-related features of volcanic strata in the hanging wall of the Schist and Mandy VMS deposits (Hidden formation). At Stop 10, located in the Western Hooke Lake Block, the synvolcanic Cliff Lake Pluton and a high temperature alteration zone within overlying volcanic strata are examined.

### ***Stop 1: Meridian-West Arm shear zone and the Missi unconformity***

#### **Stop 1.1 Meridian – West Arm Shear Zone**

##### ***Co-ordinates***

UTM, N 6068723, E 309684

##### ***Overview***

The structural relations between the Flin Flon, West Arm and Mystic Lake assemblages and ‘stitching’ intrusive rocks are

well exposed in the Meridian Creek area, Saskatchewan (Figure 12; Syme et al., 1996; Reilly, 1990, 1991, 1992; Thomas, 1989, 1990, 1991).

The West Arm ocean floor assemblage is separated from the Flin Flon arc assemblage by the Meridian-West Arm shear zone. The West Arm assemblage rocks are in tectonic contact with evolved arc plutonic rocks of the Mystic Lake assemblage along the Mystic Lake shear zone, which engulfs the entire Mystic Lake assemblage and rocks of the Birch arc assemblage to the west. West Arm assemblage units appear to be progressively eliminated from south to north between the Mystic Lake and Flin Flon assemblages. The timing of initial juxtaposition of these assemblages along the two shear corridors (D1), as well as subsequent syn-magmatic deformation (D2), is indicated by cross-cutting relations with various U-Pb dated intrusive rocks (Stern and Lucas, 1994; Lucas et al., 1996).

Both the Meridian-West Arm and Mystic Lake shear zones contain a SSE-striking, steeply west-dipping penetrative foliation (S1) associated with D1-D2 deformation. It is defined by the crystallographic alignment of in-equidimensional minerals (biotite, amphibole), “flattened” quartz grains and/or quartz-feldspar ribbons. Within intensely deformed units, the S1-parallel compositional layering is defined by sheared and/or isoclinally folded (i.e., transposed) quartz veins and both mafic and felsic veins and sheets (Reilly, 1991). Boudinage of veins and compositional layers occurs in both horizontal and vertical planes, suggesting that the shear zones accommodated a component of flattening strain. Many of the felsic veins (tonalite, aplite, and pegmatite) appear to have been emplaced during the ductile deformation event responsible for S1 and the transposed layering (Lucas et al., 1996). True mylonitic occur in narrow (cm-scale) ductile shear zones in both felsic and mafic intrusive rocks (Reilly, 1991). S1 is associated with a shallow to moderately SSE-plunging extension lineation (L1), generally defined by quartz-feldspar rods (polycrystalline aggregates) although locally by amphibole. Development of an L1 amphibole lineation and growth of oriented hornblende in the necks of boudinaged pyroxenite veins indicates metamorphism synchronous with D1-D2 deformation, probably related to plutonism (i.e., ‘regional’ contact metamorphism; cf. Lucas et al., 1996).

##### ***Stop description***

The Meridian-West Arm shear zone is a relatively narrow (<250 m) high strain corridor marked by greenschist-grade, foliated and lineated tectonites derived principally from the West Arm assemblage. Detailed study of the shear zone suggests a dextral component of shear along the contact between the tectonostratigraphic assemblages (Syme et al., 1996). In contrast, the West Arm assemblage transposed into a 100–250 m wide band of laminated mafic-felsic tectonite and mylonite adjacent to the Flin Flon assemblage. The felsic layers in the tectonite are derived from intrusive sheets, a feature it shares in common with in the Mystic Lake shear zone. Kinematic indicators are infrequently observed but include dextrally-extended veins, asymmetrically-extended and back-rotated boudins, and dextral C/S fabrics developed in protomylonite (Reilly, 1992, Lucas et al., 1996).

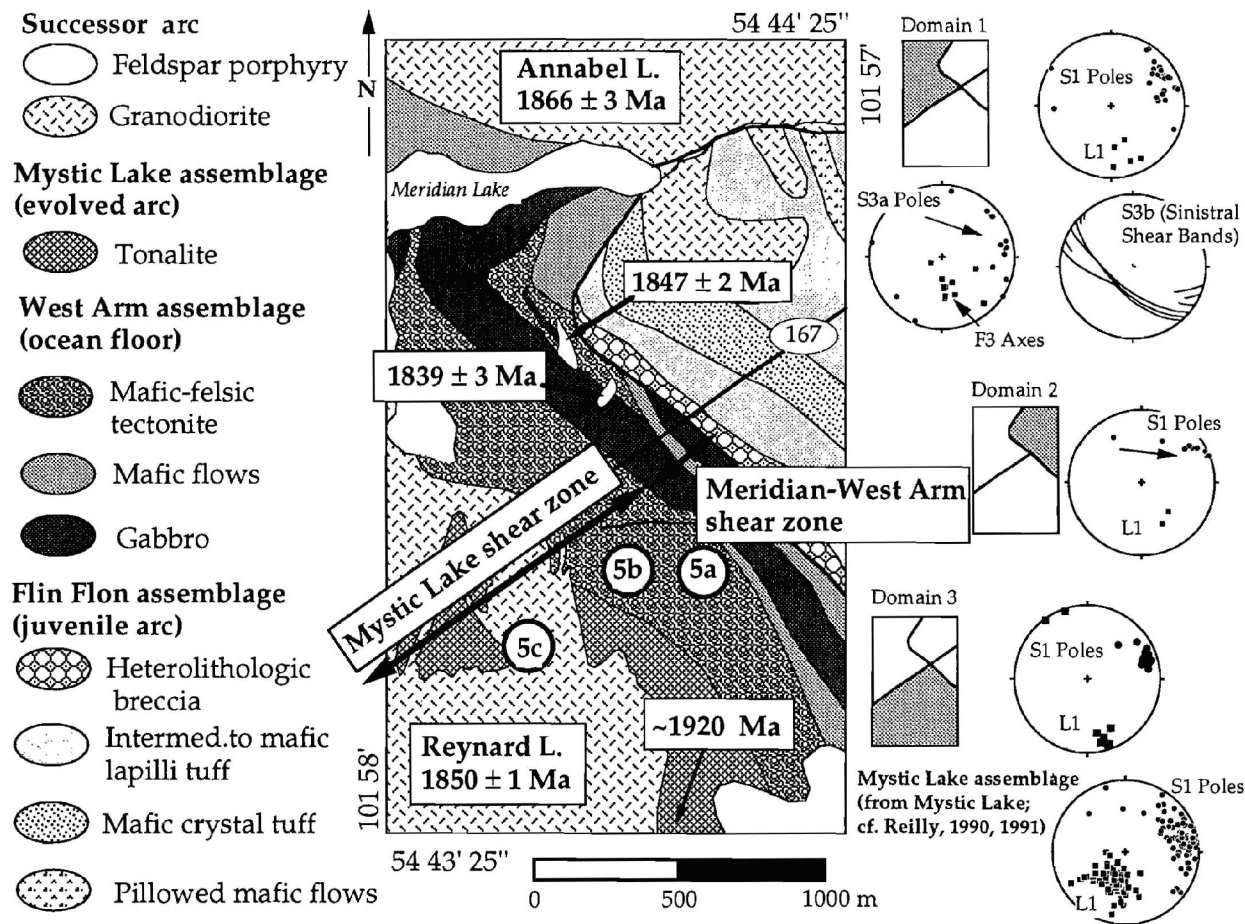


**Figure 12:** Geological map of the Meridian Creek-Hutton Bay (Meridian Lake) area (from Syme et al., 1996; after Thomas, 1990, 1992). The Meridian-West Arm shear zone includes the westernmost 50 m of the Flin Flon arc assemblage and all of the West Arm assemblage units in the map area. The Meridian-West Arm shear zone merges with the Mystic Lake shear zone in the Mystic Lake assemblage units. U-Pb age determinations are from Stern et al. (1993) and Stern and Lucas (1994). Equal area stereonet display structural data from Reilly (1990, 1991) and Lucas (pers. comm. 1996). Fabrics correlate with deformation events as follows: S1/L1 = D1-D2. Location maps for stereonet data show structural domains relative to Highway 167 and the boundary between the Flin Flon and West Arm assemblages south of Meridian Lake.

The Anabel pluton (1886 Ma ; Stern and Lucas, 1994), which cross-cuts the Flin Flon arc assemblage, the Meridian-West Arm shear zone and the tectonized West Arm assemblage of the easternmost part of the Mystic Lake shear zone (Lucas et al., 1996) provides a minimum age for the Meridian-West Arm shear zone (Thomas, 1993 and references therein). The Anabel pluton is well foliated to mylonitic within about 25–50 m of its margin; the foliation is parallel to the Meridian-West Arm shear zone foliation and probably formed during continued, post-emplacement deformation along the shear zone. Cessation of deformation along the Meridian-West Arm shear zone is bracketed by the ages of two feldspar porphyry dikes: an 1847 Ma plagioclase-phyric dike cuts across the shear zone at a low angle but contains the S1 foliation whereas an 1839 Ma K-feldspar-phyric dike cuts across the shear zone at a high angle. This result is consistent with the 1838 Ma age of the Boot-Phantom pluton (Heaman et al., 1992), which also cross-cuts the shear zone at a high-angle and does not contain the S1 foliation (Thomas, 1989).

Features to note include:

- Laminated, felsic-mafic tectonites derived from the West Arm ocean floor assemblage and syn-tectonic intrusive sheets.
- Evidence for dextral kinematics (west-side-up and to the north relative to the Flin Flon assemblage): asymmetrical-ly-extended pyroxenite veinlets with back-rotated boudins; note also that amphibole is replacing clinopyroxene.

### Stop 1.2: Missi unconformity

#### Co-ordinates:

UTM, N 6070730, E 316930

#### Overview

The Missi Group continental sedimentary rocks form a cover sequence to the 1.92–1.88 Ga tectonostratigraphic assemblages (Bruce, 1918; Ambrose, 1936; Stockwell, 1960) similar to that of the Timiskaming sequences in the Superior Province. Key features of the Missi Group siliciclastic rocks include:

- unconformable deposition on deformed rocks of the Amisk collage as well as on successor arc plutons;
- development of an oxidized paleosol (regolith) at the unconformity (Holland et al., 1989);
- removal of significant stratigraphic section along the (angular) unconformity (ca. 2 km; Bailes and Syme, 1989);
- presence of clasts derived from the 1.92–1.88 Ga assemblages (e.g., pillowed basalt, iron formation), successor arc plutons (medium- to coarse-grained granitoid rocks) and jasper (Bailes and Syme, 1989; Syme, 1987; Stauffer, 1990);
- dominated by fluvial-alluvial deposits of crossbedded and massive sandstone, with rare laminated argillite (Stockwell, 1960; Syme, 1988)
- rare trachyandesite sills (Syme, 1988)

Together, these features suggest that Missi sedimentation occurred during post-accretion arc magmatism on an uplifted and deeply incised terrain (Bailes and Syme, 1989; Stauffer, 1990), where depositional environments included alluvial fans and braided river systems. D3 structures (e.g., folds, steep belts, shear zones) and associated topography may have controlled the pattern of fluvial drainage systems and associated Missi suite sedimentation (Lucas et al., 1996). The Missi sandstone

at Flin Flon were deposited at ca. 1845 Ma, bracketed by the age of the youngest detrital zircon (1847 Ma; Ansdell et al., 1992; Ansdell, 1993) and the oldest cross-cutting intrusion (1842 ± 3 Ma Boundary Intrusion; Heaman et al., 1992). The unconformity cuts through a significant amount of basement section and is markedly angular (Stockwell, 1960; Bailes and Syme, 1989), suggesting that the basement was deformed prior to or during erosion and sedimentation, consistent with regional constraints (Lucas et al., 1996). The Flin Flon arc assemblage and Missi sedimentary cover rocks at Flin Flon were deformed and metamorphosed at greenschist to lower amphibolite grade conditions (Ambrose, 1936; Bailes and Syme, 1989; Digel and Gordon, 1995). Fedorowich et al. (1995) present biotite and hornblende Ar-Ar data that indicate peak metamorphism at 1820–1790 Ma in the Flin Flon area, coeval with regional peak metamorphism and deformation across the Trans-Hudson Orogen (e.g., Gordon et al., 1990; Ansdell and Norman, 1995; David et al., 1996).

### Stop description

The outcrop, informally called the Missi outlier (Figure 13), exposes a regolith at the unconformable contact between pillowed flows of the Carlisle Lake member of the Hidden For-

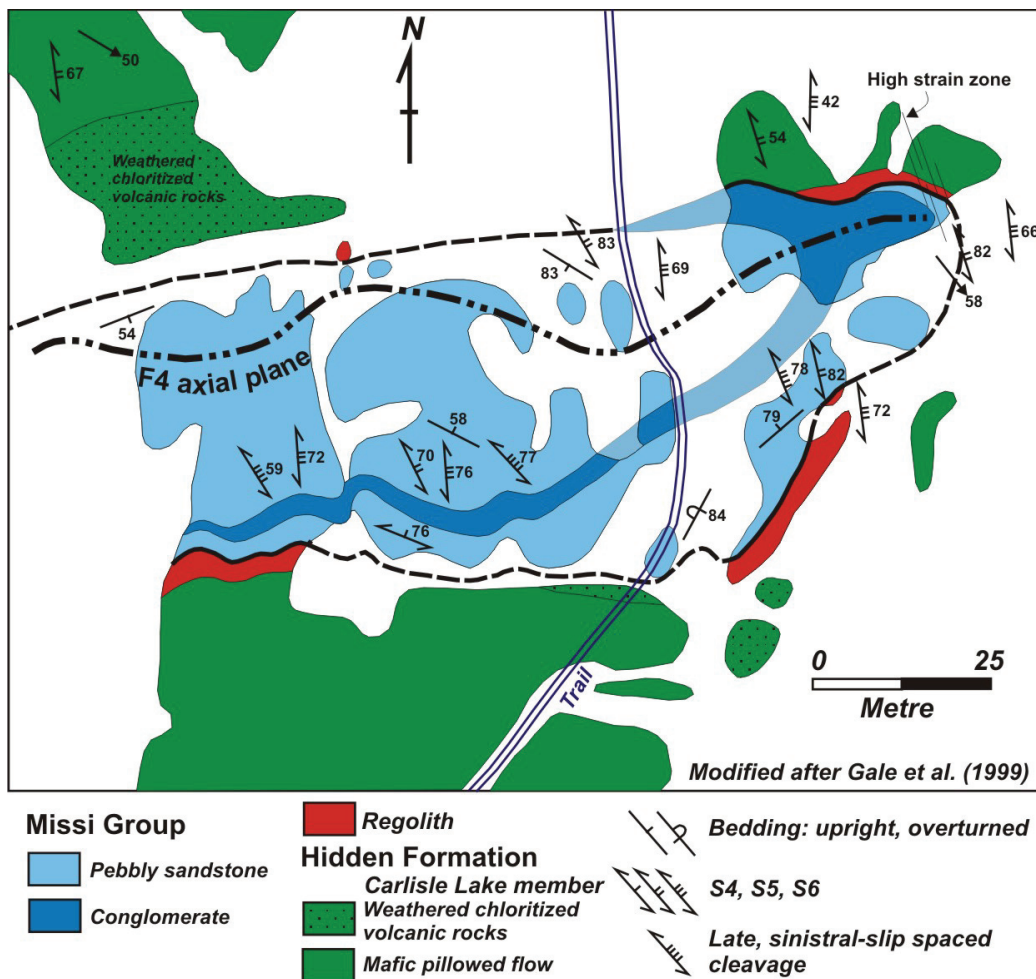


**Figure 13:** Structure of “Missi outlier”, an infolded exposure of the unconformity between Missi Group metasedimentary rocks and volcanic rocks of the Hidden formation (from Lafrance et al., accepted).

mation and fluvial conglomerate and sandstone of the Missi Group. The altered volcanic rocks that make up the regolith are strongly oxidized and red or maroon in colour up to a depth of ~ 3 m below the contact and they become pale green due to chloritization up to a depth of ~5 m below the contact (Holland et al., 1989). The regolith contains spectacular, spheroidal-weathered, pillowed volcanic rocks (corestones) with hematite Liesegang rings. The corestones decrease upward in size from the weakly weathered pillowed flow at the base of the regolith to the strongly oxidized hematite layer at the top of the regolith where they completely disappear due to the intense paleo-weathering (Holland et al., 1989).

Three generations of structures overprint the Missi outlier. The Missi outlier is folded into a tight, east-trending,  $F_4$  syncline with an axial planar, bedding-parallel  $S_4$  foliation (Gale et al., 1999). Changes in younging direction across the axial plane of the fold are given by the polarity of trough crossbeds in thick sandstone beds. The syncline is refolded by north-striking, tight to open,  $F_5$  folds, which have an axial planar, steeply-dipping,  $S_5$  cleavage.  $S_5$  varies in strike from  $330^\circ$  to  $350^\circ$  and is defined by the flattening of clasts in conglomerate. A  $D_5$  high strain with a SE-plunging stretching lineation cuts through the nose of the fold in the eastern part of the outcrop. The high strain zone and  $S_5$  are overprinted by a steeply-dipping, closely-spaced, disjunctive  $S_6$  cleavage, varying in strike from  $350^\circ$  to  $010^\circ$ .  $S_6$  is pervasive through the outlier and is dragged or refracted in sinistral fashion into a local spaced cleavage, striking  $310$ – $330^\circ$ , which is likely associated with the formation of late brittle faults.

## **Stop 2. Millrock Hill Section**

Millrock Hill is, perhaps, the most widely known and “visited” outcrop in the Flin Flon mining district. The name was derived from the coarse rhyolitic breccias that were colloquially named “Mill Rock” after the term coined by Don Sangster (Sangster, 1972) to describe coarse, felsic breccias that are typically within earshot of a mine’s mill! Millrock Hill has been mapped at various scales: Stockwell (1960) at 1:12 000 scale, Thomas (1994) at 1:5000 scale, Syme (1998) at 1:400; Price (Hudbay, unpublished map) at 1:2000 and Gibson et al. (2001) at 1:500 scale. The description and interpretations presented build upon this previous work, particularly the descriptions in Galley et al. (2002), and include results of 1:500 to 2:000 scale mapping of the on-strike extension of Millrock member lithofacies (Gibson et al., 2005, 2007, 2009a).

### **Stops 2.1 to 2.3**

#### **Stratigraphy**

A stratigraphic section illustrating lithofacies within the Millrock member of the Flin Flon formation and the Hidden formation, and location of sub-stops that will be visited at Stop 2 are shown in Figures 7 and 14. The sub-stops are described in ascending stratigraphic order and provide a complete section and description of lithofacies that comprise the Millrock member.

#### **Co-ordinates**

Stop 2.1: UTM, N 6071032, E 314395

Stop 2.2: UTM, N 6071073, E 314415

Stop 2.3: UTM, N 6071108, E 314475

#### **Stop Descriptions**

At Stop 2.1, pillowed basaltic flow lithofacies are intercalated with amoeboid breccia lithofacies. These lithofacies are volumetrically the most significant and they extend from Millrock Hill west to the Flin Flon Lake Fault. The pillowed lithofacies consist of dark green to brownish green, aphyric and subordinate feldspar phyric flows that contain up to 25% quartz (epidote)-filled amygdules, typically <5mm in size (up to 1 cm) that are concentrated toward pillow margins and are typically pipe-like in morphology and radial in orientation. The amoeboid breccia lithofacies is framework supported, and contains amygdaloidal, amoeboid-shaped fluidal fragments, and subangular blocky clasts of amygdaloidal aphyric basalt, and lesser clasts of broken and intact pillows, in a finer lapilli- to tuff-sized basaltic matrix. Within an amoeboid clast, the amygdules are concentrated toward the clast margin, which is defined by a 1–2 cm wide, rusty brown to green chilled margin that is sparsely to non amygdaloidal. The pillowed lithofacies is often discontinuous, and decreases in abundance upward. Crude bedding in the amoeboid breccia lithofacies is defined by variations in clast size, and/or by thin, pillow-thick, discontinuous flows. Irregular to lensoid, sparsely quartz phyric coherent rhyolite occurs as sills and dikes within the pillowed and amoeboid breccia lithofacies. The rhyolite is aphanitic and/or spherulitic, locally flow banded, and has sharp contacts with adjacent basaltic lithofacies.

At Stop 2.2, a 10–15 m thick, sparsely quartz phyric (<5%, <2mm) rhyolite sill has a sharp, planar, and slightly sheared lower contact with the amoeboid breccia lithofacies and is slightly discordant to stratigraphy (Gibson et al., 2001). The base of the sill is massive and weakly in situ brecciated, and the interior is massive and faintly flow banded. The upper margin of the sill is in situ brecciated (alteration around fractures imparts a pseudobreccia appearance) and locally appears pumiceous (up to 30% fine, 1mm quartz amygdules). The upper contact with the basaltic scoria lithofacies is chilled and sharp. The sill was emplaced into the mafic volcanoclastic unit at or near the contact between the amoeboid breccia and conformably overlying scoria lithofacies. The scoria lithofacies is 6 m thick at this locality but thickens abruptly, over a 150 m strike length, where it attains a maximum thickness of 30m. It consists of scoriaceous, aphanitic and aphyric, basaltic fragments in a fine, lapilli to tuff-sized mafic matrix. The scoriaceous basalt clasts have intact (unbroken) chilled margins, and a vesicle distribution that is typical of spatter (bombs) as described for the underlying amoeboid breccia lithofacies. The bomb-like shape of the clasts, their scoriaceous nature and amygdule distribution, intact chilled margins, tuff- to angular lapilli-sized matrix, absence of bedding and intercalated flows are characteristics consistent with their generation by subaqueous fire fountain eruptions (Figure 8; Devine, 2003; Gibson et al., 2009a). The abrupt lateral increase in thickness of this unit from 6 to 30 m

# Millrock Hill Section

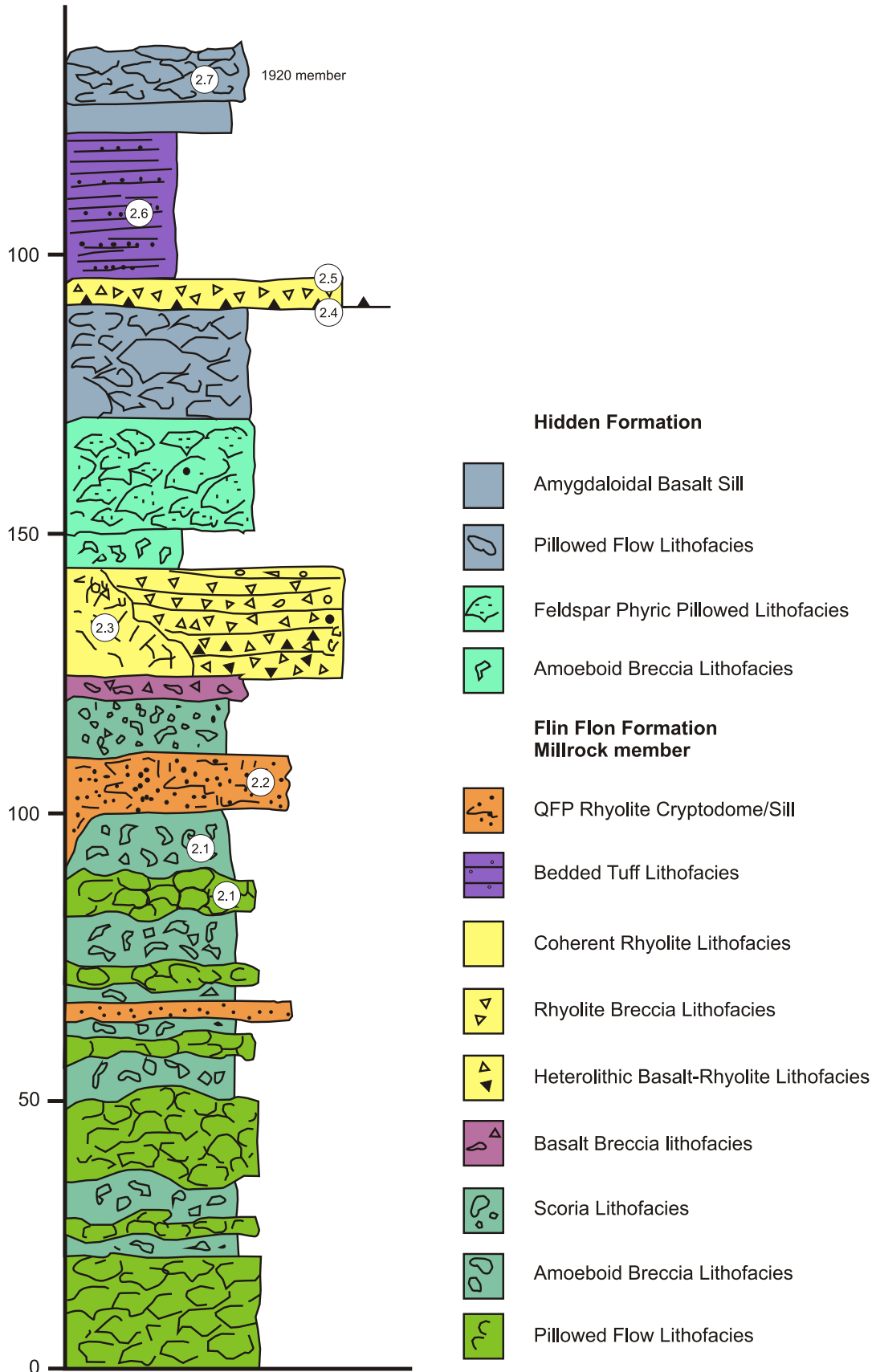


Figure 14: Idealized stratigraphic section through the Millrock member at Millrock Hill, showing the lithofacies and stop locations (Gibson et al., 2011).

indicates that this unit was erupted and deposited within a restricted, synvolcanic fault-bounded basin. Faults which bound this basin do not appreciably offset overlying units, indicating that they are synvolcanic.

The rhyolitic sill and basaltic scoria lithofacies are overlain by a 30–35 m thick unit comprised of coarse heterolithic basalt-rhyolite breccia and rhyolite breccia lithofacies. The basalt-rhyolite breccia lithofacies has a limited lateral extent (approximately 300 m) and contains abundant quartz-phyric (<3 mm, <10% quartz and or feldspar phenocrysts) rhyolitic clasts that ranges up to 2 m in size. The rhyolite clasts are typically white weathering, block- or slab-like in form, and are massive or flow banded. Some rhyolite blocks exhibit *in situ* brecciation, or have jigsaw fit fractures that are typical of blocks derived through autoclastic fragmentation (i.e., McPhie et al., 1993; Gibson et al., 1999). Subordinate, brown weathering, aphyric, mafic clasts (1–20 cm) are angular, non-amygdaloidal to scoriaceous. Clast counts indicate that the rhyolite clasts increase in size towards the top of the section (Devine, 2003). The matrix is fine-grained and mafic; the fine reddish-coloured, lapilli-sized clasts within the matrix are identical to the chilled margins of amoeboid and scoria clasts in the underlying units. Overall, the lithofacies is clast-supported, very poorly sorted, and locally displays crude bedding, graded bedding and, in one locality a large scour channel. The rhyolite breccia lithofacies conformably overlies the rhyolite-basalt breccia lithofacies and contains block to tabular clasts of quartz-phyric rhyolite (<8%, 2–8 mm quartz and feldspar phenocrysts), some of which have a jigsaw fit, or are *in situ* brecciated. This monomictic lithofacies fines upwards, has bed thicknesses <1.5m, and is neither vertically or laterally extensive. The dual mafic and felsic character of the basalt-rhyolite breccia lithofacies is interpreted to be a product of multiple sources (Devine, 2003; Gibson et al., 2006). The basalt clasts and matrix components are interpreted to have been derived from an external source (i.e., the margins of the depositional basin) and/ or from the underlying mafic volcanoclastic lithofacies. The rhyolitic clasts are interpreted to have been derived from nearby syndepositional, quartz-phyric, rhyolite flows or domes and transported by high concentration mass flows generated during periods of dome collapse triggered, perhaps, by over steepening during growth, or by mild phreatomagmatic eruptions that were initiated by or accompanied, collapse (Figure 8; Gibson et al., 2006). The occurrence of larger rhyolite clasts up section may be attributed to the increase in size and proximity of the rhyolite dome(s) over time (Devine, 2003). Rapid thickness variations of some units indicate that syn-sedimentation subsidence occurred during their deposition.

At stop 2.3, a coherent quartz phyric rhyolite flow (< 8% quartz crystal, < 3–8mm in size) weathers a distinctive yellow-white colour and is light greenish yellow on fresh surface. The coherent rhyolite ranges up to 13 m thickness and is characterized by a massive to flow-banded interior that grades outward into an inner zone of *in situ* breccia that grades outwards into an intact but clast rotated, chaotic, non-bedded breccia with lapilli-sized clasts that are commonly flow-banded and are interpreted to be a product of autoclastic fragmentation during dome emplacement and growth (Figure 8; Devine, 2003). The autoclastic breccia grades into the rhyolite breccia lithofacies, the latter was derived from the margins of the coherent rhyolite

during dome growth and collapse. The coherent rhyolite and associated volcanoclastic lithofacies thin rapidly away from the dome, and are replaced in the section by the rhyolite-basalt breccia lithofacies. The relationships between the lithofacies are obscured by folding and local fault offsets.

The heterolithic rhyolite-basalt, rhyolite breccia and coherent rhyolite lithofacies are overlain by a 150 m thick pillowed lithofacies comprised of plagioclase phyric pillowed basalt flows and up to 40 m of aphyric massive to pillowed basalt flows and flow breccias of the Hidden formation. These basalt flows differ from those of the Millrock member by their distinctive buff weathering colour, sparse epidote-quartz hydrothermal alteration, and abundance of plagioclase phenocrysts.

## Stops 2.4 to 2.7

### Co-ordinates

Stop 2.4: UTM, N 6071020, E 314600

Stop 2.5: UTM, N 6071045, E 314625

Stop 2.6: UTM, N 6071030, E 314710

Stop 2.7: UTM, N 6071156, E 314722

### Structure

The geology of Mill Rock Hill has been controversial for many years due to complex lithofacies relationships and due to overprinting deformation. The structural pattern at Mill Rock Hill is dominated by the presence of Z-shaped folds that are parasitic to the  $F_2$  Hidden Lake syncline and that are overprinted by a NW-striking, steeply-dipping,  $S_5$  foliation defined by flattened clasts in rhyolite breccias (Gibson et al., 2001; Lewis et al., 2006).  $S_5$  becomes more pronounced in a 5 to 10 metre-wide, NW-striking, high strain zone exposed along the east side of Millrock Hill. The high strain zone has a strong SE-plunging ( $35^\circ$ ) stretching lineation and it possibly originated as an early thrust fault that was reactivated during  $D_5$ .  $S_5$  is refolded by small outcrop-scale folds that have an axial plane, ENE-striking,  $S_6$  slaty cleavage.  $S_6$  becomes more intense and rotates in anticlockwise fashion within a network of northwest-striking discrete faults, suggesting that it formed during the development of this late network of  $D_6$  sinistral faults, which dissect Millrock Hill.

Stop 2.4, is located at major fault zone within the aphyric pillowed flows and intrusions of the Hidden formation. This fault zone is the continuation of the northwest-trending thrust fault that truncates the Millrock Hill syncline to the north. Stop 2.5, located immediately east of the interpreted thrust fault exposes a rhyolite breccia lithofacies, which is interpreted to be a structural repetition of the Millrock member. Further to the east, at Stop 2.6, a bedded tuff lithofacies, typical of the uppermost Millrock member, is intruded by fine-grained and aphanitic basalt sills and a younger, fine-grained felsic intrusion of the Phantom Lake series. The bedded tuff lithofacies consist of thin-bedded to laminated, to thick-bedded basaltic tuff. Scoriaceous basaltic lapilli define crude layers within some beds or occur as isolated lapilli. Fine, <5mm, round to elliptical, light coloured accretionary lapilli occur within some beds. A

pillowed lithofacies of the overlying Hidden formation (1920 unit) is exposed at Stop 2.7 (Figure 14), but is separated from the Millrock bedded tuff lithofacies by green weathering, aphanitic, and quartz-amygdaloidal aphyric basalt sills (?).

**NOTICE:** Stops 3 through 5 and Stop 7 are on the Hudbay Plant property. This area is restricted to the public and entrance requires the permission of Hudbay.

### **Stop 3. South Main Section**

In this cross section we examine lithofacies that comprise the Millrock member and the lowermost units of the Hidden formation. The traverse begins within the Millrock member approximately 500m west-northwest of the South Main shaft. All lithofacies and the location of the sub-stops are shown on Figures 7 (3.1 to 3.4) and 15. Descriptions of Stops 3.3–3.7 are modified from Galley et al. (2002).

#### **Co-ordinates**

Stop 3.1: UTM, N 6071850, E 314172

Stop 3.2: UTM, N 6071850, E 314172

Stop 3.3: UTM, N 6071633, E 314634

Stop 3.4: UTM, N 6071707, E 314731

Stop 3.5: UTM, N 6071707, E 314731

Stop 3.6: UTM, N 6071581, E 314683

Stop 3.7: UTM, N 6071401, E 314634

#### **Stop Descriptions**

At Stop 3.1 a fault occurs at the contact between a basaltic, bedded tuff lithofacies, which is typical of the uppermost Millrock member, with a megabreccia lithofacies that is typical of the basal portion of the Millrock member. The fault trends northwest, dips steeply to the east, and is crudely parallel to strata. It is interpreted to be a thrust fault that placed an “older” megabreccia lithofacies on a “younger” bedded tuff lithofacies within the Millrock member. The megabreccia lithofacies contains blocks of massive, aphyric to sparsely plagioclase phyric, amygdaloidal basalt that include intact pillows, broken pillows, massive basalt and blocks of pillowed flows that range up to 50m in size. The blocks have sharp contacts with the matrix. Irregular, intact to broken amygdaloidal, amoeboid clasts of aphyric basalt locally dominate the lithofacies and are often associated with subrounded scoriaceous basalt lapilli; the latter may define crude scoria-rich beds. The matrix consists of angular, plate-like lapilli and fine, mafic tuff. The breccias are poorly sorted, with local evidence of crude bedding and fine upwards to Stop 3.2, where the breccias consist of angular and lesser amoeboid clasts of aphyric amygdaloidal basalt and scoria. Local, discontinuous, scoria-rich beds and thin pillowed flows occur within the upper part of the finer, megabreccia lithofacies. Dikes and sills of fine- to medium-grained, variably feldspar and pyroxene phyric basalt, irregular aphyric amygdaloidal basalt, and quartz and feldspar phyric rhyolite cross cut the megabreccia as do younger Phantom Lake and Boundary intrusions. The coarse volcanoclastic lithofacies is interpreted to have been emplaced primarily as high concentration mass flow or debris

flow, derived through the collapse of synvolcanic fault scarps during episodic subsidence. The breccias define a primary synvolcanic, fault bounded sub-basin within the interpreted larger scale Flin Flon cauldron (Figure 10). The amoeboid clasts are interpreted as spatter and along with the scoriaceous lapilli may be a product of mild fire-fountain eruptions that accompanied subsidence. The thin pillowed flows intercalated with the coarse block-rich breccias are interpreted to be a product of episodic effusive eruptions that occurred within the South Main “sub-basin”.

The bedded tuff lithofacies at Stop 3.3, is located southwest of and along strike from the coherent rhyolite and breccia lithofacies that comprise the South Main flow-dome complex. It consists of rusty weathering, pyritic, thin- to medium-bedded basaltic tuff that stratigraphically overlies an aphyric pillowed flow whose base defines the top of the megabreccia lithofacies. The bedded tuff is overlain by a heterolithic, tuff lithofacies that consists of thin-bedded, mafic and felsic tuff intercalated with lapilli tuff containing quartz phyric rhyolite lapilli and lesser basaltic lapilli. The felsic lapilli were interpreted to be locally derived from detritus that was shed from the adjacent South Main rhyolite flow-dome complex (Bailes et al., 2003). This sulphide-rich bedded volcanoclastic lithofacies is considered to represent the Flin Flon mine stratigraphic interval.

At Stop 3.4, a coherent rhyolite lithofacies, of the South Main rhyolite flow-dome complex, has a thickness of 100m and consists of three facies: a lower aphyric, a middle quartz-plagioclase phyric autoclastic pumice breccia, and an upper coarsely quartz phyric flow-banded facies. The flow-dome complex is cross-cut by numerous synvolcanic mafic intrusions as well as a prominent Boundary intrusion breccia; the latter will be examined at Stop 3.5. Lower phases of the South Main flow-dome complex are well exposed in large outcrops to the northwest.

Plug and dike-like bodies of the Boundary Intrusion suite consisting of meladiorite, pyroxenite and felsic derivatives were emplaced into folded supracrustal rocks, including sedimentary rocks of the c.a. 1845 Ma Missi Group (Syme and Forester, 1977). Emplacement of these intrusions was locally accompanied by prominent brecciation of the country rocks and earlier crystallized phases of the intrusions themselves. At Stop 3.5, a Boundary intrusion breccia, cored by meladiorite, cuts sharply across the South Main rhyolite flow-dome complex and its contact with overlying pillowed lithofacies of the Hidden formation.

Stop 3.6 is located at the base of a 40(+) m thick, aphyric pillowed flow lithofacies. The lithofacies is characterized by pillows with prominent radial pipe amygdules and mega pillows up to 15m in diameter that were likely feeder tubes for the pillowed flow. The pillowed lithofacies overlies another aphyric pillowed lithofacies that also contains pillows with prominent radial pipe amygdules, but with amoeboid forms and is cross-cut by highly irregular synvolcanic dikes. The contact between the two pillowed lithofacies is traceable for 350 m along strike. At Stop 3.7, the pillows contain prominent and very photogenic radial pipe amygdules.

# South Main Section

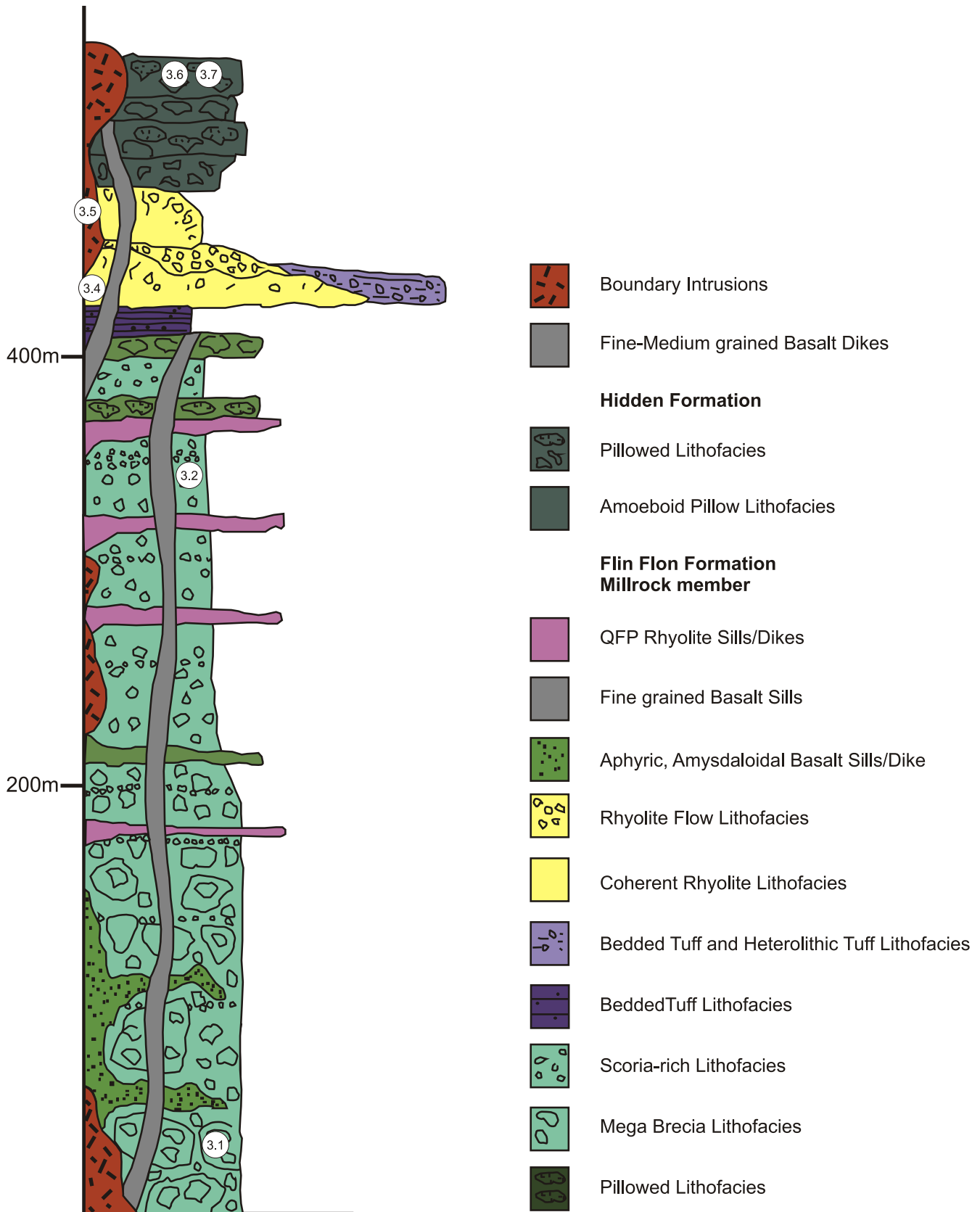


**Figure 15:** Idealized stratigraphic section through the Millrock member at South Main showing the lithofacies and stop locations (Gibson et al., 2011).

# Smelter Section

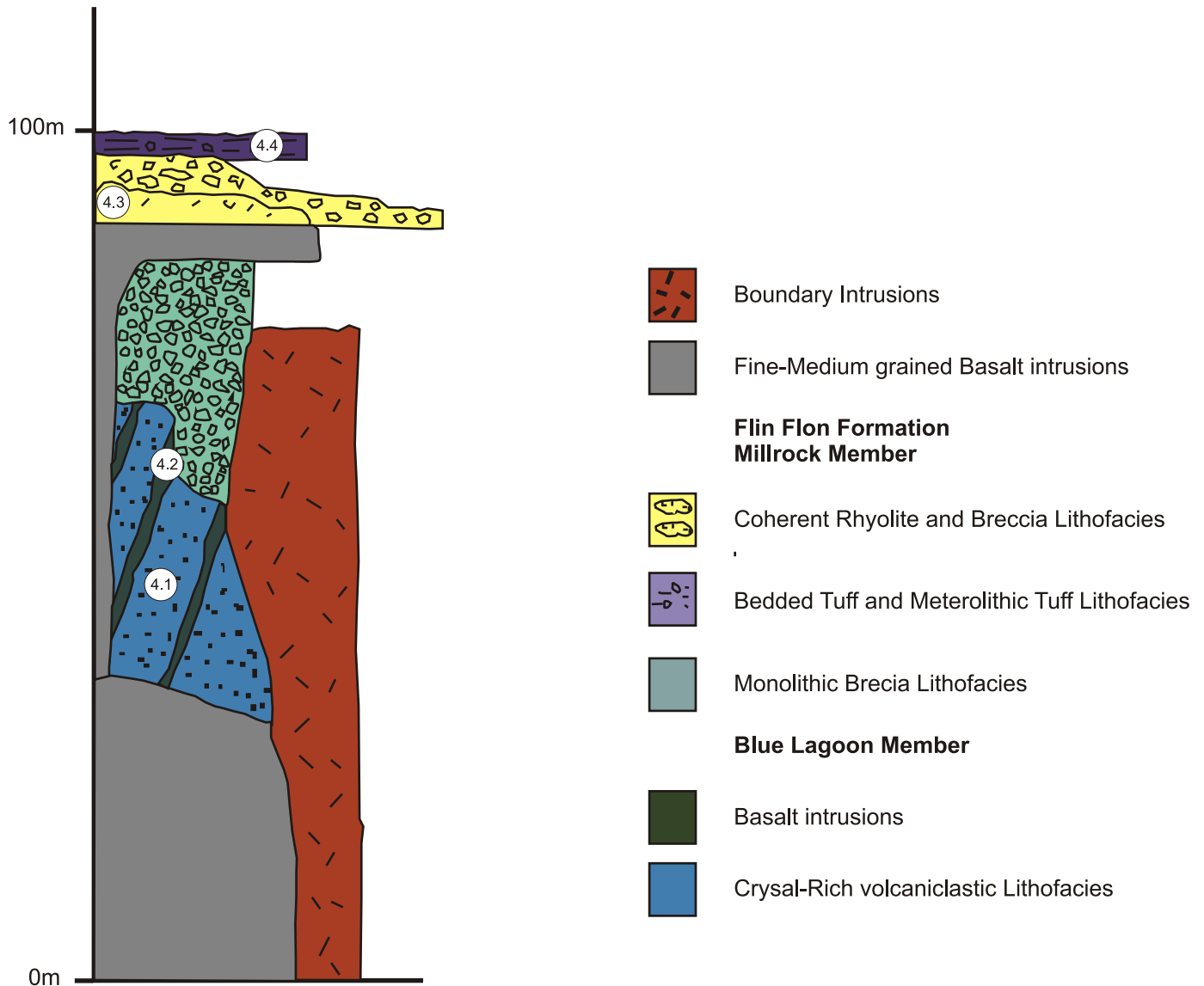


**Figure 16:** Idealized stratigraphic section through the Millrock member at the Smelter section showing the lithofacies and stop locations (Gibson et al., 2011).

## Stop 4. Smelter Section

In this cross-section evidence for an angular unconformity between the Blue Lagoon and Millrock members will be examined. Lithofacies exposed in this section and the locations of sub-stops are shown in Figures 7 and 16. Stop descriptions are modified from those of Syme et al. (1996), Galley et al. (2002), as modified by Devine (2003).

### Stops 4.1 to 4.8: Blue Lagoon member

#### Co-ordinates

Stop 4.1: UTM, N 6073524, E 314100

Stop 4.3: UTM, N 6073677, E 314217

Stop 4.5: UTM, N 6074770, E 314020

Stop 4.6: UTM, N 6074840, E 314115

Stop 4.7: UTM, N 6074780, E 314035

Stop 4.8: UTM, N 6075145, E 314090

#### Stop Descriptions

The stratigraphic succession starts with a crystal-rich volcanoclastic lithofacies of the Blue Lagoon member at Stop 4.1. The lithofacies is a thickly bedded plagioclase crystal tuff and lapilli tuff. Plagioclase crystals comprise 12–40% (>0.1–1.5 cm) of the lithofacies and primary features are obscured by recrystallization and alteration. The angular unconformity between Blue Lagoon crystal-rich volcanoclastic lithofacies and an overlying, monolithic breccia lithofacies of the Millrock member is best exposed at Stop 4.2. The unconformity surface is sharp, unfaulted and truncates bedding in the crystal

tuffs at a high angle. Thin (1 m) mafic sills in the crystal tuff and lapilli tuff are also clearly truncated at the unconformity; the dikes have chilled margins and amygdaloidal interiors. The angular unconformity is interpreted to be a product of synvolcanic faulting prior to emplacement of the Millrock member. The Millrock monolithic breccia lithofacies weathers a dark green colour, is poorly sorted and clast supported. It contains angular to subangular clasts (up to 40cm) of epidote altered, aphyric, amygdaloidal basalt (5–25 % quartz amygdules < 1cm) in a fine-grained, tuff-sized matrix. Quartz phyric rhyolite lapilli comprise <1% of the unit. The lithofacies is crudely bedded and locally displays normal grading. The aphyric amygdaloidal basalt clasts in this lithofacies are smaller but the same as those within the megabreccia at South Main; these two lithofacies are interpreted to be stratigraphically equivalent, with the monolithic basalt breccia lithofacies representing a more distal facies.

Coherent and breccia rhyolite lithofacies conformably overly the monolithic basalt breccia lithofacies at Stop 4.3 and are interpreted to define a rhyolite flow, referred to as the Mine rhyolite (Galley et al., 2002). The rhyolitic lithofacies have been traced on surface, in underground workings, and in exploration drilling for approximately 3 km. They attain a maximum thickness of 150 m northwest of the smelter complex and thin to the north and to the south. A framework-supported, monomictic breccia lithofacies composed of angular to subrounded, quartz-phyric rhyolite fragments in a finer, tuff-sized matrix occurs at the base. The rhyolite clasts contain 1–2% euhedral quartz phenocrysts (0.4–1.2 mm) and 4% euhedral tabular plagioclase phenocrysts (0.4–2 mm). The basal breccia facies is overlain by a coherent lithofacies (UTM 6073677N; 314217E) that contains <5% euhedral quartz phenocrysts (0.2–2.5 mm), 7% euhedral plagioclase phenocrysts (0.2–1.2 mm) and attains a maximum thickness of 50m. The coherent lithofacies, which is interpreted to comprise a flow interior, grades upwards into an upper, clast supported breccia lithofacies (UTM 6073629N, 314217E), which contains irregular to tabular slabs of flow banded rhyolite ranging up to 1.9 m long that have the same phenocryst population as the underlying coherent lithofacies. The flow banded slabs comprise 5–20% of the breccia and occur in a matrix composed of angular to subangular rhyolite lapilli in a dark grey rhyolite tuff-sized matrix. The Mine rhyolite is correlated with coherent rhyolite domes, cryptodomes and sills exposed at Millrock Hill and at South Main; however, the Mine rhyolite has a U-Pb zircon age of 1.9 Ga in contrast to 1.88 Ga U-Pb zircon ages obtained from the Millrock and South Main rhyolite (Stern et al., 1999). The reason for this age discrepancy is uncertain at this time.

Stop 4.4 is a virtual stop of a bedded tuff and heterolithic tuff lithofacies that comprise a 35 m thick unit, which overlies the Mine rhyolite (referred to as the ‘Railway volcanics’ by Bailes and Syme, 1989). The bedded tuff lithofacies is thick to thin-bedded and is intercalated with the heterolithic tuff lithofacies that contains quartz amygdaloidal, aphyric basalt clasts and quartz and feldspar phyric rhyolite clasts that range from 2 to 24 cm long and 2–18cm in width (average size of 9 x 5 cm) (Devine, 2003). The “Railway volcanoclastic” unit is interpreted to be the time-stratigraphic equivalent of the coarser rhyolite and rhyolite-basalt breccia lithofacies at Millrock Hill

(Stop 2.2), and the bedded tuff and heterolithic tuff lithofacies (Stop 3.3) at South Main. At these localities, the rhyolitic component of these lithofacies is interpreted to have been emplaced by submarine mass flows that were ultimately derived from syndepositional rhyolite domes.

On route to the lower Callinan Stop, typical volcanoclastic lithofacies that comprise the Blue Lagoon member are examined at Stops 4.5–4.8 (Figure 7); lithofacies descriptions at each Stop are modified from Devine (2003). Stop 4.5 is typical of the crystal-rich tuff and lapilli tuff lithofacies of the Blue Lagoon member. It contains 12–40% plagioclase crystals from 0.1 to 2 cm in size within a finer, tuff-sized, mafic matrix; locally the lapillistone facies is totally comprised of plagioclase crystals and is devoid of a finer matrix. The crystal-rich tuff and lapilli tuff lithofacies are crudely bedded, and conformably overly a matrix-supported tuff-breccia lithofacies that grades upward into the lapilli tuff lithofacies. The tuff breccia and lapilli tuff lithofacies contain clasts of feldspar phyric and aphyric basalt in a mafic, tuff-sized matrix containing up to 10 % plagioclase crystals. Possible mechanisms to explain the abundance of crystals include: pyroclastic fragmentation of highly crystallized (phyric) magma, primary and secondary eruptive fractionation, and or reworking of pre-existing, unconsolidated, volcanoclastic deposits, (i.e., Cas and Wright, 1987). The feldspar crystal-rich tuff and lapilli-tuff units are interpreted to have been derived by pyroclastic fragmentation of crystal-rich magmas, such as those that produced the intercalated pillowed flows, which have a plagioclase phenocryst content of 12–20% (Devine, 2003). The higher crystal content of the volcanoclastic lithofacies as compared their coherent extrusive lithofacies is interpreted to reflect crystal concentration processes during explosive submarine pyroclastic eruptions (sorting during eruption column generation and collapse) and their subsequent emplacement by subaqueous, pyroclastic flows and, where plagioclase crystals are the only component and bedforms do not indicate reworking or mass flow transport, by pyroclastic fall (Gibson et al., 2009a).

Located some 100 m east and up-section from Stop 4.5, a coarse heterolithic block-rich lithofacies at Stop 4.6 occurs at the top of the Blue Lagoon member. The coarse volcanoclastic lithofacies contains plagioclase-phyric basalt blocks in a fine, recrystallized, tuff-sized matrix containing 5% plagioclase crystals. Depositional units range from 3 to 4m in thickness, and are poorly size sorted and chaotic. These features suggest transportation by mass flows and, along with the occurrence of clasts of breccia (feldspar-phyric blocks in a feldspar-rich matrix) up to 1.5 m in size, suggest derivation from the redeposition of pre-existing volcanoclastic deposits (Figure 10). The mass flows may have been triggered by synvolcanic faulting, during subsidence, which generated debris flows composed of previously emplaced volcanoclastic deposits.

The coarse heterolithic block-rich lithofacies at Stop 4.6 is conformably overlain by thin bedded to laminated tuff and crystal tuff lithofacies of the Millrock member at Stop 4.7. This lithofacies weathers a rusty brown colour due to oxidized sulphides and occurs approximately 100m up-dip of the Dan VMS occurrence. Plagioclase crystals within the tuffs abruptly decrease in abundance upwards, and are absent in the upper-

most portion of the thin-bedded tuff. The Millrock bedded tuff lithofacies is now buried by construction debris, but similar bedded tuffs displaying flame, ball and pillow structures, as well as cross-bedding are well exposed some 100m to the north at Stop 4.8. However, at Stop 4.8 the bedded tuff lithofacies is underlain by a coarse, heterolithic breccia lithofacies of the Millrock member that is identical to that at Stop 5.4. The continuation of the Millrock bedded tuff lithofacies between Stops 4.7 and 4.8, and the marked absence of Millrock Hill heterolithic breccia lithofacies at Stop 4.7, where the Millrock bedded tuff sits directly on the Blue lagoon member suggest the presence of a synvolcanic fault between Stops 4.7 and 4.8 (Figure 7). The absence of Millrock heterolithic basalt breccia lithofacies at Stop 4.7, suggests that it was uplifted relative to Stop 4.8 before the onset of Millrock member volcanism (Figures 7 and 10). Blue Lagoon detritus within the Millrock heterolithic breccia lithofacies at Stop 5.3 may have been derived from the Blue Lagoon member in the adjacent, uplifted block of Stop 4.7.

## **Stop 5. Lower Callinan Section**

### **Stops 5.1 to 5.2**

#### **Co-ordinates**

Stop 5.1: UTM, N 6075705, E 313535

Stop 5.2: UTM, N 6075560, E 313753

#### **Stop Descriptions**

In this section, lithofacies typical of the Club, Blue Lagoon and Millrock members will be examined. At Stop 5.1, the Club member consists of three lithofacies, coherent rhyolite, rhyolite breccia and bedded tuff. The coherent rhyolite facies consists of massive, aphyric, aphanitic, rhyolite that is conformable, but in sharp contact with the overlying breccia lithofacies. The breccia lithofacies contains clasts of aphyric rhyolite in a fine, tuff-sized, mafic matrix. The lithofacies is thick bedded, typically normally graded and the rhyolite clasts have identical trace and REE compositions to the underlying coherent rhyolite lithofacies (Devine, 2003). The range in size and abundance of rhyolite fragments, and the absence of other clast types indicates that the rhyolite clasts have not been transported a great distance, and are derived from a single source. This coupled with their angular and blocky form, and the occurrence of *in situ* brecciated or jigsaw fit clasts suggests the clasts are a product of autoclastic fragmentation, and that they were emplaced by mass flows along the flanks of the growing flow dome represented by the underlying coherent lithofacies (Devine, 2003). Multiple normally graded beds suggest depositional units were emplaced quickly, one after another, through successive periods of dome growth and collapse. The fine, tuff-sized mafic matrix has a separate mafic provenance and may have ultimately been derived from contemporaneous explosive basalt volcanism.

The bedded tuff lithofacies conformably overlies the rhyolite breccia facies and is texturally similar to the mafic tuff matrix of the latter lithofacies. The bedded tuff lithofacies is interpreted to be a product of explosive basaltic volcanism and to have been emplaced by fall (suspension) and low concentra-

tion mass flows. The contact with the overlying Blue Lagoon member is conformable, sharp and defined by the abrupt appearance of plagioclase crystals within the mafic tuff.

The purpose of Stop 5.2 is to examine multi-generational peperite that developed where feldspar phyric and aphyric basaltic dikes and sills intruded massive, crudely bedded, crystal tuff lithofacies of the Blue Lagoon member that contains 5–20% plagioclase crystals (<5mm in size). The sparsely feldspar phyric, fine-grained sill is characterized by irregular, aphanitic chilled contacts and numerous fractures that increase in abundance and decrease in spacing towards the sill-crystal tuff contact. Irregular to fluidal apophyses of the sill extend into the crystal tuff, where they are fractured, *in situ* brecciated, and brecciated to form blocky peperite; the peperite is interpreted to be a product of quench fragmentation during emplacement of the sill into the wet, unconsolidated tuffs (Gibson et al., 2003a).

The crystal tuff away from the sill contact contains irregular, wispy and brecciated fragments of aphyric basalt that lack the feldspar crystals found within the adjacent sill. The wispy, fluidal to amoeboid clasts of aphyric basalt are not associated with a coherent intrusion and are interpreted to be an earlier formed, fluidal (blocky) peperite, which formed by the total disintegration of an initial basalt magma that was emplaced into the unconsolidated crystal tuff (Gibson et al., 2003a).

Basalt sills exposed on the immediately adjacent outcrop to the east crosscut earlier sills and rarely develop peperite (UTM 6075580, 313765). Their contacts with the crystal tuff are more uniform and straight, which suggests that at this stage the crystal tuff was essentially lithified and that there were no significant rheological differences between the tuff and earlier sills (Gibson et al., 2003a). This outcrop also displays a sharp but irregular contact between the Blue Lagoon crystal tuff lithofacies and a 75 m thick heterolithic breccia lithofacies of the Millrock member. Although conformable, the base of the Millrock lithofacies is erosive as it scours into, and contains fragments of the underlying crystal-rich beds of the Blue Lagoon member; the contact is also folded about a northwest-trending fold axis (parallel to the D2 Hidden Lake Syncline). The Millrock heterolithic breccia lithofacies (UTM 6075575, 313795) is framework supported and contains wispy- to plate-like to angular blocks and lapilli of amygdaloidal, aphyric basalt and minor clasts of feldspar phyric basalt and crystal tuff in a fine, tuff-sized matrix that contains up to 5% plagioclase crystals, which decrease in abundance with distance from the contact (Devine, 2003). The breccia lithofacies is crudely bedded and normally graded. A tentative interpretation for the monolithic basalt breccia lithofacies is that it is a product of phreatomagmatic pyroclastic eruptions that developed in response to the emplacement of basalt magma into unconsolidated and wet Blue Lagoon crystal tuff (Gibson et al., 2003a). The heterolithic breccia lithofacies was transported and emplaced by high concentration mass flows and may represent a primary pyroclastic deposit or a re-deposited, syneruptive equivalent. Aphanitic, aphyric sparsely amygdaloidal basalt dikes and sills that intrude the lithofacies have distinct autobrecciated margins with peperite. These intrusions are identical in texture and composition to the aphanitic aphyric basalt clasts within the lithofacies, and are interpreted to have

intruded their own, unconsolidated volcanoclastic deposits (Gibson et al., 2003a)

**Hazard:** *This exposure occurs along the edge of the outcrop, above a cliff.*

### **Stops 5.3 to 5.5**

#### **Co-ordinates**

Stop 5.3: UTM, N 6075518, E 313910

Stop 5.4: UTM, N 6075595, E 313934

Stop 5.5: UTM, N 6075625, E 313970

#### **Stop Descriptions**

The purpose of Stops 5.3 to 5.5 is to examine heterolithic breccia and bedded tuff lithofacies that comprises the Millrock member in the Callinan fault block (section 8 of Figures 4 and 7). The lithofacies at Stops 5.3 to 5.5 and the location of the sub-stops are shown in Figure 7. At Stop 5.3, the crystal tuff lithofacies of the Blue lagoon member consists of crudely bedded, plagioclase crystal tuff and lapilli tuff similar to those observed at Stops 4.1 and 4.5. The contact with the Millrock member is not exposed, but is interpreted to be conformable. Note that this outcrop is interpreted to be a thrust fault repeat of the same contact exposed to the west at Stop 5.2. The inferred thrust fault lies in the valley floor and is not exposed.

At Stop 5.4 the heterolithic breccia lithofacies is similar to that at Stop 5.2, and it attains a maximum thickness of 150m. It consists of framework supported beds (80 % clasts) that are moderate to poorly sorted, range from 0.4 to 6m in thickness, and contain clasts of angular, wispy- to plate-like, aphyric, aphanitic basalt, feldspar phyrlic basalt, and minor medium-grained gabbro that range up to 1.4 m in size, within a finer, tuff-sized, mafic matrix that contains <1% feldspar crystals (Devine, 2003). The upper portion of the lithofacies fines abruptly and then continuously from thick – to medium-bedded lapillistone and lapilli tuff to thin-bedded and laminated mafic tuff, with cross bedding and scours particularly well developed within the finer-grained, tuff beds. Thin (<20cm) lenses of crystal tuff and blocks of crystal tuff occur near the transition from lapilli tuff to tuff.

The relatively large thickness (up to 150 m) and confined lateral extent of this lithofacies suggest its emplacement into a distinct fault-block basin (the Callinan fault block). The lack of thinner, fine-grained beds between the coarser tuff breccia and lapillistone beds and the disorganized clast fabric with respect to bedding suggests these units were emplaced quickly and by high-concentration mass flows. They are interpreted to be syn-eruptive, resedimented, pyroclastic deposits (Devine, 2003). The presence of numerous aphanitic, aphyric basalt clasts that are angular, irregular, and have unbroken shapes and slightly chilled margins suggest this unit may have formed by initial phreatomagmatic explosive eruptions with subsequent syn-eruptive redeposition (as proposed for the similar lithofacies at Stop 5.2; Gibson et al., 2003a). The crystal tuff lenses and blocks of crystal tuff within the upper most beds of this lithofacies are interpreted as detritus derived from Blue Lagoon

member in the adjacent fault block to the south (Stops 4.6 and 4.7) that was uplifted and exposed by faulting prior to or during Millrock member volcanism (Gibson et al., 2009a). As at Stop 5.2, the aphanitic, aphyric basalt dikes and sills that intrude the heterolithic breccia lithofacies have autobrecciated margins with peperite, and are interpreted to have intruded their own, unconsolidated volcanoclastic deposits (Gibson et al., 2003a).

The bedded tuff lithofacies at Stop 5.5 also defines the top of the Millrock member and consists of thin-bedded to laminated mafic tuff and lesser, lighter coloured felsic tuff; soft sediment slump structures are common. The tuff is plane bedded, although some beds show erosive lower contacts, and is intruded by basalt sills. The bedded tuff lithofacies weathers a rusty red-brown colour and occurs approximately 250 m up-dip and plunge from the Callinan VMS deposit.

The bedded tuff lithofacies defines the top of the Millrock member in all structural blocks from Millrock Hill (and south) to Callinan in the north where it ranges in thickness from 5 to 50m (+) thickness (Figure 7). It is dominantly composed of basalt tuff, but locally contains a minor rhyolitic “tuff” component towards its base (Tardif, 2003). It also contains minor lapilli-sized scoria and lesser lithic clasts, feldspar crystals, and beds containing accretionary lapilli. It is typically plane bedded, but locally cross bedded, and often displays structures attributed to soft-sediment deformation during slumping. The large volume of bedded tuff, its significant areal extent, ubiquitous occurrence in all fault blocks, and its basaltic composition, which is identical to the composition of associated basalt flows (no geochemical evidence for input of external detritus), are consistent with an origin through pyroclastic eruptions (Figure 10; mixed strombolian magmatic and hydrovolcanic eruptions; Gibson et al., 2009a). Bed forms suggest it was emplaced by suspension sedimentation and low concentration mass flows. The occurrence of accretionary lapilli indicate the eruption column was, at least in part, subaerial and the common occurrence of cross bedding and less commonly ripples suggests reworking by bottom currents during hiatuses in eruption and deposition (Gibson et al., 2009a).

### **Stop 6. Beaver Road Anticline**

The stops through the Beaver Road anticline will demonstrate: 1) field evidence for defining primary synvolcanic subsidence, 2) the relationship between volcanism, subsidence, and hydrothermal alteration, 3) the influence of primary synvolcanic structures on later deformation, 4) how strata composed predominately of massive flows deform and fold; and 5) features characteristic of thrust faults and their reactivation. The locations of the sub-stops are shown in Figures 17, 18 and 19.

### **Stops 6.1 to 6.10**

#### **Co-ordinates**

Stop 6.1: UTM, N 6071210, E 313892

Stop 6.2: UTM, N 6071550, E 313910

Stop 6.3: UTM, N 6071900, E 313968

Stop 6.4: UTM, N 6071230, E 314085

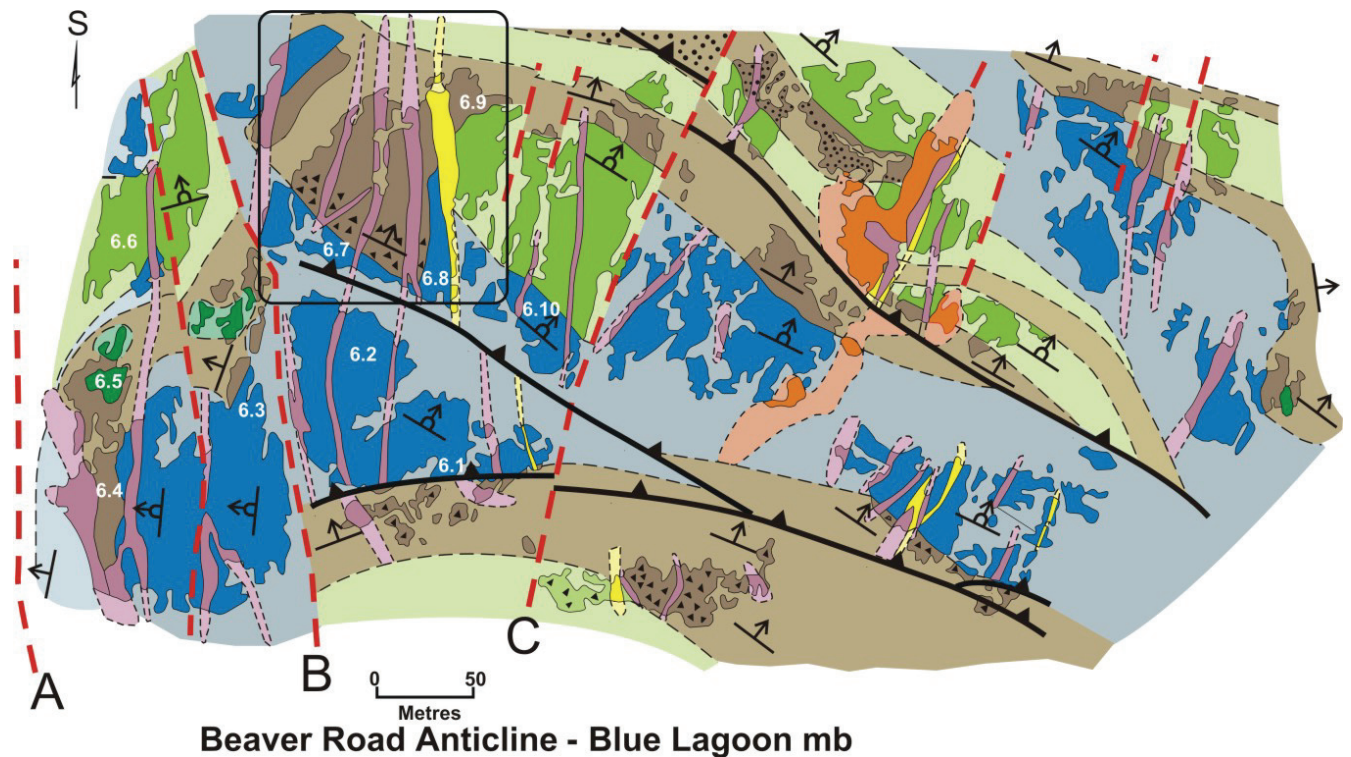


**Figure 17:** Simplified geology and structure within the Blue Lagoon member at the Beaver Road Anticline, showing Stop locations (after Gibson et al., 2007). Units are as follows: light green with black triangles, coarse basaltic volcanoclastic lithofacies; brown, volcanoclastic lithofacies comprised of coarse block-rich and megabreccia facies, massive crudely bedded tuff and well bedded tuff lithofacies with variable amounts of feldspar crystals and scoria (black dots); blue, feldspar phryic pillowed basalt lithofacies (10–15 % feldspar); green, aphyric to sparsely feldspar phryic (<5 % feldspar) basaltic pillowed lithofacies; purple, yellow and orange indicates basaltic, rhyolitic and Boundary intrusion dikes. Area within circle is illustrated in detail in Figure 18 (Gibson et al., 2011).

- Stop 6.5: UTM, N 6071156, E 314038
- Stop 6.6: UTM, N 6171082, E 314050
- Stop 6.7: UTM, N 6071095, E 313915
- Stop 6.8: UTM, N 6071092, E 313893
- Stop 6.9: UTM, N 6071035, E 313850
- Stop 6.10: UTM, N 6071135, E 313825

### Stop Descriptions

At Stop 6.1 a basaltic tuff lithofacies is separated from feldspar phryic pillowed lithofacies of the Blue Lagoon member by a shallow, south-dipping fault that clearly truncates dikes within both lithofacies and flow contacts within the pillowed lithofacies. The fault is interpreted to be a thrust fault because it has a bedding-parallel shear foliation and a down-dip, SE-plunging, stretching lineation and is similar in strike and dip to the D<sub>4</sub> Railway-Club Lake thrust faults (Lewis et al., 2007). A mafic dike in the hanging wall of the fault underwent a clockwise rotation into the fault, and the shear foliation within the thrust fault is overprinted by dextral shear bands and asymmetric Z-shaped drag folds, suggesting that it was reactivated as a dextral transcurrent fault during D<sub>6</sub>. The thrust fault is offset along a north-northwest trending steeply dipping fault labelled B in Figure 17 which, along with other similarly oriented faults, is parallel to the Flin Flon Lake Fault (A in Figure 17). The Flin Flon Lake Fault is poorly exposed but a 3D reconstruction of

the subsurface geology by Schetselaar et al. (2010), suggests that the fault is an early, west-directed, D<sub>3</sub> thrust fault that was later reactivated as a transcurrent shear zone as indicated by dextral and sinistral shear-fabrics in several parallel and adjacent minor faults.

The feldspar phryic pillowed lithofacies at Stop 6.2 is typical of the Blue Lagoon member. Note the well-developed pillow selvages, minor interpillow hyaloclastite and shallow south dip of the flow. The pillows contain 12–15% plagioclase crystals. Continuing 30 m to the north the pillows have a sharp but irregular contact with an overlying breccia containing angular to irregular (amoeboid) fragments in a hyaloclastite matrix. The breccia is interpreted to be a flow top breccia to the underlying pillowed flow. The contact between the pillows and breccia trends west-northwest, parallel to other flow contacts within this fault block

The traverse from Stop 6.2 to Stop 6.3 transects the north-northwest trending Fault B, which is not exposed as it occupies the low ground between the two outcrops (Figure 17). Fault B coincides with a significant change in the attitude of the flows, where strata at Stop 6.2 to the west strike west-northwest and dip shallowly to the south whereas strata at Stop 6.3 to the east, strike north-northeast and dip steeply to the southeast; the horizontal movement along the fault is sinistral (Figure 17). This abrupt and rapid change in the orientation of strata which, in part, defines the Beaver Road anticline is actually more in

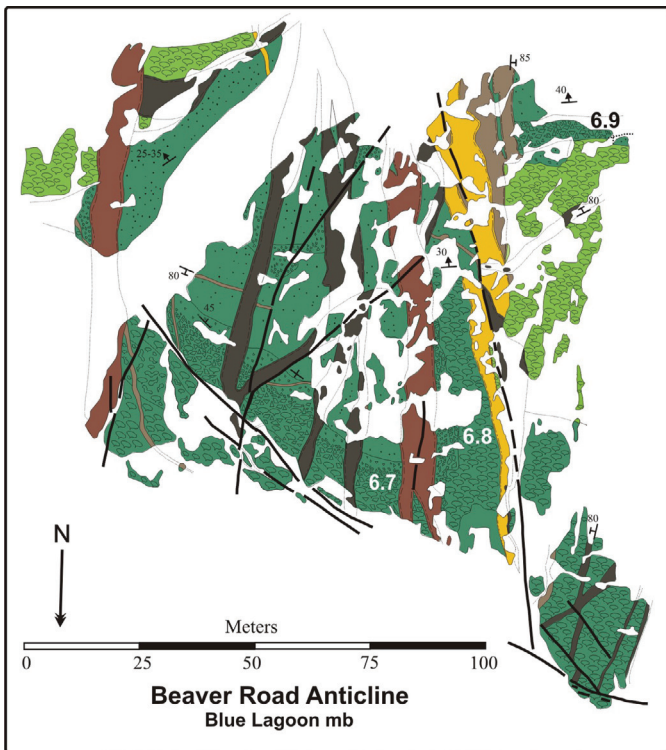


**Figure 18:** Details of synvolcanic graben showing Stop locations (after Gibson et al., 2007). Map units as follows: dark green with pillow symbol, feldspar phyric pillowed lithofacies; dark green with fine black dots, basaltic megabreccia, breccia, and tuffs with variable amounts of feldspar crystals; light green, sparsely feldspar phyric pillowed lithofacies; shades of brown and yellow, basaltic and rhyolitic dikes.

response to faulting than folding, as folding would manifest itself by a gradual change in the orientation of bedding.

At Stop 6.4, the contact between the feldspar phyric pillowed lithofacies and the overlying volcanoclastic lithofacies comprised of thin-bedded to laminated tuff and coarse, block-rich tuff breccia confirms the north-trending, steeply southeast dipping and facing orientation of the strata as does the bedding within the volcanoclastic lithofacies. Aphyric basalt sills and dikes within the volcanoclastic lithofacies have peperite along their contacts indicative of their synvolcanic emplacement.

At Stop 6.5, two large blocks (approx. 10m x 10m) of aphyric pillowed basalt occur within the volcanoclastic lithofacies (Figure 17; a third and larger block occurs 25m to the west) and this unit is interpreted to be a megabreccia, deposited by high concentration mass flows (debris flows) generated by the collapse of fault scarp walls during or after subsidence. Again the strike and dip of strata are the same as at Stops 6.3 and 6.4.

The aphyric pillowed basalt lithofacies at Stop 6.6 strikes west-southwest and dips shallowly and faces to the south. This change in bedding orientation from that at underlying Stops 6.3-6.5 is abrupt, occurs directly above the volcanoclastic unit examined at Stop 6.5, and is interpreted to define a primary, angular unconformity between strata within the same fault block (Figure 17). Thus, the abrupt change in the orientation of strata from Stop 6.2 to Stop 6.3 is a result of synvolcanic faulting along Fault B. No doubt subsequent deformation resulted in some rotation of the fault blocks and the reactivation of Fault B, but the D2 Beaver Road Anticline as illustrated on previous maps is due, in part, to block rotation during synvolcanic faulting and subsidence (Gibson et al., 2007).

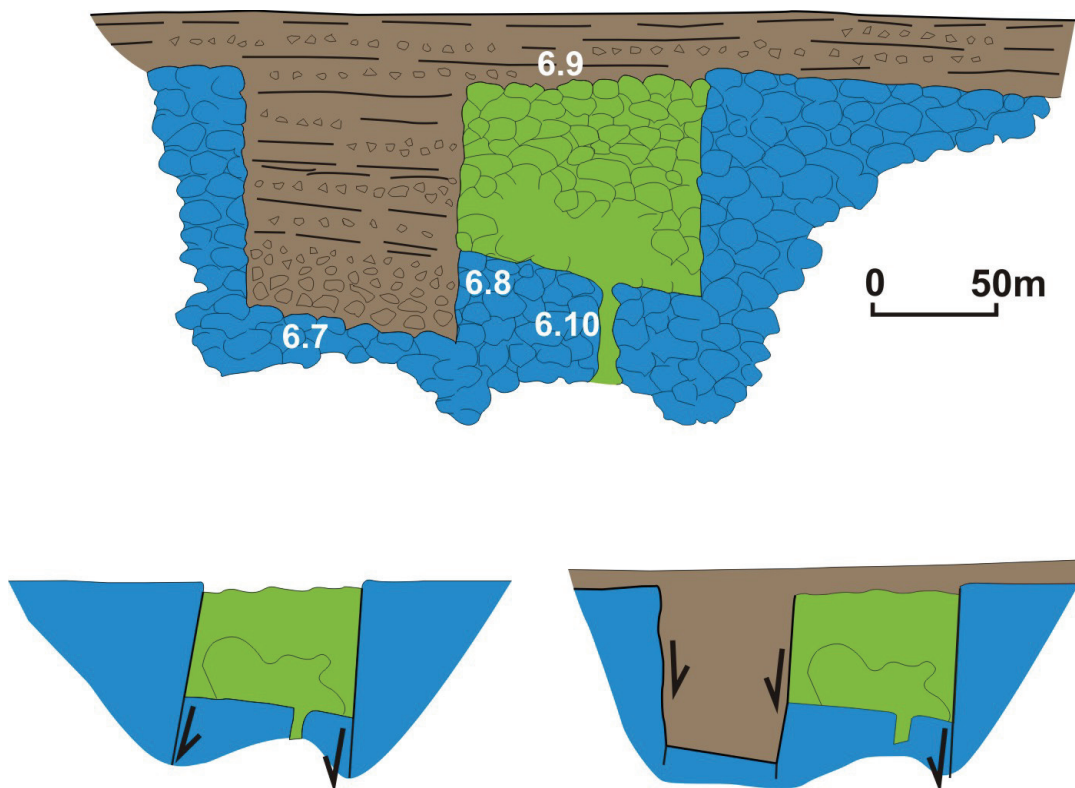


**Figure 19:** Pre-diking and pre-folding reconstruction of the area in Figures 17 and 18 showing Stop locations (after Gibson et al., 2007).

The feldspar phyric pillowed flows at Stop 6.7 are similar to those at Stop 6.2, but here they are in sharp but conformable contact with an overlying volcanoclastic lithofacies that is characterized by a coarse, block-rich tuff breccia, comprised mainly of broken pillows at the base, that grades upwards into finer lapillistone, lapilli tuff and tuff within a tuff-sized matrix containing abundant feldspar crystals (Figures 17 and 18). Medium- to thin-bedded to laminated basaltic tuff containing variable amounts of scoria, lithic lapilli and feldspar crystals occurs at the top of the volcanoclastic lithofacies. The volcanoclastic lithofacies at Stop 6.7 is correlated with that at Stops 6.3, 6.4 and 6.5 (Figure 17). Several types and generations of basalt dikes and an aphyric rhyolite dike crosscut the pillowed and volcanoclastic lithofacies; some of the basalt dikes have irregular and locally peperitic contacts with the volcanoclastic lithofacies.

At Stops 6.8, and 6.9 the contacts between the volcanoclastic lithofacies and adjacent pillowed lithofacies are examined (see details in Figure 18). The contact between the volcanoclastic lithofacies and feldspar phyric pillowed flow at Stop 6.7 trends northwest, whereas at Stop 6.8 the contact abruptly changes orientation to north-south, where it is at a high angle to bedding within the adjacent volcanoclastic lithofacies. This change in orientation continues to the south where it separates the volcanoclastic lithofacies from the aphyric pillowed lithofacies, which conformably overlies the feldspar phyric pillowed lithofacies. This north-south contact between the volcanoclastic unit and the feldspar phyric and aphyric basalt lithofacies is interpreted to be a primary, synvolcanic fault scarp wall (Figures 17 and 18; Gibson et al., 2006). However, at Stop 6.9 the volcanoclastic – aphyric pillowed lithofacies contact abruptly changes strike and returns to a northwest orientation, and bedding within the volcanoclastic lithofacies is now parallel to the contact, and to other flow contacts in the same fault block indicating that it is conformable (Figure 17). Also note that the strike extent of the aphyric pillowed facies is limited by the primary, north-northeast trending fault scarp to the east, and by the north-northeast trending Fault C to the west. This complex relationship between lithofacies, abrupt changes in strike, and conformable versus unconformable contacts can be explained by successive episodes of synvolcanic faulting, subsidence and volcanism (Figure 18; Gibson et al., 2006). As illustrated in Figure 18, initial faulting and subsidence is interpreted to have resulted in the development of a localized structural basin or graben within the feldspar phyric pillowed flows. Volcanism that accompanied or immediately followed subsidence resulted in the emplacement of an aphyric, pillowed basalt flow within the graben. Subsequent faulting, manifest by the reactivation of an earlier fault (the synvolcanic fault scarp in Figure 18) and the development of a new, parallel fault to the east resulted in the formation of a step like basin, which was subsequently filled by the volcanoclastic lithofacies such that coarse debris collected at the base of the graben and the finer tuffs and bedded tuffs extend beyond the limits of the small graben defined in Figure 19 to define a larger synvolcanic structural basin within what is now the Beaver Road anticline (Figure 17). Collapse of this basin during synvolcanic subsidence along Fault B resulted in tilting of strata within this block, and the megabreccia examined at Stop 6.5.

Epidote-quartz alteration occurs through the basaltic flows, but is locally concentrated in two areas. The first being in the pillowed lithofacies immediately adjacent to the primary synvolcanic fault scarp (Stop 6.8). The second is at Stop 6.10 where a 1m wide, north-northeast trending zone of epidote-quartz alteration crosscuts the feldspar phyric pillowed lithofacies. In both examples, the zone of intense and pervasive epidote-quartz alteration is disconformable, either adjacent to or oriented parallel to synvolcanic faults, and are interpreted to represent high-temperature hydrothermal up-flow zones.

### ***Stop 7. Upper Callinan section***

This traverse is a continuation of the Lower Callinan section (Stop 5) and focuses on coherent andesitic and basaltic flows of the Hidden formation and key structural elements, including the Railway thrust faults. The location of Stops 7.1, 7.2, 7.3, 7.4 and 7.5 are shown on Figure 20. On the walk to Stop 7.1 you will cross several large outcrops that contain thin (<1 m) screens of the bedded tuff lithofacies (as at Stop 5.5), sometimes containing quartz crystals and quartz phyric rhyolite lapilli, between the basalt and basaltic-andesitic sills which, coupled with the common occurrence of peperite, has been cited as evidence to indicate that these thick sills were emplaced into the unconsolidated, wet, Millrock member bedded tuff lithofacies during the initial stages of Hidden formation volcanism (Gibson et al., 2003b; DeWolfe et al., 2009a). The numerous basaltic and basaltic-andesitic dikes and sills encountered constitute part of a “sheeted dike-sill complex” that defines a significant zone of extension and a volcanic centre within Callinan Block and in the larger Flin Flon cauldron (Gibson et al., 2003b, 2007).

#### **Stop 7.1: Columnar jointed vent facies of the 1920 unit cryptoflow**

##### ***Co-ordinates***

UTM, N 6075231, E 314122

##### ***Stop Descriptions***

The 1920 unit occurs at the base of the Hidden formation and here consists of a coherent basaltic andesite that, along with an overlying volcanoclastic lithofacies, occupies and defines a localized fault-bounded subsidence basin (DeWolfe et al., 2009a, b). The overburden to the east of this outcrop represents a thrust fault of the same generation of the Railway fault. Directly in front of this fault in the vertical face of the large outcrop is an aphyric basaltic unit (base of outcrop and a dark green colour) in contact with the 1920 unit (upper portion of outcrop and a dark grey-blue colour). The contact between the two units is sharp and characterized by discontinuous lenses of strongly quartz-epidote altered tuff. Near the centre of this outcrop is the feeder dike for the 1920 unit cutting upwards through the underlying basalt and fanning upwards and outwards away from the vent forming a columnar jointed, massive facies of the 1920 unit. If you climb up on top of the outcrop you can observe the columnar joints in a cross sectional view. As you walk to the northeast along the line outcrops you are walking oblique to strike moving upwards through stratigraphy



## LEGEND

-  Feldspar porphyritic mafic dikes and sills
-  Feldspar and pyroxene porphyritic mafic dikes and sills
-  Fine- to medium-grained mafic dikes and sills
-  Feldspar-rich, coarse-grained dikes and sills
-  1920 unit: Basaltic andesite cryptoflow
-  Mafic volcanoclastic rocks

## SYMBOLS

-  Tuff breccia
-  Weak, patchy epidote-quartz alteration
-  Strong, patchy epidote-quartz alteration
-  CJ Columnar jointing
-  Included Tuff
-  Peperite
-  Lapillistone
-  Lapilli-tuff
-  Tuff
-  Lobe

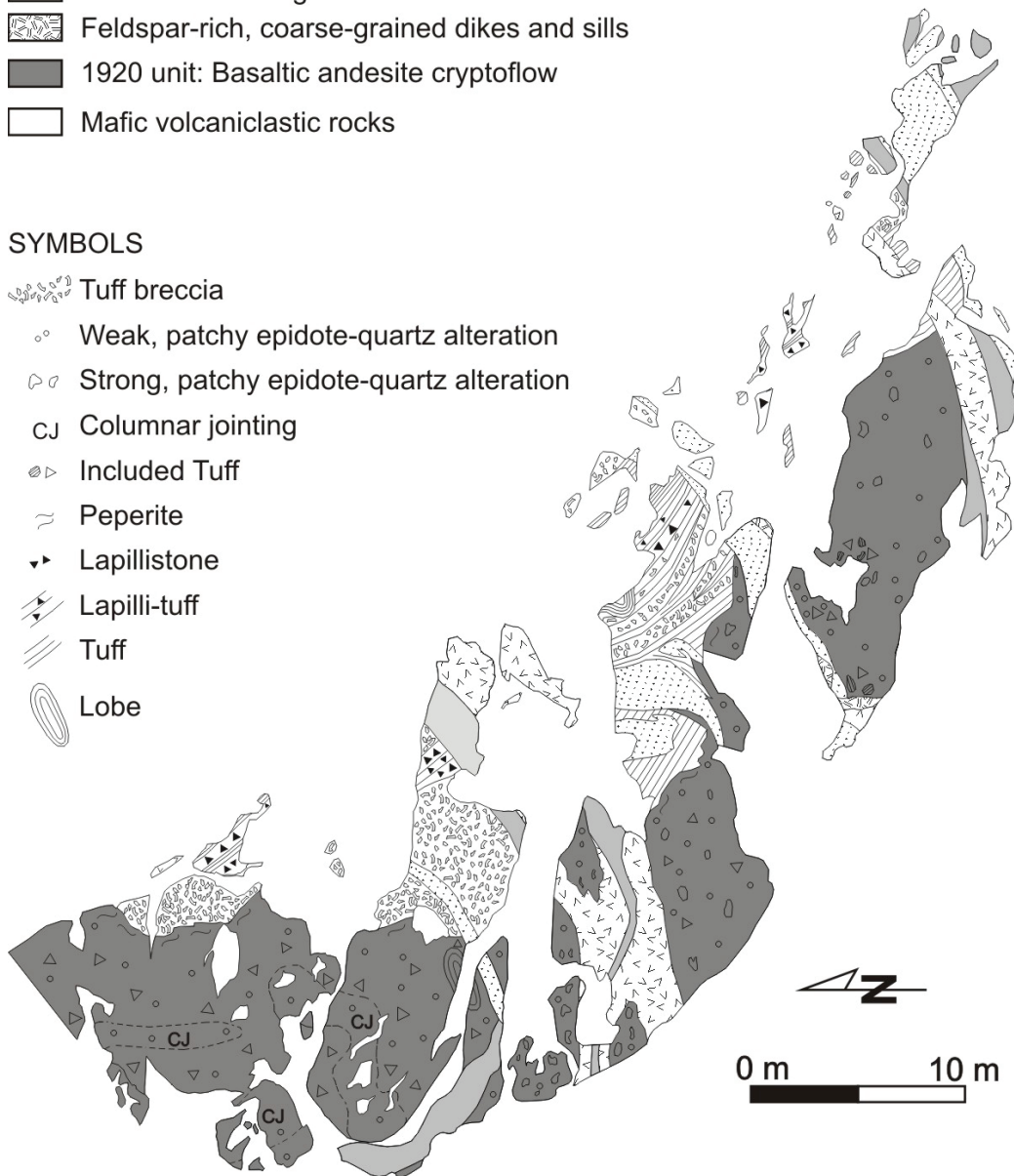


**Figure 21:** Geology of the 1920 unit at Stop 7.2 (after DeWolfe and Gibson, 2013).

between clasts, to smaller basaltic andesite fragments that are blocky to fluidal in shape within a tuff and hyaloclastite matrix. Locally the peperite is in sharp, but irregular contact with the host-volcanoclastic rocks consisting of tuff-breccia, or intercalated mafic lapilli-tuff and tuff.

Given that the 1920 unit's different lithofacies, textures and structures, and their organization within the unit, including contact relationships, are similar to those observed in subaqueous mafic flows, it is referred to as a cryptoflow. The 1920 unit was emplaced into volcanoclastic deposits that accumulated within a synvolcanic graben (DeWolfe and Gibson, 2013).

### **Stop 7.3: Sheared rhyolitic tuff breccia of the Millrock member along the Upper Railway fault**

#### **Co-ordinates**

UTM, N 6074830, E 314395

#### **Stop Description**

The Upper Railway fault is the southern splay of the north-directed Railway thrust fault, which is one of several post-Missi, east-striking, D<sub>4</sub> thrust faults that cut across the hinge of

the Hidden Lake syncline and that imbricated the VMS-hosting Millrock member.

As you walk towards a small cliff south of the railroad, the Upper Railway fault is well exposed on horizontal outcrop surfaces and at the base of the cliff as a 10 m wide shear zone that follows a horizon of polymictic tuff breccia and bedded tuff of the Millrock member (Figures 20, 22). The tuffs are stratigraphically overlain by mafic massive flows of the Reservoir member and structurally underlain by the same unit. The shear zone is characterized by a strong mylonitic S-foliation and stretching L-lineation defined by biotite and by the flattening and elongation of the clasts. The lineation plunges 30–50° to the SE, down the dip of the NE-striking mylonitic fabric. Kinematic indicators along the shear zone are at first sight puzzling because they are best developed on horizontal outcrop surface. Dextral asymmetric strain shadows around cascades of folded quartz veins and penetrative, closely-spaced (<1 cm), steeply-dipping, dextral shear bands overprint the mylonitic foliation. The intersection lineation between the shear bands and mylonitic foliation pitches within 55° of the down-dip stretching lineation along the mylonitic foliation plane (see stereonet plot in Figure 22), suggesting that the Upper Railway fault originated as a dip-slip shear zone that was later reactivated as a dextral transcurrent shear zone during D<sub>6</sub>.

Shear sense indicators related to the formation of the mylonitic S-foliation and down-dip stretching lineation are observed on vertical, west-facing, outcrop surface parallel to lineation and perpendicular to foliation. Along this surface, the S-foliation changes orientation in anticlockwise sense as it passes from tuff breccia layers to less competent, finer-grained,

tuff layers, suggesting reverse, south-side-up thrust movement along the shear zone. The orientation of the stretching lineation along the shear zone is similar to that of the regional stretching lineation in the volcanic rocks south and north of the fault. The regional stretching lineation is interpreted as a composite structure that formed during D<sub>4</sub> thrusting and that was subsequently modified during D<sub>5</sub> along the limbs of the Hidden Lake syncline.

*Climb up the cliff or hill and then walk for roughly 15 minute or 400 m eastward along the crest of the hill.*

### Stop 7.4: Sheared 1840 Ma Phantom Lake dikes and 1872 Ma gabbroic dikes along the Upper Railway fault

#### Co-ordinates

UTM, N 6075075, E 314820

#### Stop Description

Four hundred metres east of the last outcrop, the Upper Railway fault is further exposed along strike as an array of <5 m wide, S-dipping (50–60°), shear zones that host strongly foliated dikes (Figure 23). The shear zones have a strong mylonitic foliation and down-dip, SE-plunging, mineral stretching lineation, which are similar in style and orientation to those observed at the previous stop. The southernmost shear zone can be traced for 40 m in a northeasterly direction along the contact between the flow-top breccia of an underlying massive mafic flow and the polygonal-jointed base of an overlying massive flow. It then changes orientation and cuts across bedding to become

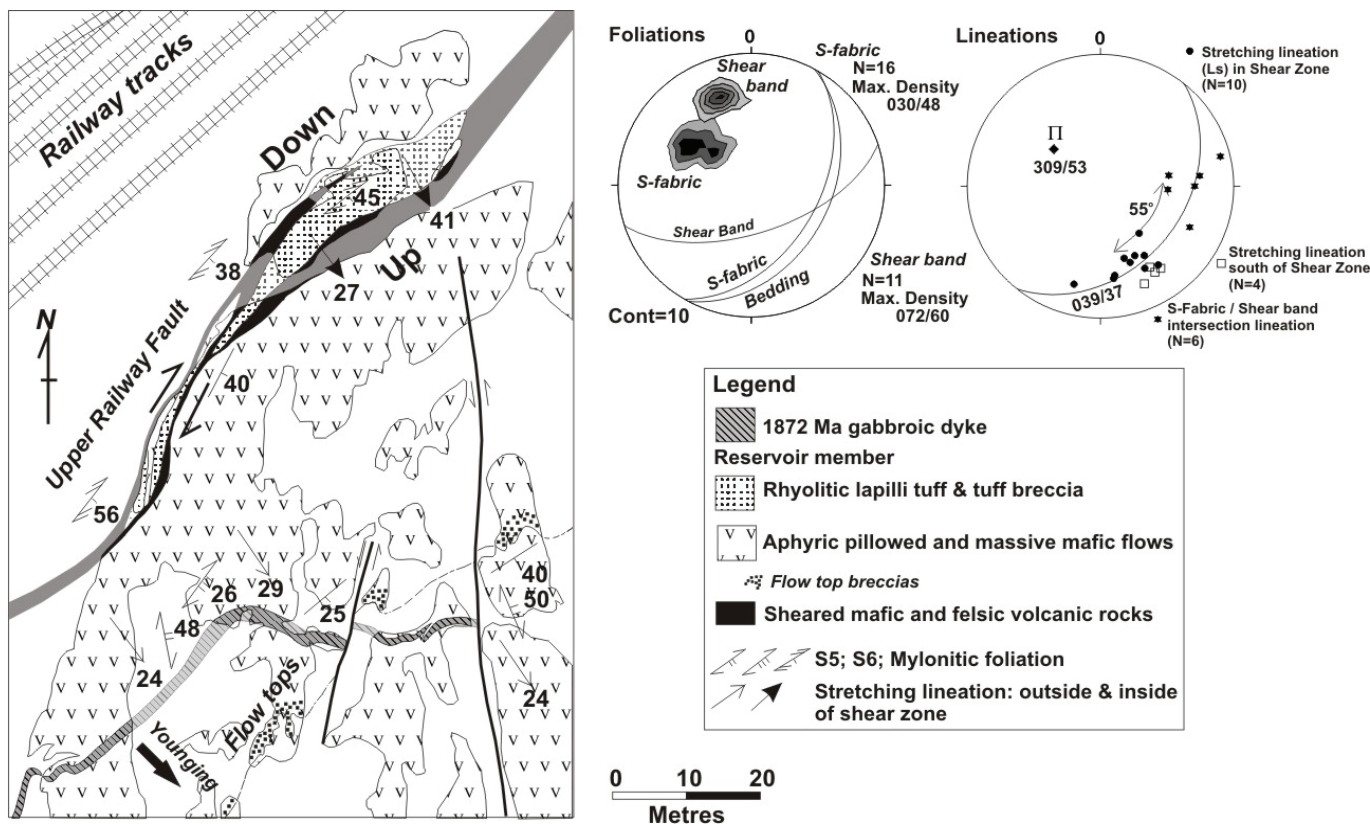


Figure 22: Details of the geology and structure of the Railway thrust faults at Stop 7.3 (after Lafrance et al., in press).

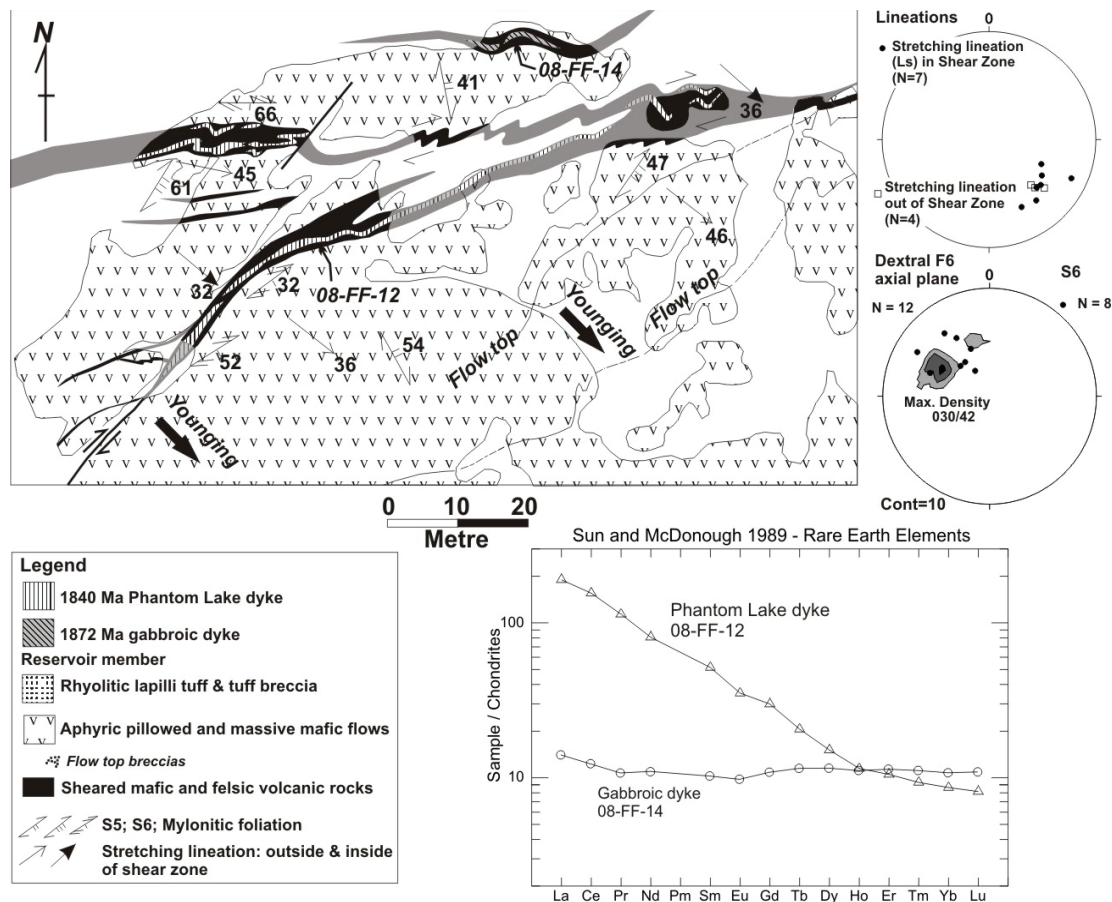


Figure 23: Geology and structure of the Upper Railway thrust fault at Stop 7.4 (after Lafrance et al., in press).

parallel to an east-striking, andesitic to dacitic dike (08-FF-12 in Figure 23), which has a similar REE pattern as ca. 1840 Ma Phantom Lake dike. Another dike (08-FF-14), which is similar in major element and REE composition to ca. 1872 Ma gabbroic dikes, is deformed within a parallel shear zone along the northern edge of the outcrop. These overprinting relationships suggest that the Upper Railway fault formed either during or after the emplacement of ca. 1840 Ma Phantom Lake dikes and it therefore postdates the deposition of the older Missi cover sequence.

The dikes and mylonitic foliation are folded by Z-shaped  $F_6$  folds with an axial plane, NNE-striking,  $S_6$  cleavage and overprinted by dextral shear bands. This confirms that the  $D_4$  Upper Railway fault was reactivated as a  $D_6$  dextral shear zone as observed at the previous stop.

Walk 400 m in a south-easterly direction to the first occurrence of Missi conglomerate.

### Stop 7.5: Missi wedge

#### Co-ordinates

UTM, N 6074955, E 315300

#### Stop Description

The Missi wedge records the complete post-Missi deformation history of the Flin Flon mining district. It consists of

shallowly-dipping Missi conglomerate and sandstone, which unconformably overlie steeply-dipping, pillowed, mafic volcanic rocks along the east limb of the pre-Missi  $F_2$  Hidden Lake syncline. Both volcanic rocks and younger Missi rocks contain a SE-plunging stretching lineation, which is spectacularly expressed by strongly elongate pebbles in conglomerate. As its orientation is similar to that of the stretching lineation along the Upper Railway thrust fault and surrounding volcanic rocks, it is interpreted to have formed during the same  $D_4$  event.

The Missi wedge was subsequently folded by upright  $F_5$  folds and overprinted by their axial plane  $S_5$  cleavage.  $F_5$  fold axes are roughly parallel to the stretching lineation which acted as a structural anisotropy that controlled the nucleation of the folds. The folds and cleavage formed during an ENE-directed compression event ( $D_5$ ) that produced the first regional NNW-striking cleavage ( $S_5$ ) across the basement-cover rocks and that reactivated the limbs of the Hidden Lake syncline and other NW-striking planar structural anisotropies as dextral shear zones.

The folded and lineated Missi wedge is transected by an array of 0.5–1 m thick, milky white, quartz veins (Figure 24). The veins are subvertical and strike north-south. They have fibrous-textured margins, massive blocky centres, and chlorite laminae with a spacing of ca. 1 cm. Thin, 1–2 cm thick, fibrous, extensional quartz veins are oriented 30° to 40° clockwise of the thicker laminated veins. Striations along chlorite laminae within the thicker veins, the dextral rotation of the lineation and Z-shaped folding of the extensional veins next to the thicker

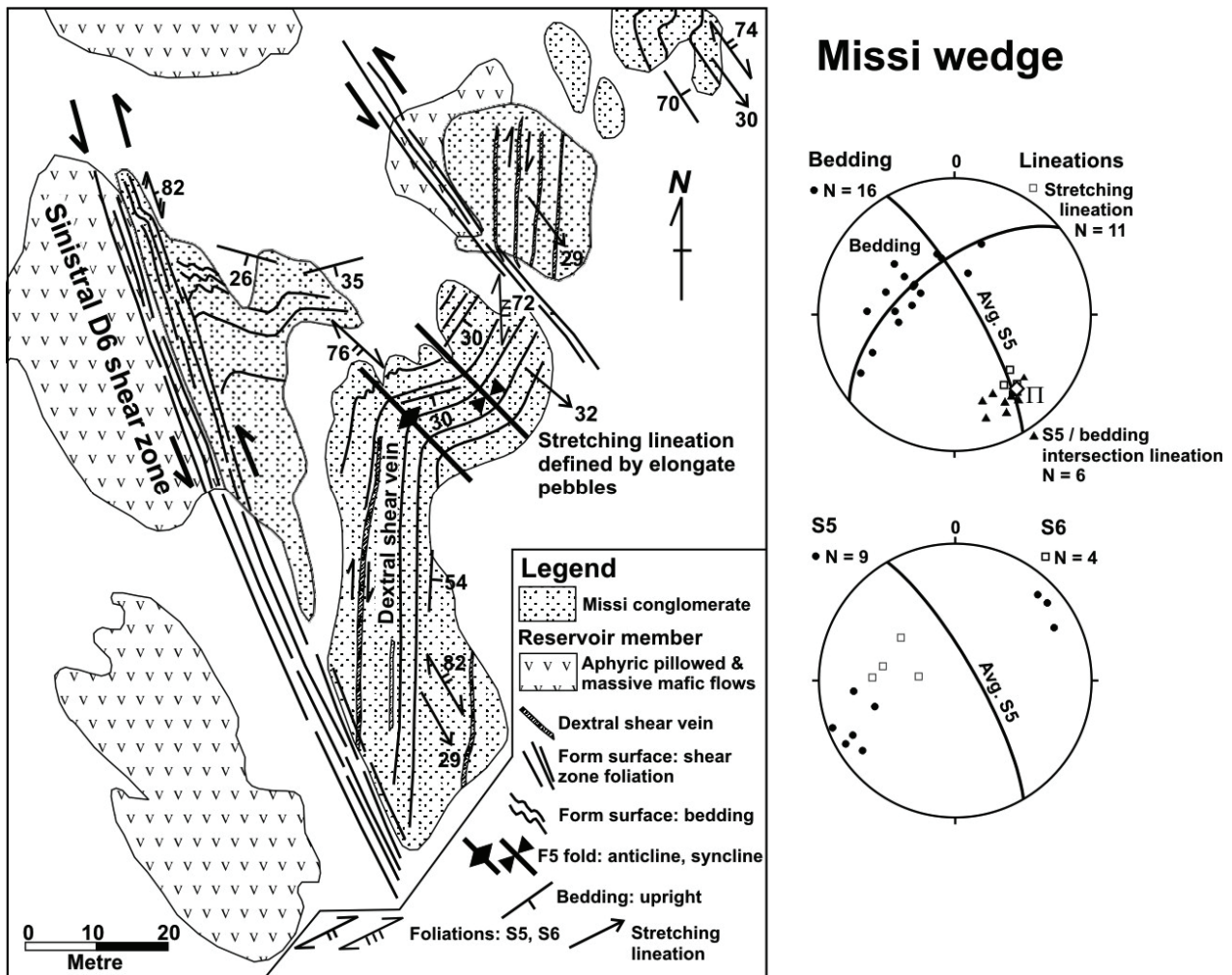


Figure 24: Geology and structure of the "Missi Wedge" area (after Lafrance et al., in press).

laminated veins suggests that the thick laminated quartz veins formed as dextral shear veins. The attitude of the two sets of veins suggest that the maximum and minimum principal stresses,  $\sigma_1$  and  $\sigma_3$ , were horizontal and oriented parallel and perpendicular, respectively, to the extensional veins, and intermediate principal stress  $\sigma_2$  was vertical and equal in magnitude to lithostatic pressure.

The veins formed during multiple repeated cycles subdivided in four stages similar to those suggested by Sibson et al. (1988) and Robert et al. (1995) for reverse faults. During pre-rupture **Stage 1**,  $\sigma_1$ ,  $\sigma_3$ , and fluid pressure increase across the shear veins. If fluid pressure increases faster than the differential stress ( $\sigma_1 - \sigma_3$ ), extensional veins form at low differential stress (i.e.  $(\sigma_1 - \sigma_3) < 4T$ , where  $T$  is the tensional strength of the rock) in the wallrocks of the shear veins. The formation of extensional veins buffers fluid pressures and allows the wallrocks adjacent to the shear veins to deform ductilely resulting in Z-shaped folding of the extensional veins and dextral dragging of the stretching lineation. During **Stage 2** rupture, further increases in the principal stresses and differential stress (i.e.,  $\sigma_1 - \sigma_3 > \sim 8T$ ) acting across the shear veins result in rupture, slip reactivation of the shear veins, and the formation of striations along chlorite laminae. The transient sudden decrease of the principal stresses

$\sigma_1$  and  $\sigma_3$  acting across the shear veins produces a switch in the orientation of the maximum principal stress  $\sigma_1$  from horizontal to vertical as the magnitude of the maximum horizontal stress drop below lithostatic pressure. During **Stage 3** sealing of the shear veins, the shear veins open as extensional fractures under vertical  $\sigma_1$  and increasing fluid pressures due to the migration of fluids from the surrounding wallrocks into the open fractures. Since the fluid pressure within the open fractures is less than in the surrounding wallrocks, the decrease in quartz solubility at lower pressures causes quartz to precipitate as fibres and/or blocky equant grains sealing the open fractures. During post-rupture **Stage 4**, the depleted fluid pressure and lower stresses adjacent to the shear veins are slowly restored as Stage 4 grades into Stage 1.

The shear veins are offset and deformed within late NNW-striking faults bounding the Missi wedge. The veins underwent anticlockwise rotation within these fault zones and are fringed by sinistral drag folds while other narrow quartz veins are offset by sinistral shear bands. Because the shear veins cut across older  $D_4$  and  $D_5$  structures, the bounding NNW-striking faults are interpreted as sinistral  $D_6$  structures. The attitude of the  $S_6$  cleavage, which is best observed at the previous stop, suggests that the compression direction was roughly ESE-WNW

during  $D_6$ . Thus during  $D_6$  compression, the E- to NE-striking Upper Railway fault was reactivated as a dextral shear zone and NNW-striking contacts between volcanic and Missi rocks at the Missi wedge were reactivated as sinistral faults or shear zones.

### Stop 8: 777 Underground Tour

Due to changing conditions underground it is not possible to exactly map out what stops and faces will be accessible on the day of the tour. What follows is a general description.

The 777 deposit was discovered in 1993 and was the third major deposit found within the Millrock member of the Flin Flon district. Drilling from underground in the Callinan mine was designed to test the down plunge extent of the Callinan ore body and to follow-up minor sulphide mineralization previously intersected in surface drillhole 4Q-64. The deposit was named after the discovery drillhole, diamond drillhole CX-777, which provided the first major intersection of the new ore body. The 777 deposit is situated between 900 and 1600m below the city of Flin Flon.

The 777 Mine is currently accessed via a 5 compartment production shaft which hosts twin 16.5 tonne production skips, a 100-man main cage for men and materials, main cage counter weight and an auxiliary hoist for moving up to 6 men. This main shaft is 1540m deep and is 6.7 m in diameter. The shaft has 5 main shaft stations, with an internal ramp linking all infrastructure. The 777 North Mine Project is currently under construction, this project will provide a ramp from surface and 300 tons per day of additional mill feed. 777 hosts 21.9 Mt (includes past production and current reserves) and is projected to produce a further 1.49 million tonnes grading 2.07g/t Au, 27.88g/t Ag, 2.80% Cu, and 4.20% Zn in 2011. It is expected to produce until 2020 from reserves of 12.285 tonnes grading 1.88 g/t Au, 27.43 g/t Ag, 1.96% Cu, and 4.33% Zn combined proven and probable reserves (Table 2).

### Mine Geology

The ore is hosted in rhyolitic and basaltic volcanic lithofacies of the Millrock Member of the Flin Flon formation. Basaltic flow and intrusive lithofacies of the overlying Hidden formation occur in the hanging wall to the deposit (Figures 25 and 26). At 777, the Millrock member is subdivided into 4 map units (Fragmental 'Andesite', Chlorite Schist, Quartz Porphyry Rhyolite, and Mafic/Felsic Tuffs). Andesite is a mine term used for the light coloured, typically altered, effusive volcanic rocks

that geochemically are classified as basalt. Lithofacies within each of these mine units, and the overlying Hidden formation are described below.

The "Fragmental Andesite" unit consists of dark green, fine-grained to aphanitic, amygdaloidal aphyric and sparsely feldspar phyrlic basalt clasts within a finer-grained, light to medium-green basaltic matrix (Figure 26). The basalt clasts are sub angular to well rounded, and range in size from 1–10cm. The "Chlorite Schist" unit consists of near massive chlorite with sections of very strongly foliated and chloritized mafic and felsic volcanoclastic lithofacies (Figure 26). It has a pronounced schistose fabric. Locally this unit contains pyrrhotite, chalcopyrite, magnetite mineralization, and it occurs only within the footwall to the 777 deposit. Sulphide Zones 15, 50, and 70 occur in this unit. The Chlorite schist unit is interpreted to be the hydrothermally altered equivalent of the Fragmental Andesite unit (locally the "QP" unit) and, as such defines the footwall alteration pipe to the 777 deposit. Its stratabound nature, with respect to the strata, is interpreted to result from transposition during deformation.

The ore is hosted in quartz porphyry rhyolite of the "QP" unit (Figure 26). The QP unit consists of coherent and volcanoclastic lithofacies. The volcanoclastic lithofacies contain subangular to subrounded fragments of QP in a finer-grained matrix that also contains quartz crystals. The massive sub units and the matrix material consists of aphanitic to very fine grained rhyolite with up to 10% blue to clear quartz eyes with trace plagioclase phenocrysts. Minor to pervasive chlorite and sericite alteration is present throughout. Mafic and lesser felsic tuff and volcanoclastic lithofacies conformably overlie the QP unit (denoted as "Tuffs" in Figure 26). The mafic (and lesser felsic) tuff lithofacies consists of massive, thick to medium bedded tuff and thinly bedded to laminated tuff. The volcanoclastic lithofacies contain lapilli-sized clasts of QP rhyolite, chlorite and or sericite altered QP rhyolite, amygdaloidal and massive sulphide in a finer-grained, mafic tuff-sized matrix. The Tuffs unit marks the top of the Millrock member. The "Flow" unit marks the base of the conformably overlying Hidden formation. It consists of a coherent basalt lithofacies that is fine-grained to aphanitic, aphyric, massive and distinctly amygdaloidal (up to 15% white amygdules filled with quartz and carbonate). Plagioclase and mafic phenocrysts occur locally as do epidote-quartz alteration patches. The Flow unit is interpreted to consist of basaltic flows and sills.

**Table 2: Ore Reserves at the 777 Mine as of January 1, 2012 (Hudbayminerals.com).**

Category	Million Tonnes	Au (g/t)	Ag (g/t)	Cu (%)	Zn (%)
<b>777</b>					
Proven	4.921	1.97	26.78	2.36	4.16
Probable	7.464	1.82	27.86	1.64	4.44

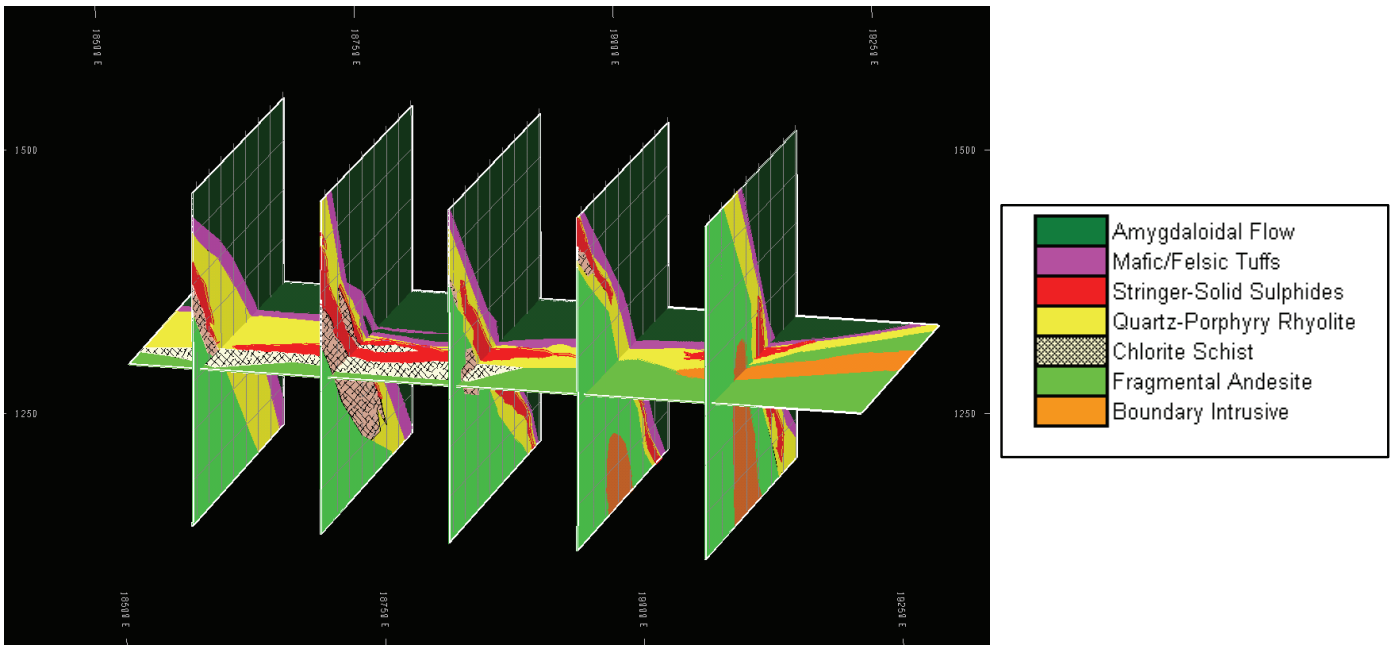


**Figure 25:** Generalized 3D Geology of the 1262 m level of the 777 Deposit (Gibson et al., 2011). Fragmental andesite, quartz-porphry rhyolite and tuffs of the 1.89 Ga Millrock member are upward facing and steeply east dipping. Amygdaloidal mafic flows of the ca. 1.88 Ga Hidden formation lie in the hangingwall. Footwall 'pipe' alteration defined by the chlorite schist lies underneath the ore body and is now tabular in shape due to superimposed multiple deformation phases. Younger 1.85 Ga gabbroic intrusions of the Boundary Intrusive suite occur in the footwall.

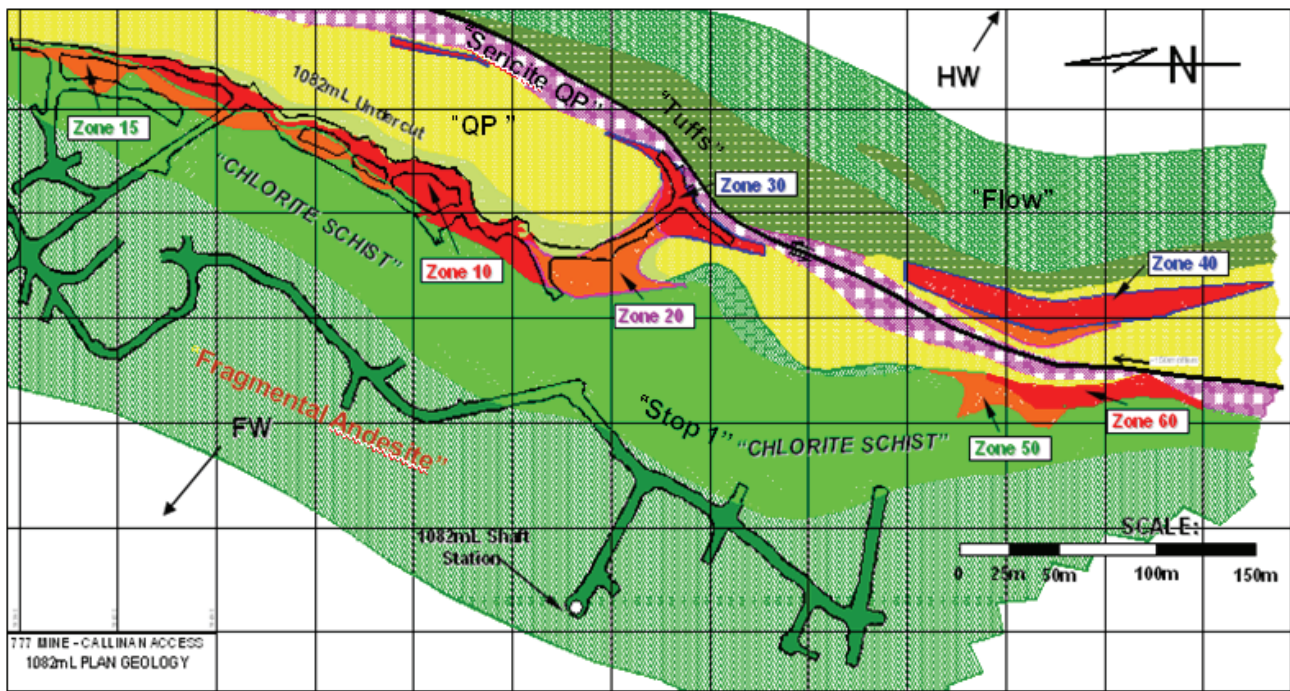


**Figure 26:** Geological map of the 1082 m level, including Stop #1 and mine map units (Gibson et al., 2011).

### The Massive Sulphide

The 777 ore zones are divided into North, South and West Zones. All 3 zones occur within the same stratigraphic interval and are associated with the same lithofacies as described above but the West zone lies within a lower thrust slice. On average, the sulphide lenses strike 010° and dip to the east at 45°. All zones have a relatively shallow plunge that trends at -35°

towards 140°. Horizontal widths through the deposit range from 2.5 to 70m in thickness. Thicker widths are observed where two or more of the ore lenses overlap. There are a total of seven distinct sulphide lenses within with the 777 deposit. Zones 10, 15, 20 and 30 occur in the North Zone, while Zones 40, 50, 60, and 70 occur in the South Zone. The sulphide lenses have been distinguished on the basis of grade and ore type, as well as their

spatial location. Zone 10 contains variable concentrations of pyrrhotite, pyrite, and chalcopyrite. Locally, minor sphalerite, arsenopyrite, chalcocite, and chlorite are present. Zones 15, 50, and 70 are hosted within the Chlorite Schist unit. They generally contain pyrrhotite, and chalcopyrite, with minor amounts of sphalerite, pyrite, arsenopyrite, and magnetite. Zones 30, 40, and 60 are Zn rich (High Zinc Lens) and contain variable concentrations of pyrite, sphalerite, and chalcopyrite. Locally, minor pyrrhotite, magnetite, and arsenopyrite are present.

**Underground tour**

A number of stops are planned on the tour to showcase each of the main underground map units, the sulphide lenses themselves, and the some of the major structures, including the thrusts (Figure 27). Where stops occur and specific details will be finalized in the days before the field trip depending on mine conditions and scheduling.

**Stop 9 – Hanging wall to the Schist Lake and Mandy ore bodies**

The Schist Lake and Mandy VMS deposits are located on the western edge of the Northwest Arm of Schist Lake, approximately 4 km southeast of the town of Flin Flon (Figure 4), and are currently inactive. Field observations suggest a major, synvolcanic structure is present in the rocks structurally over-

lying the Schist Lake and Mandy deposits and is defined by the following: a) an abrupt lateral change in lithofacies from dominantly volcanoclastic in the south to dominantly flow in the north, b) a synvolcanic dike that transitions upwards into a thin pillowed flow along this structure, and c) the presence of a megabreccia (south side) and megapillows (north side) proximal to this structure lower in stratigraphy and a spatter rampart deposit higher in stratigraphy (DeWolfe, 2009). The megabreccias, megapillows and spatter rampart are all indicative of a vent proximal environment. The synvolcanic structure most likely acted as both a magma and fluid pathway whilst accommodating movement associated with both primary subsidence, related to volcanism, and later deformation.

**Stop 9.1: Lava tubes and megabreccias within the Hidden formation: Evidence for vent proximity**

**Co-ordinates**

UTM, N 6069380, E 317125

**Hazards:** *Very steep outcrop. Use caution if approaching the southeastern margin of the large outcrop to the south. A moderate level of fitness is required to reach this field stop as the ski trail is quite steep in places (30 m of elevation gain from road to field stop).*

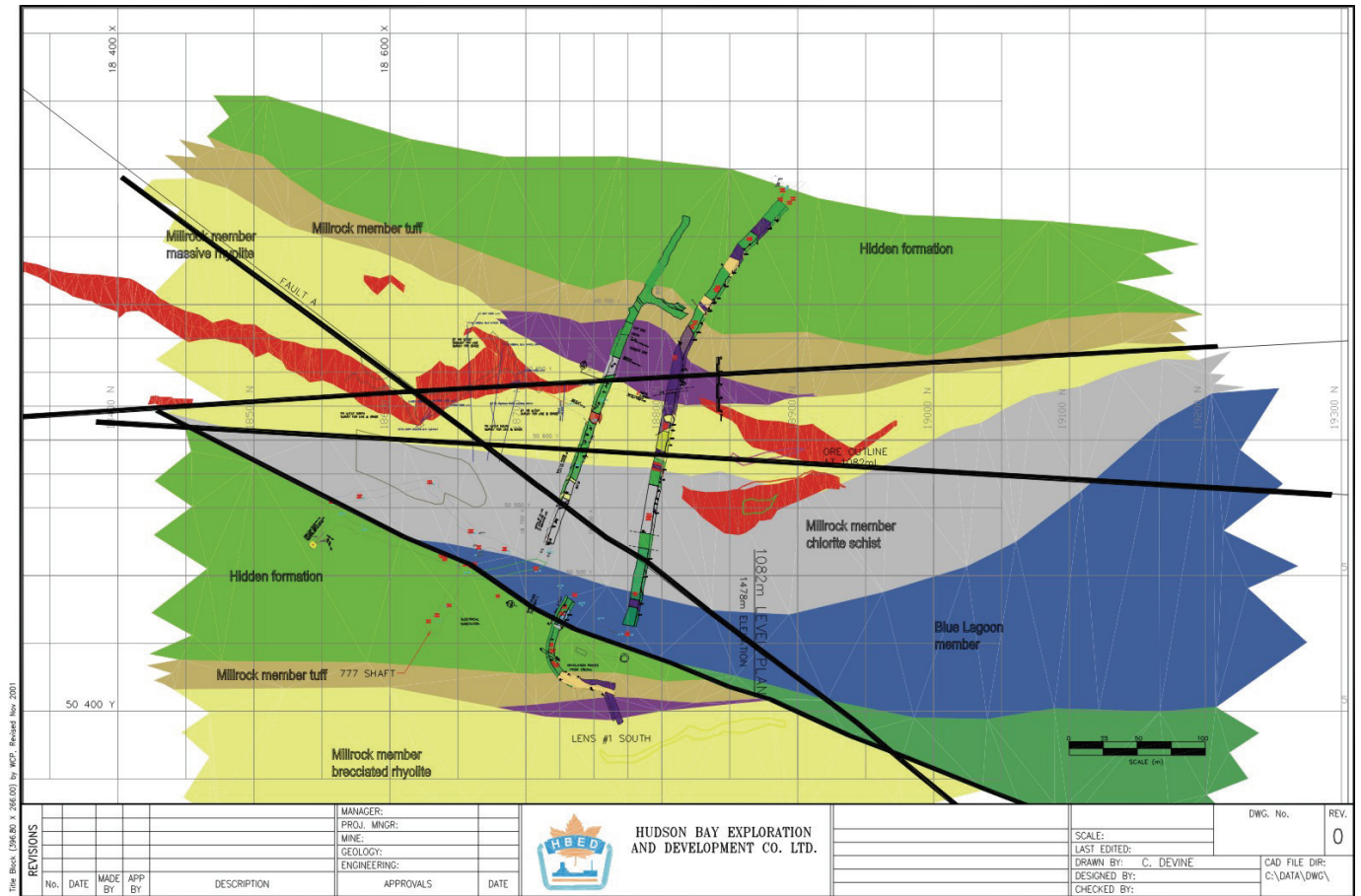


**Figure 27:** Geological map of the 1080 m level, showing thrust fault that placed Blue Lagoon footwall lithofacies overtop of Hidden formation (Gibson et al., 2011). Mapping by C. Devine, Hudbay.

**Stop Description**

As you approach the outcrops from the ski trail you will notice that there is a marked topographic feature, a narrow gully, separating a large outcrop to the north from a larger outcrop to the south. The northern outcrop contains a large basaltic lava tube surrounded by basaltic pillows, whilst the southern outcrop is dominated by breccias with a thin pillowed flow on top (Figure 28). This lateral facies transition is abrupt and marked by an aphyric mafic body, approximately 1–2 m wide, that locally cross cuts bedding lower in the stratigraphy, and changes orientation becoming parallel to bedding higher in the stratigraphy. This change in orientation corresponds with a change from massive to pillowed facies; therefore, this unit is interpreted to

represent an aphyric mafic dike, cross cutting the megabreccia and feeding a thin, pillowed flow that was extruded on top of the breccia. This dike, because it separates the megabreccia and other volcanoclastic units to the south from the basaltic flows to the north, is interpreted to have been emplaced along a synvolcanic fault, which marks the northern boundary of a subsidence structure into which the megabreccias and other volcanic debris flows were deposited. Although there is evidence of minor shearing along this dike, pillows are not truncated, and the vertical offset of the underlying plagioclase crystal-rich volcanoclastic unit along this structure is on the order of only a few metres, suggesting that this is a primary volcanic fault that has been reactivated by later deformation.

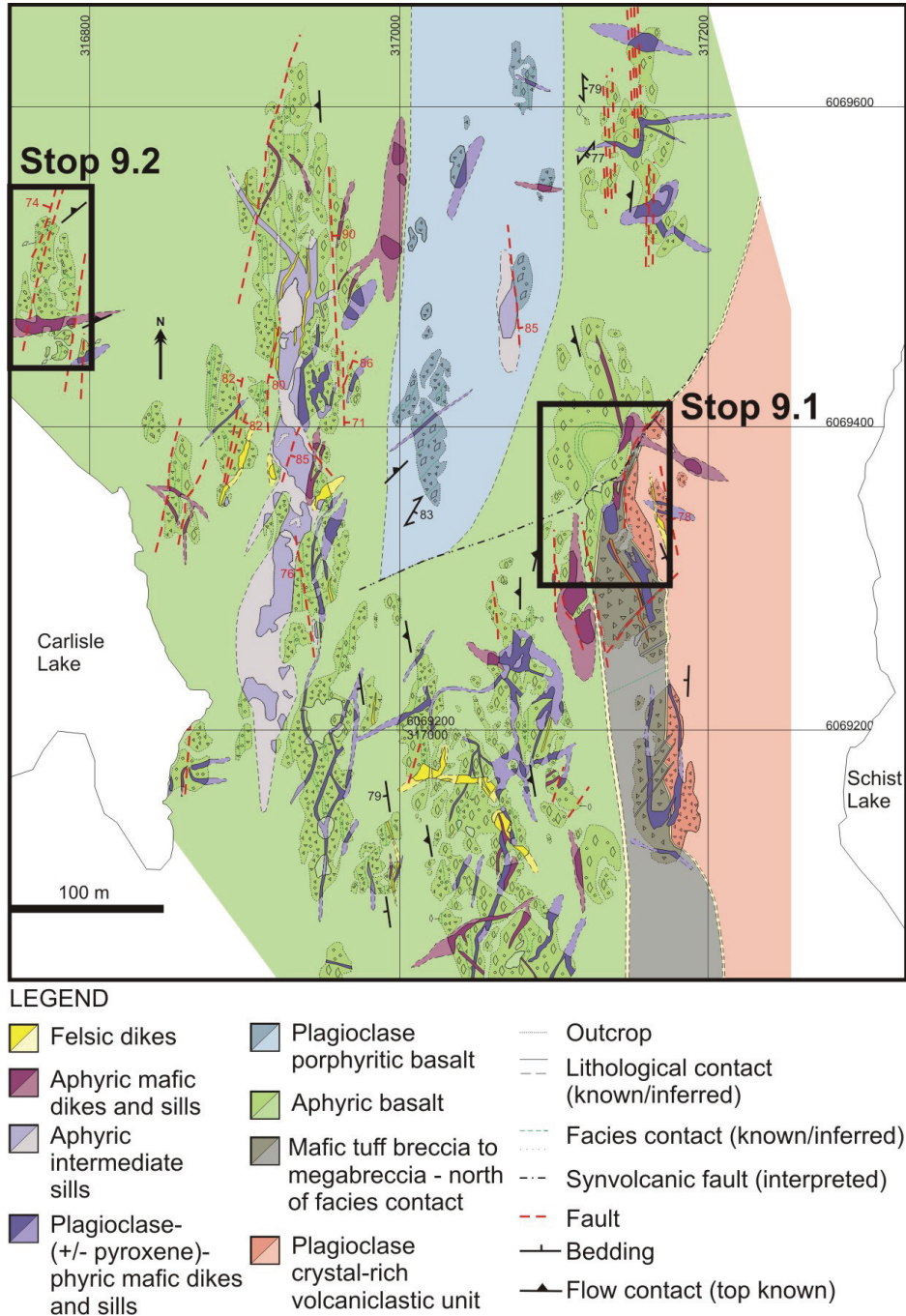


**Figure 28:** Geology and structure of the Hidden formation along the east limb of the Hidden Lake Syncline showing the location of Stops 9.1 and 9.2 (after DeWolfe, 2009).

## Stop 9.2: Spatter rampart and synvolcanic dikes within the Hidden formation: Evidence for vent proximity

### Co-ordinates

UTM, N 6069480, E 316780

### Stop Description

Coarse, fluidal breccias with minor (<10%) thin pillowed and massive flows extend approximately 450 m along strike, and have maximum thickness of 90 m. The breccia is clast supported with a reddish-brown, fine-grained tuff matrix, and is commonly intruded by thin massive to pillowed aphyric mafic sills, which can be observed on the northern tip of this outcrop.

This fluidal breccia unit is interpreted to be a spatter deposit that lies above the synvolcanic structure observed at the last stop. A synvolcanic dike, utilizing a similar synvolcanic feature occurs on the western margin of this outcrop. This synvolcanic dike is ~2 m wide and ‘sills-out’ horizontally into the surrounding spatter deposit. Where the dike propagates laterally, parallel to bedding, spatter or bombs and amoeboid blocks of aphyric quartz-amygdaloidal basalt are larger and more abundant proximal to the dike (vent), and decrease in size and number away from the dike (vent).

## Stop 10. Cliff Lake Pluton

Based on a U-Pb zircon age of  $1859 \pm 22$  Ma, the Cliff Lake Pluton was originally interpreted as single, multiphase quartz tonalite – quartz gabbro intrusion that was younger than host volcanic strata of the Hooke Lake Block ( $1891 \pm 17$  Ma) and to VMS hosting strata of the Flin Flon Block (approx 1888

$\pm 2$  Ma) (Bailes and Syme; 1989; Kremer and Simard, 2007; Simard, and Creaser, 2007). However, a recent U-Pb zircon age for the quartz gabbro phase along the west margin of the intrusion yielded an age of  $1888 \pm 1$  Ma, within error of the age of strata within Flin Flon and Hooke Lake Blocks (Rayner, 2010). The Cliff Lake Pluton and Hooke Lake Block are now divided into two intrusions and two blocks, the Western Hooke Lake Block and the Eastern Hooke Lake Block, that are separated by the Hooke Lake Fault (Figure 5). Based on recent U-Pb zircon ages, volcanic strata of the western Hooke Lake block are now interpreted to be “time equivalent” to strata of the Flin Flon Block. The younger, eastern quartz leucotonalite intrusion was emplaced into volcano-sedimentary strata of the Eastern Hooke Lake Block, whereas the older, western intrusion, consisting of quartz tonalite and quartz gabbro phases was emplaced into the Western Hooke Lake Block, and into strata of its own volcanic pile during a period of magmatic resurgence that followed cauldron subsidence and Flin Flon VMS deposit formation (Gibson et al., 2009b). The west or upper margin of the intrusion is, in part, enveloped within a high temperature (?) reaction zone.

## Stop 10.1: Contact between the Cliff Lake Pluton and the Hooke Lake Block

### Co-ordinates

UTM, N 6075241, E 317788; N 6075242, E 317758

### Stop Description

Stop 10.1 is at the contact between the quartz tonalite phase of the Cliff Lake Pluton and a pillowed flow of the Hooke Lake Block (Figure 29). The tonalite contains numerous mafic xeno-

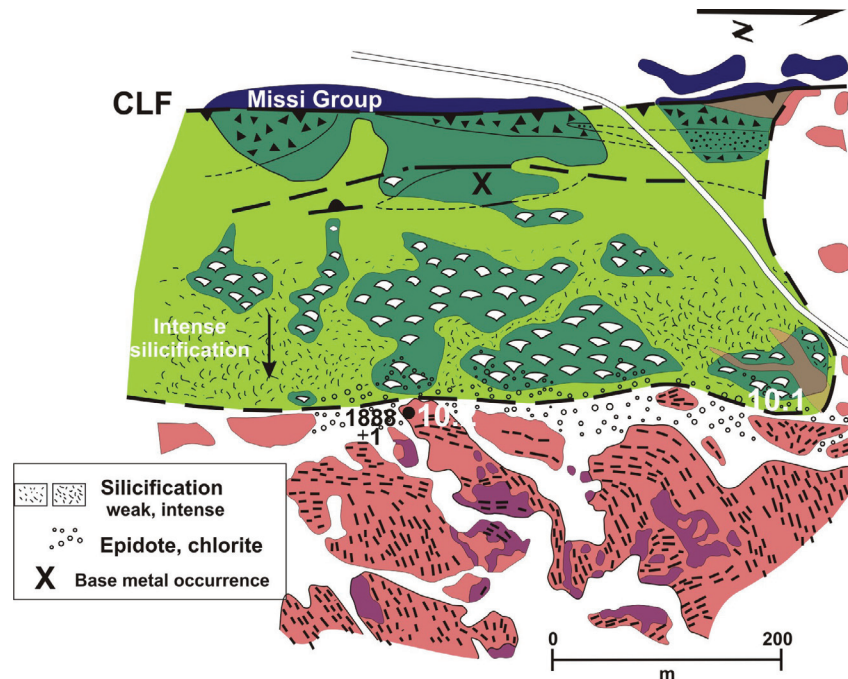


**Figure 29:** Contact between the Cliff lake Pluton (western phase) with a pillowed flow lithofacies within the Western Hooke Lake Block, showing the Location of Stop 10 (after Gibson et al., 2009b, 2011). Map units are as follows: pink and purple, tonalite and quartz-gabbro phases of the Cliff Lake Pluton (the black dashed lines denote aligned concentration of mafic xenoliths); darker green, basaltic lithofacies; white pillowed symbols, pillowed lithofacies; black triangles, volcaniclastic lithofacies; uniform green, massive lithofacies; dark blue, Missi Group sedimentary strata.

liths that define a crude layering and near the contact the tonalite is weakly chlorite and epidote altered. The adjacent pillowed flow to the west is pervasively silicified and the silicification is overprinted by epidote-quartz and a later chlorite alteration that is localized along east-west trending shears and fractures. The silicification zone extends for several 100 m from the intrusion-volcanic contact, but the epidote-quartz and chlorite alteration are restricted to within 10's of metres of the contact.

### **Stop 10.2: Contact between the Cliff Lake Pluton and the Hooke Lake Block**

#### *Co-ordinates*

UTM, N 6075010, E 317771

#### *Stop Description*

Stop 10.2 is the same contact as at Stop 10.1 except here a highly fractured and epidote-quartz and chlorite altered quartz gabbro, along with the quartz tonalite (locally with Fe-staining) is in contact with the silicified pillowed flows. The latter are pervasively epidote-quartz and chlorite altered for several metres from the contact. A pegmatitic phase of the quartz gabbro at this locality yielded the  $1888 \pm 2$  Ma U-Pb zircon age. The locations of the next two stops are shown in Figures 4 and 29 and descriptions are from DeWolfe (2008).

### **Stop 11. Icehouse member, Louis Formation, near Louis Lake**

#### **Stop 11.1: Massive and pillows lava flows of the Icehouse member**

#### *Co-ordinates*

UTM, N 6071565, E 315460

#### *Stop Description*

The Louis formation consists, from oldest to youngest, of the Tower member, Icehouse member and undivided plagioclase and pyroxene phyric basaltic flows (Figure 6). On this outcrop there are two lava flows exposed (Figure 30). All units in the area strike north and face east. The flows are part of the undivided portion of the Louis formation. The western most flow is massive and its flow-top marked by an increase in quartz amygdule content from 5 to 30% (<1–5 cm) over its upper 5 m. The contact with the overlying pillowed flow is sharp, but irregular. Pillows are <1 m in size, have thin ( $\leq 2$  cm) selvages, and contain 5–10% quartz amygdules (<1 cm). Finely laminated, epidote-quartz-altered mafic tuff commonly occurs between the pillows. At the southern edge of this outcrop, there is domain of massive lava that is in sharp contact, along strike, with the pillowed flow, but it does not truncate the pillows (Figure 30). To the west this massive domain is in sharp contact with the lower massive flow. The margin of the massive domain shows a decrease in grain-size suggesting it is a chilled contact. This domain of massive basalt, which is not laterally continuous, is

interpreted to be a lava tube, feeding the surrounding basaltic flows. Walk west to the next outcrop. This outcrop consists of a massive basaltic flow overlain by a pillowed basaltic flow of the Icehouse member (Figure 30). Continue to the west where the next outcrop is a small exposure of mafic tuff and lapilli tuff beds of the Tower member overlying aphyric basalt of the Hidden formation (Figure 30).

### **Stop 11.2: Pillow lavas, pillow breccia and overlying volcanoclastic rocks of the Icehouse member**

#### *Co-ordinates*

UTM, N 6071468, E 315430

#### *Stop Description*

At the western edge of this outcrop is the mafic tuff – lapilli-tuff of the Tower member that is overlain by massive and pillowed lava flows of the Icehouse member. The massive lava flow is in sharp contact with the overlying pillowed lava flow (Figure 30). The upper margin of the pillowed flow is irregular and broken, with a gradation over a distance of 1 m from intact pillows to pillow breccia to an overlying, normally graded, crudely bedded, heterolithic volcanoclastic unit (Figure 30). At the base of the volcanoclastic unit there is a large block (2 m x 0.75 m) of bedded tuff with very irregular margins. Overall, the volcanoclastic unit contains 50% lapilli-sized, round, aphyric to plagioclase and pyroxene phyric basalt clasts. The tuff-sized matrix is reddish brown and contains abundant plagioclase (20–25%) and pyroxene (15%) crystals. The lower 5 m of the unit is a clast supported tuff breccia bed, containing 20% large blocks (6.4–50 cm) of plagioclase and pyroxene phyric, quartz amygdaloidal basalt and 5–10%, angular to subrounded blocks of aphyric rhyodacite. The next 3–5 m marks a transition from a clast-supported tuff breccia to a matrix-supported tuff breccia bed. In this interval, there are only 5% large plagioclase-pyroxene phyric pillow fragments (>10 cm), 3–5% aphyric rhyodacite clasts (rounded and  $\leq 15$  cm), and 10–20% lapilli-sized, aphyric to plagioclase-pyroxene phyric basalt fragments. The upper 10 m of the volcanoclastic unit is a matrix supported lapillistone bed that contains 30% round, lapilli-sized basalt clasts and 5–10% subround aphyric rhyodacite clasts in a mafic, tuff-sized matrix. The poorly sorted, massive to crudely bedded tuff breccia to lapillistone unit is interpreted to have been emplaced as a mass flow that was restricted to a localized basin (DeWolfe, 2008).

### **References**

- Alt, J.C., 1999, Hydrothermal alteration and mineralization of oceanic crust: Mineral geochemistry and processes: Reviews in Economic Geology, 8, p.133-155.
- Ambrose, J.W., 1936, Progressive kinematic metamorphism in the Missi Series, near Flin Flon, Manitoba: American Journal of Science, v. 32, 5th series, p. 257-286.
- Ames, D. E., Tardif, N., Galley, A. G., Gibson, H. L. and MacLachlan, K., 2003, Hangingwall stratigraphy and hydrothermal signature of the Paleoproterozoic Flin Flon-Triple 7-Callinan VMS deposits: FF-TGI: Geological Association of Canada, Geological Association of Canada: Mineralogical Association of Canada, Vancouver, BC, Canada, May 26-28, 2003, Program with Abstracts, vol. 28.

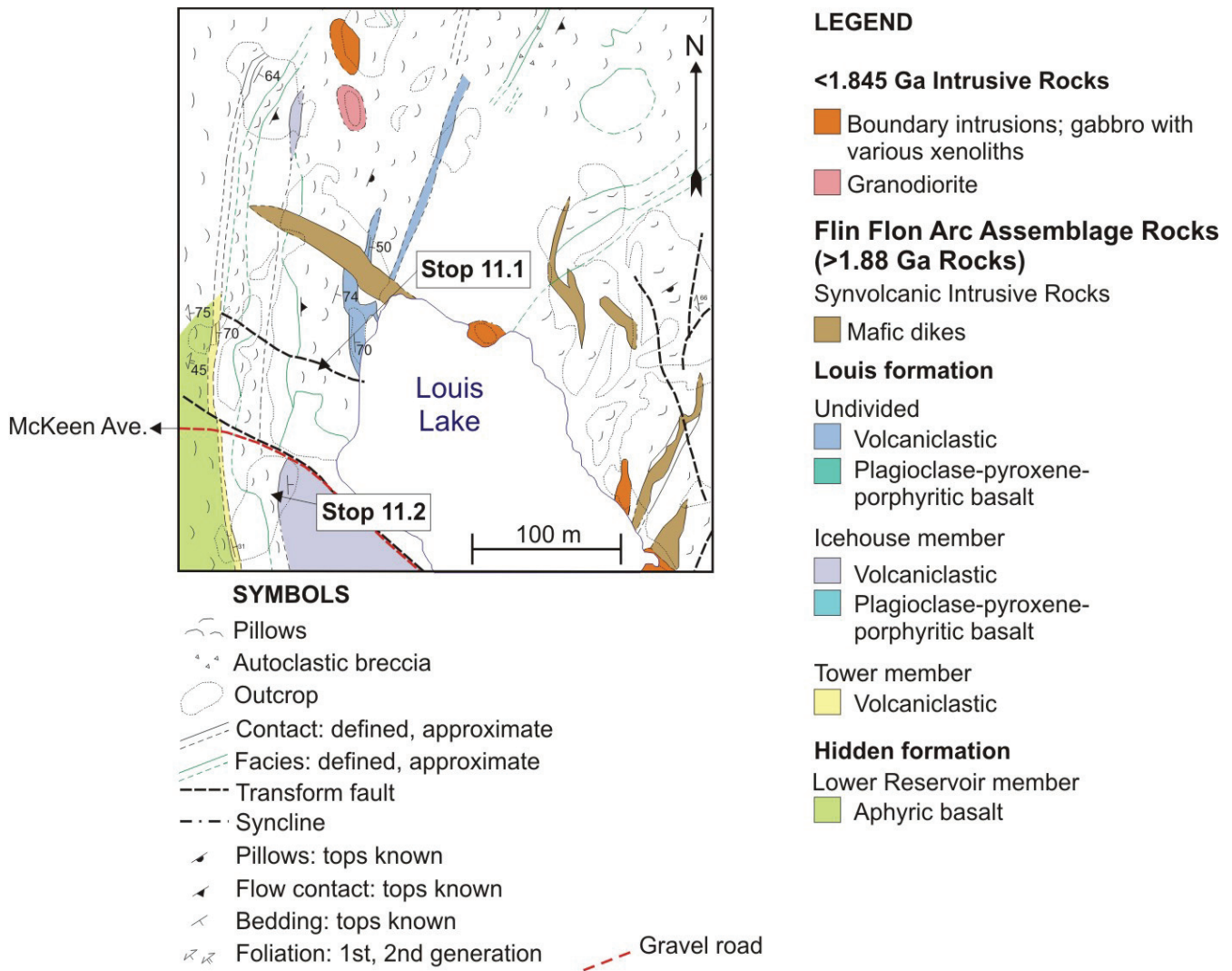


**Figure 30:** Geology and structure of the Louis formation (Ice House member at Louis Lake) showing the location of Stops 11.1 and 11.2 (after DeWolfe, 2008).

Ames, D. E., Tardif, N., MacLachlan, K. and Gibson, H. L., 2002, Geology and hydrothermal alteration of the hanging wall stratigraphy to the Flin Flon-777-Callinan volcanogenic massive sulphide horizon (NTS 63K12NW and 13SW), Flin Flon area, Manitoba: *in* Report of Activities 2002, Manitoba Industry, Trade and Mines - Geological Services, p. 20-34.

Ansdell, K.M. 2005; Tectonic evolution of the Manitoba-Saskatchewan segment of the Paleoproterozoic Trans-Hudson Orogen, Canada, *Canadian Journal of Earth Sciences*, v.42, p. 741-759.

Ansdell, K.M., 1993, U-Pb zircon constraints on the timing and provenance of fluvial sedimentary rocks in the Flin Flon and Athapuskow basins, Flin Flon Domain, Trans-Hudson Orogen, Manitoba and Saskatchewan: *in* Radiogenic Age and Isotopic Studies: Report 7, Geological Survey of Canada, Paper 93-2, p. 49-57.

Ansdell, K.M., Kyser, T.K., Stauffer, M. and Edwards, G., 1992, Age and source of detrital zircons from the Missi Group: a Proterozoic molasse deposit, Trans-Hudson Orogen, Canada: *Canadian Journal of Earth Sciences*, v. 29, p. 2583-2594.

Ansdell, K.M. and Norman, A.R., 1995, U-Pb geochronology and tectonic development of the southern flank of the Kisseynew Domain, Trans-Hudson Orogen, Canada: *Precambrian Research*, v. 72, p. 147-167.

Ashton, K. E., Lewry, J. F., Heaman, L. M., Hartlaub, R. P., Stauffer, M. R., and Tran, H. T., 2005, The Pelican Thrust Zone: basal detachment between the Archean Sask Craton and Paleoproterozoic Flin Flon – Glennie Complex, western Trans-Hudson Orogen: *Canadian Journal of Earth Sciences*, v. 42, p. 685-706

Bailes, A.H., Bray, D., and Syme, E.C., 2003, Geology of the South Main Shaft area, Flin Flon, Manitoba, Manitoba Industry, Economic Development and Mines, Manitoba Geological Survey, Preliminary Map PMAP2003-7, scale 1:5000.

Bailes, A.H. and Syme, E.C., 1989, Geology of the Flin Flon - White Lake area: Manitoba Energy and Mines, Geological Report GR87-1, 313 p + 1 geologic map at 1:20,000.

Bailey, K. A., 2006, Emplacement, petrogenesis and volcanic reconstruction of the intrusive and extrusive Myo rhyolite complex, Flin Flon and Creighton, Saskatchewan: Laurentian University, Sudbury, 123 p.

Bailey, K., Gibson, H.L., MacLachlan, K., Piercey, S. and Lafrance, B., submitted: Emplacement, Petrogenesis and Reconstruction of the Paleoproterozoic Myo Rhyolite Complex within Flin Flon cauldron subsidence structure: Implications for subsidence history and VMS formation; *submitted to* Paleoproterozoic Tectonics and Ore Deposits of the Western Trans-Hudson Orogen, Special Issue of Economic Geology.

- Banerjee, N.R., Gillis, K.M. and Muehlenbachs, K. 2000; Discovery of epidotes in a modern setting, the Tonga forearc; *Geology*, v. 28, p. 151-154.
- Banerjee, N.R. and Gillis, K.M., 2001. Hydrothermal alteration in a modern supra-subduction zone: the Tonga fore-arc. *Journal of Geophysical Research*, v. 106, p. 21737-21750.
- Barrie T.C. and Pattison J. 1999; Fe-Ti basalts, high silica rhyolites and the role of magmatic heat in the genesis of the Kam-Kotia volcanic-associated massive sulphide deposit, western Abitibi Subprovince, Canada; in Hannington M and Barrie T. (eds), *The Giant Kidd Creek Volcanogenic Massive Sulphide Deposit, Western Abitibi Subprovince, Canada*. *Economic Geology Monograph* 10, pp 577-592.
- Bleeker, W, 1990, New structural-metamorphic constraints on Early Proterozoic oblique collision along the Thompson Nickel Belt, Manitoba, Canada: *In: Lewry, J. F. and Stauffer, M. R. (eds) The Early Proterozoic Trans-Hudson Orogen of North America*, Geological Association of Canada, Special Paper, v. 37, p. 57-73.
- Bruce, E.L., 1918, Amisk-Athapapuskow Lake district: Geological Survey of Canada, Memoir 105, 91 p.
- Carmichael, I.S.E. 1967; The iron-titanium oxides of salic volcanic rocks and their associated ferromagnesian silicates, *Contributions to Mineralogy and Petrology*, v.15, p. 24-66.
- Cas, R.A.F. and Wright, J.V., 1987, *Volcanic Successions: Modern and Ancient*. Allen and Unwin, 528p.
- Coombe Consultants, 1984, *Gold in Saskatchewan: Saskatchewan Energy and Mines, Saskatchewan Geological Survey, Open File Report 84-1*.
- Corrigan, D., Galley, A. G., and Pehrsson, S., 2007, Tectonic evolution and metallogeny of the southwestern Trans-Hudson Orogen: *In: Goodfellow, W. D. (ed.) Mineral Deposits of Canada: A Synthesis of Major Deposit-types, District Metallogeny, the Evolution of Geological Provinces, and Exploration Methods*. Geological Association of Canada, Mineral Deposits Division, Special Publication v. 5, p. 881-902.
- Corrigan, D., Pehrsson, S., Wodicka, N., and de Kemp, E., 2009, The Palaeoproterozoic Trans-Hudson Orogen; a prototype of modern accretionary processes: *in: Ancient orogens and modern analogues, Geological Society Special Publications*, v. 327, 457-479.
- Davis, J. and Syme, E.C. 1994; U-Pb geochronology of late Neoproterozoic tonalities in the Flin Flon Belt, Trans-Hudson Orogen: surprise at surface, *Canadian Journal of Earth Sciences*, v.31, p.1785-1790.
- David, J., Bailes, A. H., and Machado, N., 1996, Evolution of the Snow Lake portion of the Palaeoproterozoic Flin Flon and Kibseynew belts, Trans-Hudson Orogen, Manitoba, Canada: *Precambrian Research*, v. 80, p. 107-124.
- Devine, C., 2003, Origin and emplacement of volcanogenic massive sulphide-hosting, Paleoproterozoic volcanoclastic and effusive rocks within the Flin Flon subsidence structure, Manitoba and Saskatchewan, Canada: *Laurentian University, Sudbury*, 279 p.
- Devine, C., Gibson, H., Bailes, A., Galley, A., MacLachlan, K. and Gilmore, K., 2003, Origin and emplacement of VMS-hosting, Paleoproterozoic volcanoclastic rocks within the Flin Flon Subsidence Structure, Flin Flon, Manitoba and Saskatchewan; *in Abstract Volume 28, Geological Association of Canada/Mineralogical Association of Canada Joint Annual Meeting, Vancouver, Canada*.
- Devine, C. A., Gibson, H. L., Bailes, A. H., MacLachlan, K., Gilmore, K. and Galley, A. G., 2002, Stratigraphy of volcanogenic massive sulphide-hosting volcanic and volcanoclastic rocks of the Flin Flon Formation, Flin Flon (NTS 763K12 and 13), Manitoba and Saskatchewan: *in Report of Activities 2002, Manitoba Industry, Trade and Mines - Geological Services*, p. 9-19.
- DeWolfe, Y.M. and Gibson, H.L. 2013; The facies architecture of a Paleoproterozoic andesite synvolcanic intrusion, Flin Flon, Manitoba, Canada, *Bulletin Volcanology*, v.75, p.3-14.
- DeWolfe, Y. M., 2008, Physical volcanology, petrology and tectonic setting of intermediate and mafic volcanic and intrusive rocks in the Flin Flon volcanogenic massive sulphide (VMS) district, Manitoba, Canada: *Growth of a Paleoproterozoic arc: Ph.D. thesis, Laurentian University, Sudbury*, 269p.
- DeWolfe, Y. M., 2009, Stratigraphy and structural geology of the hangingwall to the hostrocks of the Schist Lake and Mandy volcanogenic massive sulphide deposits, Flin Flon, Manitoba (part of NTS 63K12) *in Report of Activities 2009, Manitoba Science, Innovation, Energy and Mines, Manitoba Geological Survey*, p. 22-36.
- DeWolfe, Y. M. and Gibson, H. L., 2004, Physical description of the 1920 member, Hidden formation, Flin Flon, Manitoba (NTS 63K16SW): *in Report of Activities 2004, Manitoba Industry, Economic Development and Mines, Manitoba Geological Survey*, p. 24-35.
- DeWolfe, Y. M. and Gibson, H. L., 2005, Physical description of the Bomber, 1920 and Newcor Members of the Hidden Formation, Flin Flon, Manitoba (NTS 63K16SW): *in Report of Activities 2005, Manitoba Science, Technology, Energy and Mines, Manitoba Geological Survey*, p. 7-19.
- DeWolfe, Y. M. and Gibson, H. L., 2006, Stratigraphic subdivision of the Hidden and Louis Formations, Flin Flon, Manitoba (NTS 63K16SW): *in Report of Activities 2006, Manitoba Science, Technology, Energy and Mines, Manitoba Geological Survey*, p. 22-34.
- DeWolfe, Y. M., Gibson, H. L., Lafrance, B. and Bailes, A. H., 2009a, Volcanic reconstruction of Paleoproterozoic arc volcanoes: the Hidden and Louis formations, Flin Flon, Manitoba, Canada, *Canadian Journal of Earth Science*, v. 46, p. 481-508.
- DeWolfe, Y. M., Gibson, H. L. and Piercey, S. J. 2009b, Petrogenesis of the 1.9 Ga mafic hanging wall sequence of the Flin Flon, Calinan and 777 massive sulphide deposits, Flin Flon, Manitoba, Canada, *Canadian Journal of Earth Science*, v. 46, p. 509-527.
- Digel, S. and Gordon, T.M., 1995, Phase relations in metabasites and pressure-temperature conditions at the prehnite-pumpellyite to greenschist facies transition, Flin Flon, Manitoba, Canada: *in Schiffman, P., and Day, H.W., eds., Low-Grade Metamorphism of Mafic Rocks, Geological Society of America Special Paper* 296, p. 67-80.
- Emby, R.W., Jonasson, I.R., Perfit, M.R., Franklin, J.M., Tivey, M.A., Malahoff, A., Smith, M.F. and Francais, T.G. 1988; Submersible investigation of an extinct hydrothermal system on the Galapagos Ridge: sulfide mounds, stockwork zone, and differentiated lavas, *Canadian Mineralogist*, v.26, p. 517-539.
- Fedorowich, J.S., Kerrich, R. and Stauffer, M.R., 1995, Geodynamic evolution and thermal history of the central Flin Flon Domain, Trans-Hudson Orogen: constraints from structural development,  $^{40}\text{Ar}/^{39}\text{Ar}$ , and stable isotope geothermometry, *Tectonics*, v. 14, p. 472-503.
- Fisher, R. V., 1966, Rocks composed of volcanic fragments, *Earth Science Reviews*, v. 1, p. 287-298.
- Fisher, R. V. and Schmincke, H. U., 1984, *Pyroclastic rocks: Springer-Verlag, Berlin*, 472 p.
- Gale, D. F. G., Lucas, S. B., and Dixon, J. M., 1999, Structural relations between the polydeformed Flin Flon arc assemblage and Missi Group sedimentary rocks, Flin Flon area, Manitoba and Saskatchewan, *Canadian Journal of Earth Sciences*, v. 36, p. 1901-1915.

- Galley, A. G., 1993, Characteristics of semi-conformable alteration zones in volcanogenic massive sulphide districts: *Journal of Geochemical Exploration*, 48, p. 175-200.
- Galley, A.G., Bailes, A.H., Paradis, S. and Taylor, B., 2002, Volcanogenic massive sulphide-related hydrothermal alteration events within the Paleoproterozoic Snow Lake Arc Assemblage, Geological Association of Canada-Mineralogical Association of Canada Joint Annual Meeting 2002, Saskatoon, Saskatchewan, Canada, Field Trip A2 Guidebook, 94 p.
- Galley, A.G., Syme, E.C., and Bailes, A.H., 2007, Metallogeny of the Paleoproterozoic Flin Flon Belt, Manitoba and Saskatchewan: *in*: Goodfellow, W.D., ed., *Mineral Deposits of Canada: A Synthesis of Major Deposit Types, District Metallogeny, the Evolution of Geological Provinces, and Exploration Methods*: Geological Association of Canada, Mineral Deposits Division, Special Publication No. 5, p. 509-531.
- Gibson, H., Pehrsson, S., Lafrance, B., DeWolfe, M., Syme, R., Bailes, A., Gilmore, K., Devine, C., Simard, R-L., MacLachlan, K. and Pearson, B. 2011; The volcanological and structural evolution of the paleoproterozoic Flin Flon and Snow Lake mining districts: Geological Association of Canada – Mineralogical Association of Canada – Society of Economic Geologists – Society for Geology Applied to Mineral Deposits Joint Annual Meeting, Ottawa 2011, Guidebook to Field Trip 3B, 76p.
- Gibson, H.L., Lafrance, B., DeWolfe, M., Devine, C., Gilmore, K., and Pehrsson, S. 2009a. Volcanic Reconstruction and Post Depositional Modification of a Cauldron Subsidence Structure within the Flin Flon VMS District. In, Program with Abstracts, Prospectors and Developers Association of Canada, Annual Meeting, Toronto, ON.
- Gibson, H.L., Lafrance, B., DeWolfe, M., Devine, C., Gilmore, K., Pehrsson, S., and Simard, R-L., 2009b. The Volcanic and subvolcanic architecture of a VMS hosting cauldron subsidence structure at Flin Flon, Manitoba. *In*, Program with Abstracts, Manitoba Mining and Minerals Convention, Winnipeg, Manitoba.
- Gibson, H. L., DeWolfe, Y. M., Lafrance, B., Bailey, K., Devine, C., Simms, D., Gilmore, K., Bailes, A. H., Simard, R. L. and MacLachlan, K., 2007, The relationship between rifting, subsidence, volcanism and VMS deposits at Flin Flon, Manitoba: Manitoba Mining & Minerals Convention 2007, Winnipeg, Manitoba, p. 55.
- Gibson, H.L., Bailey, K., DeWolfe, M., Gilmore, K., Devine, C., Sims, D., Bailes, A. and MacLachlan, K., 2006, Evidence for cauldron subsidence at the Flin Flon Mining Camp: Implications for the location of volcanogenic massive sulphide deposits. In, Program with Abstracts, Saskatchewan Industry and Resources Convention, Saskatoon, Saskatchewan.
- Gibson, H. L., DeWolfe, Y. M., Bailey, K., Devine, C., Lafrance, B., Gilmore, K., Simms, D. and Bailes, A. H., 2005, The Flin Flon caldera: ore localization within a Paleoproterozoic synvolcanic subsidence structure defined through mapping: Manitoba Industry, Economic Development and Mines, Manitoba Mining & Minerals Convention 2005, Winnipeg, Manitoba, November 17-19, 2005, p. 49.
- Gibson, H. L., Ames, D. E., Bailes, A. H., Tardif, N., Devine, C., Galley, A. G., MacLachlan, K. and Gilmore, K., 2003a, Invasive flows, peperite and Paleoproterozoic massive sulphide, Flin Flon, Manitoba and Saskatchewan: Geological Association of Canada, Geological Association of Canada: Mineralogical Association of Canada, 2003 Joint Annual Meeting, Vancouver, Program with Abstracts, vol. 1, p. 28.
- Gibson, H. L., Devine, C., Galley, A. G., Bailes, A. H., Gilmore, K., MacLachlan, K. and Ames, D. E., 2003b, Structural control on the location and formation of Paleoproterozoic massive sulfide deposits as indicated by synvolcanic dike swarms and peperite, Flin Flon, Manitoba and Saskatchewan: Geological Association of Canada, Geological Association of Canada: Mineralogical Association of Canada, 2003 Joint Annual Meeting, Vancouver, Program with Abstracts, p. 28.
- Gibson, H. L., Bailes, A. H., Tourigny, G. and Syme, E. C., 2001, Geology of the Millrock Hill area, Flin Flon Manitoba Geological Survey, Geologic map 33, scale 1:500.
- Gibson, H. L., Morton, R. L. and Hudak, G. J., 1999, Submarine volcanic process, deposit, and environments favorable for the location of volcanic-associated massive sulfide deposits: *in* Volcanic associated massive-sulfide deposits: processes and examples in modern and ancient settings, C. T. Barrie and M. D. Hannington (eds.), *Reviews in Economic Geology*, vol. 8, p. 13-51.
- Gibson, H.L. and Kerr, D.J. 1993; Giant volcanic-associated massive sulphide deposits: with emphasis on Archean deposits: in Whiting, B.H., Hodgson, C.J. and Mason, R., eds., *Giant Ore Deposits*: Society of Economic Geologists, Special Publication number 2, p. 319-348.
- Gordon, T.M., Hunt, P.A., Bailes, A.H. and Syme, E.C., 1990, U-Pb zircon ages from the Flin Flon and Kiseynew belts, Manitoba: Chronology of crust formation at an Early Proterozoic accretionary margin: in Lewry, J.F. and Stauffer, M.R., eds., *The Early Proterozoic Trans-Hudson Orogen of North America*: Geological Association of Canada, Special Paper 37, p. 177-199.
- Harper, G.D., 1999, Structural styles of hydrothermal discharge in ophiolite/sea-floor systems: *Reviews in Economic Geology*, 8, p. 53-73.
- Heaman, L.M., Kamo, S.L., Ashton, K.E., Reilly, B.A., Slimmon, W.L. and Thomas, D.J., 1992, U-Pb geochronological investigations in the Trans-Hudson Orogen, Saskatchewan: in *Summary of Investigations 1992*, Saskatchewan Geological Survey, Saskatchewan Energy and Mines, Miscellaneous Report 92-4, p. 120-123.
- Hoffman, P. F., 1988, United plates of America, the birth of a craton: Early Proterozoic assembly and growth of Laurentia: *Annual Review of Earth and Planetary Science Letters*, v. 16, p. 543-603.
- Holland, H.D., Feakes, C.R. and Zbinden, E.A., 1989, The Flin Flon paleosol and the composition of the atmosphere 1.8 BYBP: *American Journal of Science*, v. 289, p. 362-389.
- Kremer, P. D. and Simard, R. L., 2007, Geology of the Hook Lake Block, Flin Flon area, Manitoba (part of NTS 63K12): *in* Report of Activities 2007, Manitoba Science, Technology, Energy and Mines, Manitoba Geological Survey, p. 21-32.
- Lafrance, B., Gibson, H.L., Pehrsson, S., Schetselaar, E., DeWolfe, Y. M., and Lewis, D., in press, Structural reconstruction of the Flin Flon volcanogenic massive sulfide mining district, Saskatchewan and Manitoba, Canada. *Economic Geology Special Issue "Paleoproterozoic Tectonics and Ore Deposits of the Western Trans-Hudson Orogen"*.
- Lewis, D., Lafrance, B. and MacLachlan, K., 2007, Kinematic evidence for thrust faulting and reactivation within the Flin Flon Mining Camp, Creighton, Saskatchewan: *in* Summary of Investigations 2007, Saskatchewan Geological Survey, Saskatchewan Ministry of Energy and Resources, Miscellaneous Report 2007-4.2, CD-ROM, Paper A-2, p. 10.

- Lewis, D., Lafrance, B., MacLachlan, K. and Gibson, H., 2006, Structural investigations of Millrock Hill and the Hinge Zone of the Beaver road Anticline, Creighton, Saskatchewan: *in* Summary of Investigations 2006, Volume 2, Saskatchewan Geological Survey, Saskatchewan Industry Resources, Miscellaneous Report 2006-4.2, CD-ROM, Paper A-10, p. 11.
- Lewry, J. F., and Collerson, K. D., 1990: The Trans-Hudson Orogen: extent, subdivisions and problems: *In*: Lewry, J. F. and Stauffer M. R. (eds) The Early Proterozoic Trans-Hudson Orogen of North America; Geological Association of Canada, Special Paper 37, p. 1-14.
- Lewry, J.F. and Sibbald, T.I.I. 1980; Thermotectonic evolution of the Churchill Province in northern Saskatchewan, Tectonophysics, v.68, p. 45-82.
- Lucas, S.B., Stern, R.A., Syme, E.C., Reilly, B.A., and Thomas, D.J., 1996, Intraoceanic tectonics and the development of continental crust: 1.92-1.84 Ga evolution of the Flin Flon Belt, Canada: Geological Society of America (GSA), Geological Society of America Bulletin, v. 108, no. 5, p. 602-629.
- MacLachlan, K., 2006a, Bedrock geology Douglas Lake area, Flin Flon Domain (part of NTS 63K12): Saskatchewan Geological Survey, Saskatchewan Industry and Mines, Summary of Investigations 2007, Volume 2, Miscellaneous Report 2006-4.2, Geological Map, scale 1:3 000.
- MacLachlan, K., 2006b, Bedrock geology Green Lake area, Flin Flon Domain (part of NTS 63K12): Saskatchewan Geological Survey, Saskatchewan Industry and Mines, Summary of Investigations 2007, Volume 2, Miscellaneous Report 2006-4.2, Geological Map, scale 1:3 000.
- MacLachlan, K., 2006c, Stratigraphy, structure, and silicification: new results from mapping in the Flin Flon Mining Camp, Creighton, Saskatchewan: *in* Summary of Investigations 2006, Volume 2, Saskatchewan Geological Survey, Saskatchewan Industry and Resources, Miscellaneous Report 2006-4.2, p. 25.
- MacLachlan, K. and Devine, C., 2007, Stratigraphic evidence for volcanic architecture in the Flin Flon Mining Camp: implications for mineral exploration: *in* Summary of Investigations 2007, Saskatchewan Geological Survey, Saskatchewan Ministry of Energy and Resources, Miscellaneous Report 2007-4.2, CD-ROM, Paper A-1, p. 29.
- Malinowski, M., White, D. J., Mwenifumbo, C. J., Salisbury, M., Bellefleur, G., Schmitt, D., Dietiker, B., Schetselaar, E., and Duxbury, A., 2008, Seismic exploration for VMS deposits within the Paleoproterozoic Flin Flon Belt, Trans-Hudson Orogen, Canada: *in* European Geosciences Union general assembly 2008, Anonymous, *Geophysical Research Abstracts*, 10
- Maxeiner, R.O., Corrigan, D., Harper, C.T., MacDougall, D.G. and Ansdell, K. 2005; Paleoproterozoic arc and ophiolitic rocks on the northwest-margin of the Trans-Hudson Orogen, Saskatchewan, Canada: their contribution to a revised framework for the orogen, *Precambrian Research*, v.136, p. 67-106.
- McPhie, J., Doyle, M. and Allen, R., 1993, Volcanic textures: a guide to the interpretations in volcanic rocks: CODES, Hobart, 198 p.
- Pehrsson, S. and the TGI-3 Flin Flon project team, 2009: New models and metalotects for the Trans-Hudson orogen; Exploration 2007, Manitoba Mining and Minerals Convention, online abstracts.
- Perfit M.R., Ridley W.I. and Jonasson, I.R. 1999; Geologic, Petrologic and geochemical relationships between magmatism and massive sulphide mineralization along the Eastern Galapagos Spreading Centre; *in*: Barrie CT and Hannington MD (eds) Volcanic associated massive sulfide deposits: processes and examples in modern and ancient settings. *Reviews in Economic Geology* 8:75-100.
- Rayner, N., 2010, New U-Pb zircon ages from the Flin Flon Targeted Geoscience Initiative Project 2006-2009: Flin Flon and Hook Lake blocks, Manitoba and Saskatchewan, Geological Survey of Canada, Current Research (Online) no. 2010-4, 2010: 15 pages, doi:10.4095/261489
- Reilly, B.A., 1990, Bedrock geological mapping: Mystic Lake - West Arm, Schist Lake area (Part of NTS 63K-12): *in* Summary of Investigations 1990, Saskatchewan Geological Survey, Saskatchewan Energy and Mines, Miscellaneous Report 90-4. p. 25-35.
- Reilly, B.A., 1991, Revision bedrock geological mapping: Mystic Lake - Kaminiis Lake area (parts of NTS 63K-12 and 63L-9): *in* Summary of Investigations 1991, Saskatchewan Geological Survey, Saskatchewan Energy and Mines, Miscellaneous Report 91-4. p. 9-15.
- Reilly, B.A., 1992, Early thrusting and granitoid diapirism in the southern Flin Flon greenstone belt, Saskatchewan: *in* Geological Association of Canada, Programs with Abstracts, v. 17, p. A95.
- Robert, F., Boullier, A-M. and Firdaous, K. 1995: Gold-quartz veins in metamorphic terranes and their bearing on the role of fluids in faulting; *Journal of Geophysical Research*, v. 100, No. B7, p. 12861-12879.
- Sangster, D. F., 1972, Precambrian volcanogenic massive sulphide deposits in Canada: A review, Geological Survey of Canada, Paper 72-22.
- Schetselaar, E., Pehrsson, S.J., Devine, C., Currie, M., and White, D. 2010. The Flin Flon 3D Knowledge Cube, Geological Survey of Canada, Open File 6313, 35 p.
- Sibson, R.H., Robert, F., Poulsen, K.H. 1988: High-angle reverse faults, fluid-pressure cycling, and mesothermal gold-quartz deposits; *Geology*, v. 16, p. 551-555.
- Simard, R. L. and Creaser, R. A., 2007, Implications of new geological mapping, geochemistry and Sm-Nd isotope data, Flin Flon area, Manitoba (part of NTS 63K12): *in* Report of Activities 2007, Manitoba Sciences, Technology, Energy and Mines, Manitoba Geological Survey, p. 7-20.
- Simard, R. L., MacLachlan, K., Gibson, H. L., DeWolfe, Y. M., Devine, C., Kremer, P. D., Lafrance, B., Ames, D. E., Syme, E. C., Bailes, A. H., Bailey, K., Price, D. P., Pehrsson, S., Cole, E. M., Lewis, D. and Galley, A. G., 2010, Geology of the Flin Flon area, Manitoba and Saskatchewan (part of NTS 63K12, 13): Innovation, Energy and Mines, Manitoba Geological Survey, Geoscientific Map MAP 2009-1, colour map, scale 1:10 000.
- Smith, R.L., and Bailey, R.A., 1968, Resurgent cauldrons, Geological Society of America Memoire, v. 116, p. 613-662.
- Stauffer, M.R., 1990, The Missi formation: an Apebian molasse deposit in the Reindeer Zone of the Trans-Hudson orogen, Canada: *in* Lewry, J.F. and Stauffer, M.R., eds.: The Early Proterozoic Trans-Hudson Orogen of North America: Geological Association of Canada, Special Paper 37, p. 121-141.
- Stauffer, M. R., Mukherjee, A. C. and Koo, J., 1975, The Amisk Group: an Apebian(?) island arc deposit, *Canadian Journal of Earth Science*, v. 12, p. 2021-2035.
- Stern, R. A., Machado, N., Syme, E. C., Lucas, S. B. and David, J., 1999, Chronology of crustal growth and recycling in the Paleoproterozoic Amisk collage (Flin Flon Belt), Trans-Hudson Orogen, Canada, *Canadian Journal of Earth Sciences*, v. 36, p. 1827-1807.
- Stern, R.A. and Lucas, S.B., 1994, U-Pb zircon constraints on the early tectonic history of the Flin Flon accretionary collage, Saskatchewan: *in* Radiogenic Age and Isotopic Studies: Report 8, Geological Survey of Canada, Paper 94-F, p. 75-86.

- Stern, R.A., Lucas, S.B., Syme, E.C., Bailes, A.H., Thomas, D.J., LeClair, A.D. and Hulbert, L., 1993, Geochronological studies in the Flin Flon Domain, Manitoba-Saskatchewan, NATMAP Shield Margin Project area: results for 1992-1993: in Radiogenic Age and Isotopic Studies, Report 7, Geological Survey of Canada, Paper 93-2, p. 59-70.
- Stern, R.A., Syme, E.C., Bailes, A.H. and Lucas, S.B., 1995a, Paleoproterozoic (1.86-1.90 Ga) arc volcanism in the Flin Flon belt, Trans-Hudson Orogen, Canada: Contributions to Mineralogy and Petrology, v. 119, p. 117-141.
- Stern, R.A., Syme, E.C. and Lucas, S.B., 1995b, Geochemistry of 1.9 Ga MORB- and OIB-like basalts from the Amisk collage, Flin Flon belt, Canada: Evidence for an intra-oceanic origin: *Geochimica et Cosmochimica Acta*, v. 59, p. 3131-3154.
- Stockwell, C.H., 1960, Flin Flon-Mandy area, Manitoba and Saskatchewan: Geological Survey of Canada, Map 1078A, scale 1:12 000.
- Syme, E.C. and Bailes, A.H., 1993, Stratigraphic and tectonic setting of volcanogenic massive sulfide deposits, Flin Flon, Manitoba: *Economic Geology*, v. 88, p. 566-589.
- Syme, E.C., Bailes, A.H., Lucas, S.B., 1996, Tectonic assembly of the Paleoproterozoic Flin Flon belt and setting of VMS deposits: Geological Association of Canada: Mineralogical Association of Canada, Geological Association of Canada: Mineralogical Association of Canada: Joint Annual Meeting, Winnipeg, MB, Field Trip Guidebook B1, 131 p. Syme, E.C. 1998; Ore-associated and barren rhyolites in the central Flin Flon Belt: Case study of the Flin Flon mine sequence. Manitoba Energy and Mines, Geological Services Open File Report OF98-9, 26p.
- Syme, E.C. 1987; Athapapuskow Lake Project: in Manitoba Energy and Mines, Minerals Division, Report of Field Activities, 1987, p. 30-39.
- Syme, E.C. 1988; Athapapuskow Lake Project: in Manitoba Energy and Mines, Minerals Division, Report of Field Activities, 1988, p. 20-34.
- Syme, E. C. and Forester, R. W., 1977, Petrogenesis of the Boundary Intrusions in the Flin Flon area of Saskatchewan and Manitoba, *Canadian Journal of Earth Sciences*, v. 14, p. 444-455.
- Syme, E.C., Lucas, S.B., Bailes, A.H., and Stern, R.A., 1999, Contrasting arc and MORB-like assemblages in the Paleoproterozoic Flin Flon Belt, Manitoba, and the role of intra-arc extension in localizing volcanic-hosted massive sulphide deposits, *Canadian Journal of Earth Sciences*, v. 36, no. 11, p. 1767-1788.
- Tardif, N. P., 2003, Hanging wall alteration above the Paleoproterozoic, Callinan and 777 volcanogenic massive sulphide deposits, Flin Flon, Manitoba, Canada: M.Sc. thesis, Laurentian University, Sudbury, 100 p.
- Thomas, D.J., 1989, Geology of the Douglas Lake-Phantom Lake area (Part of NTS 63K-12 and -13): in Summary of Investigations 1989, Saskatchewan Geological Survey, Saskatchewan Energy and Mines, Miscellaneous Report 89-4, p. 44-54.
- Thomas, D.J., 1990, New perspectives on the Amisk Group and regional metallogeny, Douglas Lake - Phantom Lake area, northern Saskatchewan: in Summary of Investigations 1990, Saskatchewan Geological Survey: Saskatchewan Energy and Mines, Miscellaneous Report 90-4, p. 13-20.
- Thomas, D.J. 1991, Revision bedrock geological mapping: Bootleg Lake - Birch Lake area (parts of 63K-12 and 63L-9): in Summary of Investigations 1991, Saskatchewan Geological Survey: Saskatchewan Energy and Mines, Miscellaneous Report 91-4, p. 2-8.
- Thomas, D. J., 1992, Highlights of investigations around the Flin Flon mine: reassessment of structural history: in Summary of investigations 1992, Saskatchewan Geological Survey, Saskatchewan Energy and Mines, Miscellaneous Report 92-4, p. 3-13.
- Thomas, D.J. 1993, Geological highlights of the Hamell Lake area, Flin Flon-Amisk Lake region (parts of NTS 63K-13, 63L-16): in Summary of Investigations 1993, Saskatchewan Geological Survey, Miscellaneous Report 93-4, p. 3-11.
- Thomas, D. J., 1994, Stratigraphic and structural complexities of the Flin Flon mine sequence: in Summary of investigations 1994, Saskatchewan Geological Survey, Saskatchewan Energy and Mines, Miscellaneous Report 94-4, p. 3-10.
- Wallace, R.C., 1984, Mining and Mineral Prospects in Northern Manitoba Northern Manitoba Bulletin published by Authority of Government of Manitoba
- Wentworth, C.K., 1922, A scale of grade and clast terms for clastic sediments. *Journal of Geology*, v.30, p. 377-392.
- Whalen, J.B., Syme, E.C. and Stern, R.A. 1999; Geochemical and Nd isotopic evolution of Paleoproterozoic arc-type granitoid magmatism in the Flin Flon Belt, Trans-Hudson orogen, Canada, *Canadian Journal of Earth Sciences*, v.36, p.227-250.
- White, J. D. L., McPhie, J. and Skilling, I., 2000, Peperite: a useful genetic term, *Bulletin of volcanology*, v. 62, p. 65-66.
- White, J.D.L., and Houghton, B.F., 2006. Primary volcanoclastic rocks. *Geology*, v.34, p. 677-680.